Rijksuniversiteit Groningen

Master Thesis

Optical control of donor-bound electron and nuclear spins in n-doped semiconductors

Author:
Rob Bremer

Supervisors:
Prof. Dr. Ir. C.H. van der Wal
A.R. Onur M.Sc.
Referent:
Dr. V. Malyshev

July 26, 2012

university of groningen / faculty of mathematics and natural sciences

Zernike Institute of Advanced Materials
Physics of Nanodevices Group

Contents

Chapter 1

Introduction

Motivation To perform quantum information processing, using electron spin states can be done with localized spin states. In donor doped semiconductors electrons are localized in donor-bound electron and bound exciton systems. With the help of polarized optical transitions there can be coherent electron spin states created. The big disadvantage of using donor doped semiconductors is that the decoherence time of the electron spin is very short [1]. So information stored in the electron spin is easily lost. In for example donor doped GaAs the donor-bound electron couples with around $\approx 10^5$ [2] nuclear spins (called spin bath), due to hyperfine interaction between the electron spin and the nuclear spins. Because of thermal fluctuations of the nuclear spin bath the nuclear field forms an important dephasing source. Therefore understanding the mechanisms that lead to loss of quantum information and controlling these processes is crucial. Dynamic Nuclear Polarization (DNP) can be used to reduce these fluctuations of nuclear spins in the spin bath [3–6]. DNP is the mechanism were electron spin polarization is induced, which leads to nuclear polarization. When electron spin polarization deviates from thermal equilibrium, spin polarization can be transferred between electrons and nuclei via hyperfine interaction between the electrons and the nuclei. Relatively new research area is ZnSe II-VI semiconductor. The big advantage of II-VI semiconductors is the low natural abundances of nonzero nuclear-spin isotopes in II-VI materials. The existence of zero nuclear-spin isotopes can be also isotropically purified to deplete nonzero nuclear spins [7]. In this thesis a model is build which describes the energy levels of a single electron spin that has hyperfine interaction with an arbitrary number of nuclear spins. For building physical insight we mainly focus on the case of single or a few nuclear spins with $I = 1/2$ or $I = 3/2$. These results are the basis for further investigations that study how DNP can take place. Nuclear spin decoherence times are much larger than electron spin decoherence times, so its also interesting to look for possibilities for using the nuclear spin to store quantum information. This thesis explores the possibilities for optical transitions between nuclear spin states which directly give rise to a nuclear spin polarization. To be able to investigate optical transitions between nuclear spin states, a description of the coupling between the electron and the nuclear spins in the spin bath is needed. For inducing nuclear spin flips, the ability to selectively couple different nuclear spin states is needed. For the possibility of selective coupling with a laser to optical transitions between different spin states, the dipole coupling selection rules for different polarizations of laser light are important.

Experimental reference In an external magnetic field the donor-bound electron in the ground state, called D^0, has two possible Zeeman split levels corresponding to electron spin up and down. These states can be optically excited to higher energy levels, where the lowest excited state excists of a bound exciton state, labeled with D^0X. In an external magnetic field the electrons form a spin singlet state and the spin projections of the hole will be Zeeman split into four levels. In experiments with n-doped GaAs the excited state D^0X is shown to be optically resolvable. In the experiment of figure 1, taken from reference [8], two lasers are coupled between the ground state and an excited state. With different polarizations light transitions can be selectively coupled

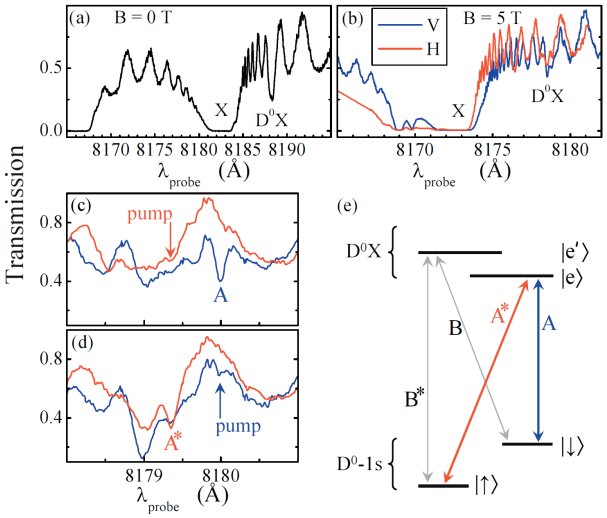

FIG. 1. (Color) (a) Transmission spectroscopy at B=0 T. (b) Transmission at B=5.0 T for H and V polarization. (c) Pump-assisted spectroscopy with H-polarized pumping at the A^* transition shows enhanced absorption for the A transition for the scan with a V-polarized probe (blue trace) but not with an H-polarized probe (red trace). (d) Complementary to (c), V-polarized pumping at A shows enhanced absorption for the A^* transition with an H-polarized probe. (e) Energy levels and optical transitions of the D^0-D^0X system.

between different spin states. One is coupled with the ground state with electron spin up and the other with electron spin down. This scheme is called a lambda scheme. Such an lambda scheme in figure 1, can be used to induce DNP. The levels in figure 1 represent only the electronic states. In reality, due to electron-nuclear angular momentum coupling, each of these levels is split into many hyperfine levels. When we have more insight in this hyperfine splitting and the corresponding optical transition strengths, it is in principle possible to treat the interaction of the full system with one or more optical fields within the density matrix formalism. A preliminary study of how this should be done is covered in appendix A. The main part of this thesis has the goal to understand the hyperfine structure in simplified representations of the D^0X system, as well as the corresponding optical transition rates.

Outline thesis In chapter 2 is explained that a hydrogen like model is used to describe the energy levels of the ground state D^0 and the excited state D^0X. The concepts of the spin-orbit coupling and hyperfine coupling are worked out. These couplings are important to be able to describe the electron spin and nuclear spin states. The last part of chapter 2 will explain what happens with these energy levels when applying an external magnetic field. These Zeeman splitting provides optically resolvable energy levels which are needed to be able to selectively couple lasers on resonance to specific electron spin states. In chapter 3 selection rules for different polarizations laser light are worked out. These selection rules are needed to be able to describe the coupling of a laser to specific nuclear spin states and also to describe the strongly allowed spontaneous emission from the excited states. In chapter 4 all the concepts from chapter 2 are combined. An example of a ground state D^0 with one nuclear spin 1/2 is worked out including Hyperfine coupling and Zeeman splitting. This example illustrates how the field dependent energy diagrams are constructed and the field dependent mixing of spin states is explained. This mixing of spin states has influence on the selection rules. In chapter 5 a few systems with different number of nuclei coupled to the donor-bound electron/hole are worked out. These magnetic field dependent energy level diagrams are used to construct transition schemes, which sketches the strongly allowed transitions between

spin states in low and high field. A model in Mathematica is build to calculate the energy levels of a donor system coupled with multiple nuclei (Appendix E). In chapter 6 the transition schemes derived in chapter 5 are used to investigate the possibilities for inducing nuclear polarization by coupling laser light with certain polarization. To keep track of populations in the system, rate equation can be set up with the density matrix formalism. In appendix A the concept of density matrix formalism is introduced and a three-level lambda system (shortly introduced in figure 1) is worked out with an extension to four levels.

Chapter 2

Energy levels

2.1 Introduction

In this chapter it is described how the hydrogen model is used to describe the energy levels of the ground state and the excited state. The band structures and their corresponding quantum numbers in the semiconductor are important, because these determine the quantum numbers of the donor-bound electron and hole. The different spin states of the donor-bound electron and hole are described with the help of the spin-orbit coupling. The hyperfine coupling between the donor-bound electron and the nuclear spin states in the spin bath is explained. After defining all the energy levels and their degeneracies, the Zeeman splittings due to an applied external magnetic field are worked out. These Zeeman splittings are important to be able to investigate the possible transitions between optically resolvable energy levels.

2.2 Hydrogen like orbitals

When semiconductors are doped with low concentration of donor atoms, at low temperatures the donor electron will bound to the donor site. For GaAs the bohr radius of the bound electron will spread out approximately 100-200 lattice sites. When exciting an electron from the valence band an excited state is created. These excited states are very complicated [9] and not yet fully understood. There is still no consistent picture of what these excited states look like. But the most used description of the lowest excited states are that of a three particle complex [10], which consist of two electrons in a spin singlet state and a hole. Because the two electrons are in a spin singlet state, they will not contribute to effects involving couplings with the spin. The hole however does contribute to spin coupling effects. So the ground state D^0 contains one electron and

(a) Ground state D^0 of the donor-bound electron.

(b) Excited state D^0X of the donor system.

Figure 2.1: The ground state of the donor-bound electron consists of an electron bound to the positive charged donor atom. The excited state exists of two bound electrons in a spin singlet and an hole.

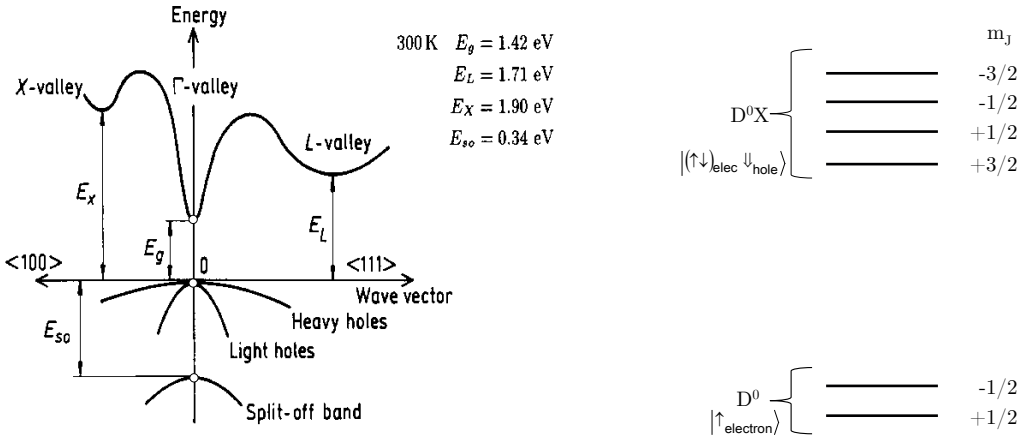

(a) Band Structure GaAs [11]. (b) Energy levels.

Figure 2.2: Figure a) shows the band structure of GaAs. The three lower bands belong to the valence band and the highest band belongs to the conductance band. Figure b) shows the possible spin projections for the electron in the ground state D^0 and for the hole spin in the excited state D^0X.

the excited state contains one hole which is of interest. Because of this hydrogen like structure of the system, this can be described with the hydrogen model.

2.3 Band structure

The band structure of a semiconductor determines the character of the bound electron and hole. In this paragraph a short introduction is given what the band structure of GaAs or ZnSe looks like and what their corresponding quantum numbers are for the ground state and excited state. In figure 2.2a the highest band is the conductance band. Electrons in the conductance band have a s-like orbital. The valence band contains three bands, namely the heavy/light-hole bands and the split-off band. Electrons in the valence band have p-like orbitals. p-like orbitals have orbital angular momentum $L = 1$ and because here only the hole with spin $S = 1/2$ is considered, the total angular momentum J has two possible values $J = |L - S| = \frac{1}{2}$ and $J = L + S = \frac{3}{2}$. The heavy hole band has the quantum numbers $J = \frac{3}{2}, m_J = \pm\frac{3}{2}$ and the light hole band has $J = \frac{3}{2}, m_J = \pm\frac{1}{2}$. The split-off band has quantum numbers $J = 1/2$ and $m_J = \pm\frac{1}{2}$. The heavy hole and light hole bands at $k = 0$ are strictly degenerate only in absence of strain. In a quantum well structure there can be a splitting induced between the heavy-hole and light-hole energy bands. For a quantum well structure with a height of 5nm the heavy hole ans light hole bands are separated by 100 meV [12]. In this thesis a model is build where the heavy/light-hole bands are strictly degenerate.

The energy difference between the heavy/light hole bands and the split-off band is due to spin-orbit coupling. In figure 2.2a this energy splitting between the heavy/light hole band and the split-off band is indicated with E_{SO}. This energy splitting due to spin-orbit coupling is explained in more detail in section 2.4. The energy splitting between the ground state D^0 and the excited state D^0X is almost the same as the gap energy in the semiconductor, in the figure indicated with E_g.

When looking at possible transitions between the valence band and conductance band at a particular point in the bandstructure at the point $k = 0$ (in figure 2.2a indicated with three open circles), electrons can be excited from the split-off band or the higher heavy/light-hole bands to the conductance band. When exciting an electron from the valence band to the conductance band, the hole left behind has the properties of what the electron had in that band. In figure 2.2b the quantum numbers of the ground state and the lowest excited state are summarized.

2.4 Spin orbit coupling

To explain the splitting between the heavy/light hole band and the split-off band a closer look at the spin-orbit coupling is needed. Also the spin-orbit coupling determines the quantum number J, which stands for the total angular momentum $L+S$. J is important because this also determines which projections m_J there are possible for a certain energy level. In chapter 3 it becomes clear that the projections m_J are important for the dipole selection rules.

The spin-orbit interaction is the interaction between the electron magnetic moment and the magnetic field generated by the motion of the electron in the static electric field of the nucleus. The electron moves with a velocity $\vec{v} = \frac{\vec{p}}{m_e}$ in the static electric field $\vec{E}$ of the nucleus. In the reference frame of the electron there appears a magnetic field $\vec{B'} = -\frac{1}{c^2}\vec{v}\times\vec{E}$. Because the electron has an intrinsic magnetic moment $\vec{M_S} = q\vec{S}/m_e$, the interaction energy can be written as

$$H_{SO} = -\vec{M_S}\cdot\vec{B'} \tag{2.1}$$

$\vec{E}$ can be written as $-\frac{1}{q}\frac{d}{dr}V(r)\hat{r}$ with $V(r) = -\frac{e^2}{r}$ substituting this in B' the expression for B' becomes

$$\vec{B'} = -\frac{1}{c^2}\vec{v}\times\vec{E} = \frac{1}{qc^2}\frac{1}{r}\frac{d}{dr}V(r)\frac{\vec{p}}{m_e}\times\vec{r} \tag{2.2}$$

The cross product between $\vec{p}$ and $\vec{r}$ can be written as the total angular momentum vector $\vec{l}$

$$\vec{P}\times\vec{R} = -\vec{L} \tag{2.3}$$

where the classical vectors are replaced by quantum operators, here represented with capitals. The expression for H_{SO} becomes

$$H_{SO} = \frac{1}{m_e^2c^2}\frac{1}{R}\frac{d}{dR}V(R)\vec{L}\cdot\vec{S} = \frac{e^2}{m_e^2c^2}\frac{1}{R^3}\vec{L}\cdot\vec{S} \tag{2.4}$$

Introducing the $|J, m_J\rangle$ basis The spin-orbit term depends on a product of two angular momenta, the orbital angular momentum vector $\vec{L}$ and the electron spin vector $\vec{S}$. The product of the two operators does not have eigenstates defined in either of the two bases $|L, m_L\rangle$ or $|S, m_S\rangle$. One way to describe the eigenstates of this product of two operators is to define a new vector space as a product of the two vector spaces $|L, m_L\rangle|S, m_S\rangle$. But a more useful construction of a new basis is $|J, m_J\rangle$, where $\vec{J} = \vec{L} + \vec{S}$. In this new basis $|J, m_J\rangle$ the spin-orbit operator is diagonal. The eigenstates of $|J, m_J\rangle$ can be expressed in that of $|L, m_L\rangle|S, m_S\rangle$ with the help of Clebsch-Gordan $C^J_{m_L m_S}$ coefficients

$$|J, m_J\rangle = \sum_{m_L, m_S} C^J_{m_L m_S}|L, m_L\rangle|S, m_S\rangle \tag{2.5}$$

were the Clebsch-Gordan coefficients are defined in equation 3.21. This relation between the two bases is useful to obtain the orbital angular momentum L and its projection m_L from a $|J, mJ\rangle$ state. The values for m_L determine mostly whether electric dipole transitions between energy states are possible or not. This is explained in chapter 3.

In this new basis $|J, m_J\rangle$ the spin-orbit coupling term can be rewritten in terms of operators with eigenvalue defined in this new basis.

$$\begin{gathered}\vec{J}^2 = \left(\vec{L}+\vec{S}\right)^2 = \vec{L}^2 + \vec{S}^2 + 2\vec{L}\cdot\vec{S} \\ \vec{L}\cdot\vec{S} = \tfrac{1}{2}\left(\vec{J}^2 - \vec{L}^2 - \vec{S}^2\right)\end{gathered} \tag{2.6}$$

Where each of these operators $\vec{J}^2$, $\vec{L}^2$, $\vec{S}^2$ has an eigenstate in the $|J, m_J\rangle$ basis. Namely $\hbar^2(J(J+1))$, $\hbar^2(L(L+1))$ and $\hbar^2(S(S+1))$.

Spin-orbit energy splitting The expectation value of the spin-orbit term is the matrix element

$$\Delta E_{SO} = \langle R(r)Y(\theta,\phi)| H_{SO} |R(r)Y(\theta,\phi)\rangle \tag{2.7}$$

where the eigenfunctions are a product of the angular and radial solutions of the Schrödinger equation. The matrix element can be written as a product of two elements depending on different variables. These steps are described in more detail in paragraph 3.1.

$$\Delta E_{SO} = \frac{e^2}{m_e^2 c^2} \langle R(r)| \frac{1}{R^3} |R(r)\rangle \langle Y(\theta,\phi)| \vec{L}\cdot\vec{S} |Y(\theta,\phi)\rangle \tag{2.8}$$

where the expectation value of $1/R^3$ is

$$\langle R(r)| \frac{1}{R^3} |R(r)\rangle = \int_0^\infty \frac{1}{r^3} R_{n,l}^2(r) r^2 dr \tag{2.9}$$

with $R(r)$ the radial depending part of the eigenfunctions for hydrogen (shortly introduced in section 3.1). The angular part with the help of equation 2.6 becomes

$$\begin{aligned} \langle Y(\theta,\phi)| \vec{L}\cdot\vec{S} |Y(\theta,\phi)\rangle &= \langle J, M_J| \vec{L}\cdot\vec{S} |J, M_J\rangle \\ &= \tfrac{\hbar^2}{2} \{J(J+1) - L(L+1) - S(S+1)\} \end{aligned} \tag{2.10}$$

Combining the expectation values of the radial and angular parts for the spin-orbit coupling

$$\Delta E_{SO} = \frac{\hbar^2 \beta_{SO}}{2} \{J(J+1) - L(L+1) - S(S+1)\} \tag{2.11}$$

with all constants in front collected in the constant β_{SO}. The spin-orbit energy splitting occurs between different values of J. The spin-orbit term does not depend on the projections m_J. So the energy bands of the heavy/light hole bands does not split up relative to each other due to spin-orbit effect. There is a splitting induced between the split-off band and the heavy/light hole band. Using equation 2.11 the spin-orbit energy shift for the heavy/light hole band with $J = 3/2$ is

$$\Delta E_{SO}^{3/2} = \frac{\hbar^2 \beta_{SO}}{2} \{3/2(3/2+1) - 1(1+1) - 1/2(1/2+1)\} = \frac{\hbar^2 \beta_{SO}}{2} \tag{2.12}$$

For the split-off band with J=1/2 the energy shift due to spin-orbit coupling is

$$\Delta E_{SO}^{1/2} = \frac{\hbar^2 \beta_{SO}}{2} \{1/2(1/2+1) - 1(1+1) - 1/2(1/2+1)\} = -\hbar^2 \beta_{SO} \tag{2.13}$$

So the the splitting between the heavy/light hole bands and the split of band has an energy separation

$$\Delta E_{SO}^{3/2} - \Delta E_{SO}^{1/2} = \frac{3}{2} \hbar^2 \beta_{SO} \tag{2.14}$$

2.5 Hyperfine coupling

The nucleus has just like an electron an intrinsic angular momentum. The spin for the nucleus is labeled with $\vec{I}$. The corresponding magnetic moment is labeled by $\vec{M}_I$. The magnetic moment of the nucleus can be expressed in terms of the nuclear spin.

$$M_I = g_n \vec{\mu_n} \vec{I}/\hbar \tag{2.15}$$

where $\vec{\mu}_n = q_n \hbar / 2M_n$, with M_n the mass of the nucleus. The hyperfine interaction is the interaction of the moment $\vec{M}_I$ of the nucleus with the magnetic field $\vec{B}_e$ produced by the electron. The interaction term is

$$H_{hf} = -\vec{M}_I \cdot \vec{B}_e \tag{2.16}$$

When writing out the magnetic field produced by the electron, the hyperfine interaction term in the Hamiltonian becomes [13]

$$H_{hf} = -\frac{\mu_0}{4\pi}\left\{\frac{e}{m_e R^3}\vec{L}\cdot\vec{M}_I + \frac{1}{R^3}\left[3\left(\vec{M}_S\cdot\hat{R}\right)\left(\vec{M}_I\cdot\hat{R}\right) - \vec{M}_S\cdot\vec{M}_I\right] + \frac{8\pi}{3}\vec{M}_S\cdot\vec{M}_I\delta\left(\vec{R}\right)\right\} \tag{2.17}$$

where R is the distance between the two dipoles $\vec{M}_I$ and $\vec{M}_S$ and $\hat{R} = \vec{R}/R$ is the unit vector parallel to the line joining the dipoles, pointing towards the electron dipole. The first term describes the interaction between the nuclear moment $\vec{M}_I$ and the magnetic field produced by the orbital motion of the electron's charge. The field produced is $\vec{B}_{orbital}(0) = -(\mu_0/4\pi)e\vec{L}/m_e R^3$. The second term represents the interaction between the nuclear magnetic moment and the magnetic dipole field created by the electron density outside the nucleus. The third term is the Fermi contact term, which describes the interaction of the magnetic moment of the nucleus with the magnetic field created by the electron density inside the nucleus ($\vec{R} = 0$).

For the calculation of the expectation value of the hyperfine interaction for a 1s orbital, the contribution of the first term in equation 2.17 leads to the matrix $\langle L = 0, m_L = 0|\,\vec{L}\,|L = 0, m_L = 0\rangle$, which is clearly zero. The second term is zero because of spherical symmetry. The remaining term is the expectation value for the Fermi contact term for the 1S level is equal to the matrix element

$$\langle n = 1; l = 0; m_L = 0; m'_S; m'_I| - \frac{2\mu_0}{3}\vec{M}_S\cdot M_I\delta(\vec{R})\,|n = 1; l = 0; m_L = 0; m'_S; m'_I\rangle \tag{2.18}$$

here $\vec{M}_I$ and $\vec{M}_S$ are rewritten as $\vec{M}_I = g_n\mu_n\vec{I}/\hbar$ and $\vec{M}_S = g_e\mu_B\vec{S}/\hbar$, with $g_e \approx -2$ for a free electron (The following convention about the g-factor of the electron is used, in which the sign of the g factor is positive when the dipole moment is parallel to its angular momentum and negative when it is antiparallel. This would have the advantage that it could be applied consistently in any situation. Such a choice would require the g factors for the electron orbital and electron spin angular momenta to be negative. This is briefly discussed in the reference [14]).

$$\mathcal{A}_k\,\langle m'_S; m'_I|\,\vec{I}\cdot\vec{S}\,|m_S; m_I\rangle \tag{2.19}$$

Only a fraction of the magnetic moment of the total electron is inside the nucleus. The radius of the nucleus is small compared to the electron density function, so the electron density function squared is considered constant inside the nucleus. The hyperfine coupling constant A_k between the electron and a nucleus at a distance $\vec{R}_k$, the hyperfine coupling constant for a nucleus at a distance k lattice sites from the center of the electron density function is [15]

$$\mathcal{A}_k = Av_0\left|\Psi(\vec{R}_k)\right|^2 \tag{2.20}$$

Where A is based on the average over the hyperfine coupling constants for the isotopes in the semiconductor of interest, weighted by there relative abundances. v_0 is the volume of the crystal unit cell containing one nuclear spin, and $\left|\Psi(\vec{R}_k)\right|$ is the electron envelope function. When considering only one nucleus, the electron density function will have its center at the location of the nucleus. The square amplitude at the origin is $|\Psi_{n,l=0}(0)|^2 = \frac{1}{\pi}\left(\frac{Z}{na_0}\right)^3$, where the radial function R_{nl} can be found in table 3.1. The hyperfine interaction term in the Hamiltonian can be written as

$$\text{For } D_0\text{: } H_{hf} = \mathcal{A}_k\vec{I}_k\cdot\vec{S} \tag{2.21}$$

Introducing the $|F, m_F\rangle$ basis Both $\vec{I}$ and $\vec{S}$ has its own vector space with theire eigenvalues. To be able to describe the eigenstates of the product of the two operators there has to a new basis $|FM_F\rangle$ defined. Just like explained in paragraph 2.4. F is defined as the total angular momentum

$\vec{F} = \vec{J} + \vec{I}$. This new basis is needed to be able to write the product of the operators in the Fermi contact term in operators which have theire eigenstates in this new basis.

$$\begin{aligned} \vec{F}^2 &= \left(\vec{I} + \vec{S} + \vec{L}\right)^2 = \vec{I}^2 + \vec{S}^2 + \vec{L}^2 + 2\vec{I}\cdot\vec{S} + 2\vec{S}\cdot\vec{L} + 2\vec{I}\cdot\vec{L} \\ \vec{I}\vec{S} &= \tfrac{1}{2}\left(\vec{F}^2 - \vec{L}^2 - \vec{I}^2 - \vec{S}^2\right) - \vec{I}\cdot\vec{L} - \vec{S}\cdot\vec{L} \end{aligned} \tag{2.22}$$

In the energy levels with s orbitals, $\vec{L}$ is zero and we get with the help of equation 2.22 the expression for $\vec{I}\vec{S}$ in this new basis

$$H_{hf} = \mathcal{A}\vec{I}\vec{S} = \frac{\mathcal{A}}{2}\left(\vec{F}^2 - \vec{I}^2 - \vec{S}^2\right) \tag{2.23}$$

Now the matrix elemetn in equation 2.19 can be calculated with the help of equation 2.23.

$$\langle F; m_F| \frac{\mathcal{A}}{2}\left(\vec{F}^2 - \vec{I}^2 - \vec{S}^2\right)|F; m_F\rangle = \frac{\mathcal{A}\hbar^2}{2}\left(F(F+1) - I(I+1) - S(S+1)\right) \tag{2.24}$$

For the excited state D^0X the hole are in p-like orbitals, with the consequence that the density function at the lattice sites is zero. The fact that the contact term gives no contribution for an electron in a p orbital has led to the claim that electrons in p orbitals and holes do not interact with nuclear spins. But there is still a contribution from the dipole-dipole interaction and the orbital interaction terms, which gives a coupling constant that is about 10 percent of that of the coupling constant of the s electron in the ground state with opposite sign [16]. The effective interaction term for the dipole-dipole and orbital interaction is studied by J. Fischer and W. A. Coish [17] and turned out it can be written as

$$\text{For } D^0X\text{:} \quad H_{hf} = \mathcal{A}\vec{I}\cdot\vec{J} \tag{2.25}$$

which contains now the first two terms of equation 2.17. And the energy shift relative to the spin-orbit energy becomes now simply

$$\Delta E_{hf} = \frac{\mathcal{A}\hbar^2}{2}\left(F(F+1) - I(I+1) - J(J+1)\right) \tag{2.26}$$

This energy shift due to hyperfine coupling is an additional shift to the energy shift above the spin-orbit coupling splitting. The expectation value of the Fermi contact term depend on the quantum number F and not on the projection m_F.

2.6 Multiple coupled nuclei

The donor electron has hyperfine interaction with the nuclear spins on the lattice sites inside its bohr radius. This model looks at the coupling between the donor electron spin and multiple nuclear spins at equal distance and equal nuclear spin. In this paragraph is explained why this approuch is needed and that with this approuch the total interaction with multiple nuclei can be rewritten in the form of equation 2.26.

To describe the coupling between the electron and the nuclear spins in the spin bath, the hyperfine coupling contribution of each nucleus is summed over.

$$H_{hf} = \sum_k^N \mathcal{A}_k \vec{I}_k \vec{J} \tag{2.27}$$

To calculate the expectation value of this hyperfine coupling term with multiple nuclei, the inner product of the operators should be rewritten like in equation 2.22. Because the coupling constants are not equal, defining a total $F = \sum_k^N \vec{I}_k + \vec{J}$ to be able to rewrite the product of operators, is not possible with the approach as used in equation 2.23 or 2.26. Considering only the nuclei at the

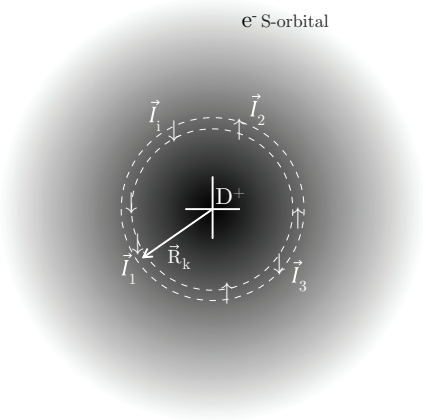

Figure 2.3: Hyperfine coupling with multiple nuclei at the same distance R_k. The white cross in the middle indicates the donor site, with its positive charged nucleus D^+. The black gradient illustrates the spherical symmetric electron density function of an electron in the s orbital.

same distance from the center of the electron density function, sketched in figure 2.3, can overcome this problem. The coupling constant $\mathcal{A}_k$ contains the radial dependence given in equation 2.20. When looking only at the nuclei at the same distance the value for $\left|\Psi(\vec{R}_k)\right|^2$ is for each nucleus the same. $\mathcal{A}_k$ is replaced by $A_R = N_R\mathcal{A}_k$, were N_R is the number of nuclei at a distance R_k as sketched in figure 2.3. When looking at the coupling between the electron and nuclei at the same distance R_k, $\mathcal{A}_R$ can be taken outside the summation.

$$H_{hf} = \mathcal{A}_R \sum_i^{N_R} \vec{I}_i \vec{J} \tag{2.28}$$

the summation here is only over the nuclei which are at the same distance R_k. When considering all nuclear spins I_i with the same value, for GaAs 3/2 for ZnSe assumed 1/2, the sum over all I_i's can be replaced with a total vector I_{tot}. The general rule for vector addition holds I_{tot} runs from $|I_1 - I_2|$ to $I_1 + I_2$ and results in

$$\vec{I}_{tot} = \begin{cases} \text{even number of nuclei:} & 0, 1, ..., N \cdot I_i \\ \text{odd number of nulcei:} & I_1, I_1 + 1, ..., N \cdot I_i \end{cases} \tag{2.29}$$

The first term equals to all nuclear spin vectors anti-parallel and the last term corresponds to all nuclear spin vectors parallel. The steps in between are of the size one. The interaction term can be written in terms of this total nuclear spin vector

$$H_{hf} = \mathcal{A}_R \vec{I}_{tot} \vec{J} \tag{2.30}$$

Defining a basis with this new total nuclear spin vector is possible by defining a total angular momentum vector $\vec{F} = \vec{I}_{tot} + \vec{J}$. In this new basis the expectation values for the hyperfine coupling term can be easily calculated in the same way as in equation 2.26. The difference now is that the nuclear spin vector $\vec{I}_{tot}$ can take more values than the nuclear spin vector for one nucleus, so the number of energy splittings will increase. When extending the model to coupling with all nuclei, the contribution of all the rings, containing nuclei at same distance, should be included.

2.7 Zeeman splitting

When applying an external magnetic field B_0, due to the magnetic momenta of the electron and nuclei, the energy levels split up due to Zeeman splitting. The Zeeman term corresponding to an applied external magnetic field B_0 in the $\hat{z}$ direction these shifts are

$$\begin{aligned} H_Z &= -\omega_0 \left(g_L L_z + g_e S_z\right) - \omega_n g_n I_z \\ H_Z &= -\omega_0 \left(g_L L_z + g_e S_z + g_I I_z\right) \end{aligned} \tag{2.31}$$

The g_e and g_n are the gyro magnetic factors of the electron and nuclei. In the second line of equation 2.31 the gyro magnetic factor of the nucleus g_I contains the nuclear mass, $g_I = g_n \frac{m_e}{M_n}$. For a free electron $g_e \approx -2$ or $g_e \approx +0.41$ for GaAs (see [14] for the used sign convention). ω_0 and ω_n are the Larmor frequencies of the electron and nuclei and are defined like

$$\begin{aligned} \omega_0 &= \tfrac{e}{2m_e} B_0 \\ \omega_n &= \tfrac{e}{2M_n} B_0 \end{aligned} \tag{2.32}$$

The Zeeman energy is much smaller than the spin-orbit coupling($\hbar\omega_0 << \hbar^2\beta_{SO}$) for the range of applied external magnetic fields in this thesis. The spin orbit coupling is of the order of electron volt and the Zeeman splitting is of the order micro electron volt. The term $-\omega_0 \left(g_L L_z + g_e S_z\right)$ can be rewritten as function of J_z. With the help of the Wigner-Eckart theorem, L and S can be written in terms of J

$$\begin{aligned} \vec{L} &= \frac{\langle \vec{L}\cdot\vec{J} \rangle_{E_0,L,S,J}}{J(J+1)\hbar^2} \vec{J} \\ \vec{S} &= \frac{\langle \vec{S}\cdot\vec{J} \rangle_{E_0,L,S,J}}{J(J+1)\hbar^2} \vec{J} \end{aligned} \tag{2.33}$$

where the inner products can be rewritten as

$$\begin{aligned} \vec{L}\cdot\vec{J} &= \vec{L}(\vec{L}+\vec{S}) = \vec{L}^2 + \tfrac{1}{2}(\vec{J}^2 - \vec{L}^2 - \vec{S}^2) \\ \vec{S}\cdot\vec{J} &= \vec{S}(\vec{L}+\vec{S}) = \vec{S}^2 + \tfrac{1}{2}(\vec{J}^2 - \vec{L}^2 - \vec{S}^2) \end{aligned} \tag{2.34}$$

Now L and S can be rewritten

$$\begin{aligned} &\hbar\omega_0(g_L L_z + g_e S_z) = \\ &\hbar\omega_0 \left[g_L \tfrac{J(J+1)+L(L+1)-S(S+1)}{2J(J+1)} + g_s \tfrac{J(J+1)-L(L+1)+S(S+1)}{2J(J+1)} \right] J_z \\ &= \hbar\omega_0 g_J J_z \end{aligned} \tag{2.35}$$

The Zeeman terms from equation 2.31 becomes

$$H_z = -\omega_0 \left(g_L L_z + g_e S_z + g_I I_z\right) = -\omega_0 \left(g_J J_z + g_I I_z\right) \tag{2.36}$$

where g_J is called the Landé factor

$$g_J = \frac{g_L \left(J(J+1) + L(L+1) - S(S+1)\right)}{2J(J+1)} + \frac{g_s \left(J(J+1) - L(L+1) + S(S+1)\right)}{2J(J+1)} \tag{2.37}$$

Three different regimes for field strengths Energy levels for all magnetic fields can be calculated analytically with the help of the hyperfine coupling described in paragraph 2.5 and the Zeeman term derived in the previous paragraph. So the three regimes that will be described are not used to produce the field dependent energy diagrams in this thesis, but are only used for physical interpretation of the results. There are three different regimes of magnetic field strengths, where

the energy splitting can be interpreted in different ways. In weak magnetic fields the Zeeman term can be seen as a perturbation on the hyperfine term, which results in an offset due to hyperfine coupling plus an energy splitting of each level due to projections of the total angular momentum F. At high fields the hyperfine term can be seen as a perturbation on the Zeeman term, which results in overall energy splittings due to Zeeman splitting of the spin projections in the magnetic field and within these overall splitting, there will be a splitting due to hyperfine splitting. In the intermediate field strengths there will be a continues transition between these two descriptions. The three regimes will be explained in more detail.

Weak field Zeeman effect ($\hbar\omega_0 << \mathcal{A}\hbar^2$) For weak external magnetic fields the total angular momentum $\vec{J}$ and the nuclear spin angular momentum $\vec{I}$ are on resonance. The Zeeman terms of the electron and the nucleus can be combined

$$H_z = -\omega_0 \left(g_J J_z + g_I I_z\right) = -g_F \omega_0 F_z \tag{2.38}$$

with the Landé factor g_F defined like

$$g_F = \frac{g_J(F(F+1) - I(I+1) + J(J+1))}{2F(F+1)} + \frac{g_I(F(F+1) + I(I+1) - J(J+1))}{2F(F+1)} \tag{2.39}$$

So at zero field there are the energy offsets due to the hyperfine interaction given in equation 2.26. When increasing the field the degenerate energy levels evolve according to the Zeeman term $-g_F\omega_0 F_z$. Each hyperfine level contains $2F+1$ degenerate levels, m_F running from $-F, -F+1, ..., F$, so each degenerate level at zero field split up into $2F+1$ levels.

High field Zeeman effect ($\hbar\omega_0 >> \mathcal{A}\hbar^2$) For high field $\vec{I}$ and $\vec{J}$ are decoupled, so they are described with $-\omega_0 \left(g_J \hat{J}_z + g_I \hat{I}_z\right)$. Because the two terms are decoupled the Zeeman term cannot be described any more (is not diagonal) in the basis $|F, mF\rangle$. At the high field limit the Zeeman term is diagonal in the basis $|m_J m_I\rangle$

$$-\omega_0 \left(g_J \hat{J}_z + g_I \hat{I}_z\right) |m_J m_I\rangle = -\hbar\omega_0 \left(m_J + m_I\right) |m_J m_I\rangle \tag{2.40}$$

m_J has values running from $-J, ..., +J$, so the energy level split up into $2J+1$ energy levels. The hyperfine coupling term is in high field considered as a perturbation to the Zeeman term. So the hyperfine interaction produces an offset from the Zeeman split energy level. The Hyperfine interaction

$$\langle m_J m_I | \, \mathcal{A}\vec{I} \cdot \vec{J} \, | m_J m_I \rangle \tag{2.41}$$

can be calculated in the same basis $|m_J m_I\rangle$ with the use of the relation

$$\vec{I} \cdot \vec{J} = I_z J_z + \frac{1}{2}\left(I_+ J_- + I_- J_+\right) \tag{2.42}$$

where the last two terms are diagonal in this basis and cancel each other. The remaining term is

$$\langle m_J m_I | \, \mathcal{A} I_z J_z \, | m_J m_I \rangle = \mathcal{A}\hbar^2 m_J m_I \tag{2.43}$$

So inside a Zeeman split bundle due to a projection of m_J there are splittings, which corresponds to a different projections of m_I.

Intermediate field Zeeman effect ($\hbar\omega_0 \approx \mathcal{A}\hbar^2$) At an intermediate field $\vec{I}$ and $\vec{J}$ are partial decoupled. There will be a continues transition between the two descriptions when increasing the magnetic field. States cannot be described in either the basis $|J, m_J\rangle$ or $|F, m_F\rangle$. In this intermediate field the states are not purely in a state $|F, m_F\rangle$ or $|J, m_J\rangle$, but contain a mixture of spin states. This mixture of spin states is worked out in chapter 4.

Chapter 3

Electric dipole transition and selection rules

3.1 Introduction

In this chapter the concept of dipole coupling between electron states and applied electric fields is explained. Also the selection rules for transitions for different polarizations and incoming directions are determined. To describe the dipole transition strength, the dipole operator and the eigenfunctions need to be specified. Starting with the Schrödinger equation for the hydrogen atom in its most general form

$$\left(\frac{-\hbar^2}{2m_e}\bigtriangledown^2 + V(r)\right)\psi = E\psi \tag{3.1}$$

The solution to this differential equation can be found as a product of two functions depending on the radial depending part and the angular depending part

$$\psi = R(r)Y(\theta,\phi) \tag{3.2}$$

Where $Y_l^m(\theta,\phi)$ are the angular momentum eigenfunctions. Some examples for the spherical harmonics are summed in table 3.1 and a few expressions for $R_{n,l}$ are given in table 3.1. Solutions to the Schrödinger equation are standing waves which give a time-independent charge distribution of the electron. To look at transitions between these standing waves a time-dependent perturbation theory is needed. The results of this time-dependent perturbation is described by Fermi's Golden rule. This states that the transition rate is proportional to the square of the matrix element of

$R_{n,l}(r)$	$Y_l^m(\theta,\phi)$
$R_{1,0} = 2\left(\frac{Z}{a_0}\right)^{3/2} e^{-\rho}$	$Y_0^0 = \frac{1}{2}\sqrt{\frac{1}{\pi}}$
$R_{2,0} = \left(\frac{Z}{2a_0}\right)^{3/2} (2-\rho)\, e^{-\rho}$	$Y_1^{-1} = \frac{1}{2}\sqrt{\frac{3}{2\pi}} e^{-i\phi}\sin\theta$
$R_{2,1} = \left(\frac{Z}{2a_0}\right)^{3/2} \frac{2}{\sqrt{3}}\rho e^{-\rho}$	$Y_1^0 = \frac{1}{2}\sqrt{\frac{3}{\pi}}\cos\theta$
	$Y_1^{-1} = -\frac{1}{2}\sqrt{\frac{3}{2\pi}} e^{i\phi}\sin\theta$

Table 3.1: some values for $R_{n,l}$'s and Y_l^m's, with ρ defined as $\frac{Z}{n}\frac{r}{a_0}$.

the perturbation. The transition rates are defined as [18]

$$\begin{aligned}\Gamma^{abs}_{i\to f} &= \frac{\pi e^2\rho(\omega_{fi})}{\epsilon_0\hbar^2 m_e^2\omega_{fi}^2}\left|\langle\Psi_f|\, e^{i\vec{k}\vec{r}}\hat{e}_{rad}\cdot\vec{p}_e\,|\Psi_i\rangle\right|^2\\ \Gamma^{stm}_{i\to f} &= \frac{\pi e^2\rho(\omega_{if})}{\epsilon_0\hbar^2 m_e^2\omega_{if}^2}\left|\langle\Psi_i|\, e^{i\vec{k}\vec{r}}\hat{e}_{rad}\cdot\vec{p}_e\,|\Psi_f\rangle\right|^2\end{aligned} \tag{3.3}$$

were $\Gamma^{abs}_{i\to f}$ is the transition rate for radiation induced absorption and $\Gamma^{stm}_{i\to f}$ is the rate for stimulated emission. ρ is the energy density of radiation, $\hat{e}_{rad}$ is the polarization vector and the integral is in the Dirac notation, i stands for initial state of the system and f stands for final state. Before calculating the integral a simplification can be made. When the wavelength of the incoming beam is larger than the the size of the electron bound electron, the spacial dependence of the oscillating incoming field can be neglected. The approximation made is

$$\begin{aligned}e^{i\vec{k}\vec{r}} &= 1 + i\vec{k}\vec{r} + ...\\ &\approx 1\end{aligned} \tag{3.4}$$

this is called the dipole approximation and gives the simplification for the interaction matrix

$$\langle\Psi_f|\, e^{i\vec{k}\vec{r}}\hat{e}_{rad}\cdot\vec{p}_e\,|\Psi_i\rangle \approx \langle\Psi_f|\,\hat{e}_{rad}\cdot\vec{p}_e\,|\Psi_i\rangle \tag{3.5}$$

$\vec{p}_e$ can be rewrite with the commutation relation $[H_0,\vec{r}] = \frac{\hbar\vec{p}_e}{im}$, were H_0 is the unperturbed Hamiltonian

$$-i\frac{m_e}{\hbar}\langle\Psi_f|\,\hat{e}_{rad}\cdot[H_0,\vec{r}]\,|\Psi_i\rangle = \frac{im}{\hbar}\omega_{fi}\langle\Psi_f|\,\hat{e}_{rad}\cdot\vec{r}_e\,|\Psi_i\rangle \tag{3.6}$$

Now plugging this expression back into equation 3.3 the rates become

$$\begin{aligned}\Gamma^{abs}_{i\to f} &= \frac{\pi}{\epsilon_0\hbar^2}\left|\hat{e}_{rad}\cdot\vec{\mu}_{if}\right|^2\rho(\omega_{fi})\\ \Gamma^{stm}_{i\to f} &= \frac{\pi}{\epsilon_0\hbar^2}\left|\hat{e}_{rad}\cdot\vec{\mu}_{if}\right|^2\rho(\omega_{if})\end{aligned} \tag{3.7}$$

where $\vec{\mu}_{if}$ is the electric dipole moment

$$\vec{\mu}_{if} = \langle\Psi_f|\, e\cdot\vec{r}|\Psi_i\rangle \tag{3.8}$$

The integral can be written as a product of two integrals both depending on different variables [19]

$$\langle f|\,\hat{e}_{rad}\cdot\vec{r}|i\rangle \equiv D_{12}I_{ang} \tag{3.9}$$

where D_{12} is the radial integral

$$D_{12} = \int_0^\infty R_{n_2,l_2}(r)|r|R_{n_1,l_1}(r)r^2dr \tag{3.10}$$

and I_{ang} is the angular integral

$$I_{ang} = \int_0^{2\pi}\int_0^{\pi} Y_{l_2}^{m_2}(\theta,\phi)\hat{e}_{rad}\cdot\hat{r}Y_{l_1}^{m_1}(\theta,\phi)\sin\theta d\phi d\theta \tag{3.11}$$

with $\hat{r} = \vec{r}/|r|$.

3.2 Polarizations incoming beam

Before determining which transitions are possible with different polarizations and directions of an incoming beam, a well defined reference frame is needed to be able to define the polarization and propagation direction of incoming electric fields. With the help of a static external magnetic field it is possible to define a reference frame. The reference frame can be defined with its z-axis along the magnetic field. Looking at Π and σ polarizations of the incoming beam. Π polarized light is defined as a linear polarized oscillating electric field, for example $\Pi^x_{k_z}$ is an incoming beam in the z direction, with its electric field oscillating in the x direction, see figure 3.1a. Sigma polarized light is a combination of two linear polarizations perpendicular to each other and with a relative phase shift of $\pi/2$. For example $\sigma^+_{k_z}$ is defined as an incoming beam in the z direction and the electric field rotating in the x-y plane, see figure 3.1b.

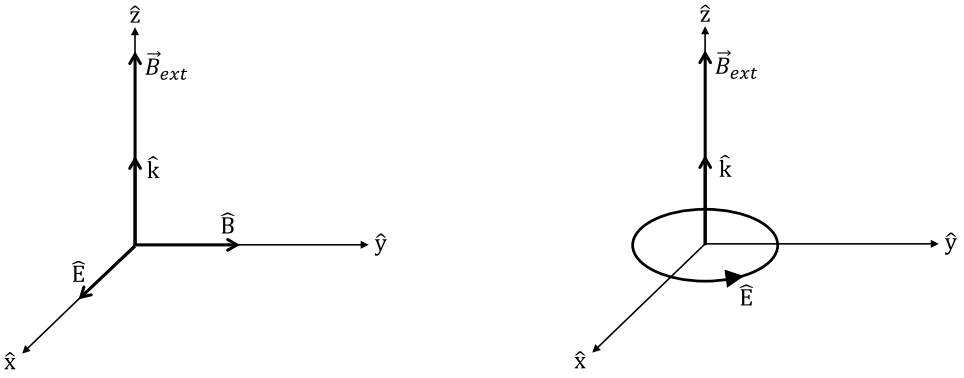

(a) $\Pi^x_{k_z}$ polarized light

(b) $\sigma^+_{k_z}$, or right-handed, polarized light

Figure 3.1: Example of incoming beams with propagation directions in the z-axis (Faraday configuration), with different polarizations.

Faraday and Voight configuration There are two classifications of situations depending on the propagation direction of the incoming beam. In a Faraday configuration the incoming beams propagate parallel to the applied external magnetic field, so theire electric and magnetic field components are perpendicular to the field. The situations sketched in figure 3.1 are in a Faraday configuration. When the propagation direction is perpendicular to the applied external magnetic field the system is called to be in the Voight configuration. Often used terminology for polarizations are horizontal and vertical polarized light. For example horizontal and vertical polarized light in a Voight configuration correspond with: polarizations $\Pi^y_{k_x}$ or $\Pi^x_{k_y}$ for horizontal light and $\Pi^z_{k_x}$ or $\Pi^z_{k_y}$ for vertical polarized light. All other possible polarizations and propagation directions are summed in table 3.2.

3.3 Dipole transition rates and selection rules

Transitions are possible for certain polarizations when the matrix element $\langle f|\, \hat{e}_{rad} \cdot \vec{r}\, |i\rangle$ is non-zero. Both for stimulated emission and for excitation the same electric dipole $\vec{\mu}_{if}$ from equation 3.8 determines which transitions are possible. For calculating this matrix element, its useful to express all terms in Y^m_l's. Not only the initial and final state, but also the dipole operator. When expressing the integral in Y^m_l's it is very easy to determine for which values of m and l the integral is non-zero.

Only the angular integral I_{ang} is interesting for determining if this matrix element is non-zero, because the radial integral always gives a non-zero constant. The angular integral I_{ang} from equation 3.11 can be calculated by describing $\hat{r}$ in spherical coordinates.

$$\hat{r} = \frac{1}{r}\left(x\hat{e}_x + y\hat{e}_y + z\hat{e}_z\right) = \sin\theta\cos\phi\hat{e}_x + \sin\theta\sin\phi\hat{e}_y + \cos\theta\hat{e}_z \tag{3.12}$$

Expressing these in spherical harmonics

$$\begin{aligned}
\sin\theta\cos\phi &= \sqrt{\tfrac{2\pi}{3}}\left(Y_1^{-1} - Y_1^1\right) \\
\sin\theta\sin\phi &= i\sqrt{\tfrac{2\pi}{3}}\left(Y_1^{-1} + Y_1^1\right) \\
\cos\theta &= \sqrt{\tfrac{4\pi}{3}}Y_1^0
\end{aligned} \tag{3.13}$$

Writing the angular integral in spherical harmonics for the example of an incoming beam $\Pi^x_{k_z}$ the angular integral becomes

$$\langle f|\, \hat{e}_{rad} \cdot \hat{r}\, |i\rangle \propto \int_\Omega Y^{*m_f}_{l_f}(\theta,\phi)(Y_1^{-1} - Y_1^1)(\theta)Y^{m_i}_{l_i}(\theta,\phi)d\phi d\theta \tag{3.14}$$

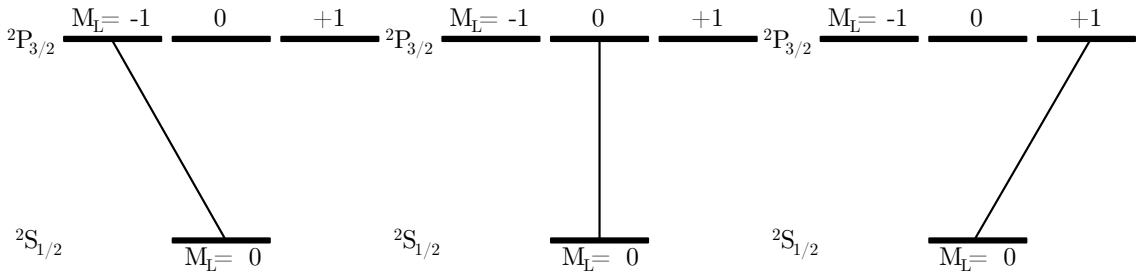

(a) Allowed transitions for q=-1 (b) Allowed transitions for q=0 (c) Allowed transitions for q=+1

Figure 3.2: Possible transitions with dipole coupling between energy states of ${}^2S_{1/2}$ and ${}^2P_{3/2}$. The lines connecting the energy levels represent allowed transitions for both radiation induced absorption and stimulated emission. The ground state and excited states are now indicated with Russel Saunder symbols ${}^2S_{1/2}$ and ${}^2P_{3/2}$. The superscript indicates the multiplicity, the number of possibilities for J. The letters S and P indicates the value for L, respectively 0 and 1 for the ground and excited state. The subscript indicates the value for J, which is the total angular momentum $L + S$.

In general the dipole operator is proportional to Y_l^q with a certain q, or like in the example in equation 3.14 as a sum of Y_l^m's with different q's. Where q is the value for m_l of the incoming beam. For the example in equation 3.14 q has the values ± 1.

$$\int_\Omega Y_{l_f}^{m_f} Y_1^q Y_{l_i}^{m_i} d\phi d\theta \tag{3.15}$$

Selection rules If this integral is non-zero the transition is allowed. With the help of the addition rule [19] of spherical harmonics the integral of three Y_l^q's can be evaluated. The addition rule of spherical harmonics state that the product of two spherical harmonics can be rewritten as a sum of two new spherical harmonics.

$$Y_{l_2}^{m_2} \cdot Y_{l_1}^{m_1} = A Y_{l_1+l_2}^{m_1+m_2} + B Y_{l_1-l_2}^{m_1+m_2} \tag{3.16}$$

And with the help of

$$\int_\Omega Y_{l'}^{m'} Y_l^m d\phi d\theta = \delta_{l',l} \delta_{m',m} \tag{3.17}$$

The angular integral over the three spherical harmonics become

$$\int_\Omega Y_{l_3}^{m_3} Y_{l_2}^{m_2} Y_{l_1}^{m_1} d\phi d\theta = A \delta_{l_3,l_1+l_2} \delta_{m_3,m_1+m_2} + B \delta_{l_3,l_1-l_2} \delta_{m_3,m_1+m_2} \tag{3.18}$$

The integral is non-zero when both of the next statements are agreed

$$\begin{aligned} &\Delta l = l_3 - l_1 = \pm 1 \\ &\Delta m = m_3 - m_1 = q, \text{ with } q = -1, 0 \text{ or } +1. \end{aligned} \tag{3.19}$$

In figure 3.2 is summarized which transitions are allowed for the different polarizations q. The lines connecting the ground level with the excited levels represent both excitations and emissions with that particular polarization. In table 3.2 all possible propagation directions and polarizations of incoming beams with theire corresponding dipole operator expressed in Y_l^q's are summarized.

3.3.1 Selection rules including spin-orbit interaction

When also spin-orbit coupling is considered, described in paragraph 2.4. The number of energy levels increases and also the selection rules have to be adjusted. When the energy states are

Polarization	q	$\hat{r} \cdot \hat{e}_{rad} \propto$	Δl	$\Delta m_l = q$	$^2S_{1/2} \Leftrightarrow ^2 P_{3/2}$
$\Pi^z_{k_x,k_y}$	0	$Y_1^0(\theta)$	± 1	0	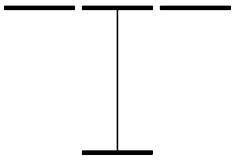
$\Pi^x_{k_z,k_y}$	± 1	$Y_1^{-1}(\theta) - Y_1^1(\theta)$	± 1	± 1	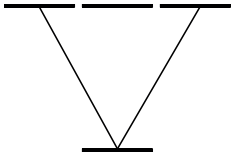
$\Pi^y_{k_x,k_z}$	± 1	$Y_1^{-1}(\theta) + Y_1^1(\theta)$	± 1	± 1	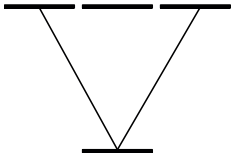
$\sigma^-_{k_z}$	-1	$Y_1^{-1}(\theta, \phi)$	± 1	-1	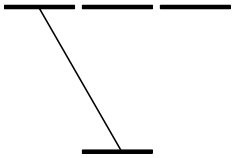
$\sigma^+_{k_z}$	$+1$	$Y_1^{+1}(\theta, \phi)$	± 1	$+1$	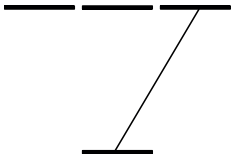
$\sigma^-_{k_y}$	$0, \pm 1$	$Y_1^{-1}(\theta, \phi) - Y_1^1(\theta, \phi) - Y_1^0(\theta, \phi)$	± 1	$0, \pm 1$	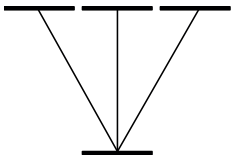
$\sigma^+_{k_y}$	$0, \pm 1$	$Y_1^{-1}(\theta, \phi) - Y_1^1(\theta, \phi) + Y_1^0(\theta, \phi)$	± 1	$0, \pm 1$	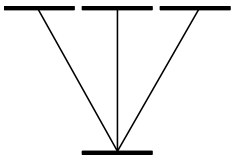
$\sigma^-_{k_x}$	$0, \pm 1$	$Y_1^{-1}(\theta, \phi) + Y_1^1(\theta, \phi) - Y_1^0(\theta, \phi)$	± 1	$0, \pm 1$	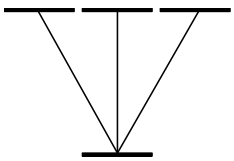
$\sigma^+_{k_x}$	$0, \pm 1$	$Y_1^{-1}(\theta, \phi) + Y_1^1(\theta, \phi) + Y_1^0(\theta, \phi)$	± 1	$0, \pm 1$	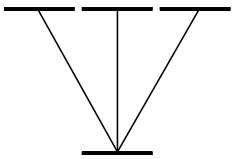

Table 3.2: Possible transitions, excitations and emissions for all different polarizations and propagation directions

described in the basis $|J, m_J\rangle$, the selection rules are determined like before, by looking at the non-zero transition rates. The transition rate in this new basis is calculated with the matrix element

$$\langle J', m'_J| \hat{e} \cdot \vec{r} |J, m_J\rangle \tag{3.20}$$

Like in the previous paragraph the easiest way to evaluate the transition rates is by first writing every term in Y_l^m's. To be able to write the eigenstates $|l, s, J, m_J\rangle$ a basis transformation to $|Lm_L\rangle |Sm_S\rangle$ is needed [20]. The physical idea why a basis transformation is needed here, is that the driving field only couples to the orbital part of the state. Transitions can take place between two energy levels where the electron spin stay unchanged. So for states in the $|J, m_J\rangle$ basis the underlying states in the $|m_L, m_S\rangle$ are of importance. As described in equation 2.5 the $|J, m_J\rangle$ states are a superposition of $|m_L, m_S\rangle$ states. These transitions with keeping the electron spin unchanged can however induce a electron spin flip, because the electron in the excited state can spontaneously fall back into a different spin state. This is made more clear in paragraph 3.4

Basis transformation Spin orbit coupling Starting with writing out the Clebsch-Gordan coefficients from equation 2.5 [21].

$$C^j_{m_L m_S} = \langle LM_L SM_S\, |JM_J\rangle = (-1)^{-L+S-M_J} \sqrt{2J+1} \begin{pmatrix} L & S & J \\ L_L & M_S & -M_J \end{pmatrix} \tag{3.21}$$

Here the Clebsch-Constant is written in the form of a Wigner 3j symbol, which can be computed using the Racah formula which results in a single value (at the website of MathWorld [22] the explicit calculations are shown). Plugging this basis transformation twice in equation 3.20, once for the bra, once for the ket and recombine the two Wigner 3j symbols into one Wigner 6j and one 3j the result is [23]

$$\begin{aligned} \mu_{eg} &= e(-1)^{L'+S-M'_J} \sqrt{(2J+1)(2J'+1)} \\ &\times \begin{Bmatrix} L' & J' & S \\ J & L & 1 \end{Bmatrix} \begin{pmatrix} J & 1 & J' \\ M_J & q & -M'_J \end{pmatrix} \langle \alpha' L'| \, |r| \, |\alpha L\rangle \end{aligned} \tag{3.22}$$

where the last part $\langle \alpha' L'| \, |r| \, |\alpha L\rangle$ is the radial integral which will give an extra constant factor just like described for equation 3.10. The matrix with round brackets is the Wigner 3j symbol again and the matrix with the curly brackets is the Wigner 6j symbol. For both matrices there are rules for which these give nonzero results. The general form for the Wigner 3j symbol is

$$\begin{pmatrix} j_1 & j_2 & j_3 \\ m_1 & m_2 & m_3 \end{pmatrix} \tag{3.23}$$

There are 4 rules which apply for Wigner 3j symbols, wherefore it is nonzero [22]:

$$\begin{aligned} &\text{rule 1}: \quad m_1 + m_2 + m_3 = 0 \\ &\text{rule 2}: \quad j_1 + j_2 + j_3 \text{ has to be integer,} \\ &\qquad\quad \text{but when } m_1 = m_2 = m_3 = 0,\ j_1 + j_2 + j_3 \text{ has to be an even integer} \\ &\text{rule 3}: \quad |m_i| \leq j_i \\ &\text{rule 4}: \quad |j_1 - j_2| \leq j_3 \leq j_1 + j_2 \end{aligned} \tag{3.24}$$

The general form of the Wigner 6j symbol can be written as

$$\begin{Bmatrix} j_1 & j_2 & j_3 \\ J_1 & J_2 & J_3 \end{Bmatrix} \tag{3.25}$$

The Wigner 6j can be split up into four triads [24], which have to obey two rules for which the Wigner 6j symbol is nonzero. The four triads are (j_1, j_2, j_3), (j_1, J_2, J_3), (J_1, j_2, J_3) and (J_1, J_2, j_3). The rules are

$$\begin{aligned} &\text{rule 1} \quad \text{the elements in each triad } (x_1, x_2, x_3) \text{ have to satisfy the triangle rule:} \\ &\qquad\quad |x_1 - x_2| \leq x_3 \leq x_1 + x_2 \\ &\text{rule 2} \quad \text{sum over the elements in a triad has to be an integer} \end{aligned} \tag{3.26}$$

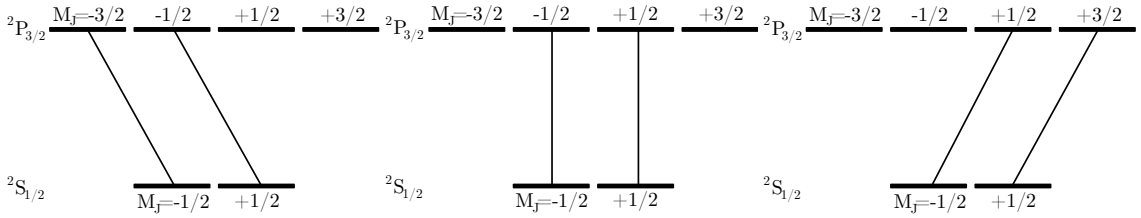

(a) Allowed transitions for q=-1 (b) Allowed transitions for q=0 (c) Allowed transitions for q=+1

Figure 3.3: Possible transitions between the energy states of $^2S_{1/2}$ and $^2P_{3/2}$. The lines connecting the energy states represent the allowed transitions for both excitation and stimulated emission for an incoming beam with a polarization q. The ground state has now two possible states, namely states corresponding with electron spin up and down. The excited state exist of four possible spin states, corresponding with the four different possibilities of the projection of $J = 3/2$.

Selection rules spin-orbit coupling Filling in the quantum numbers for the states in the energy levels $^2S_{1/2}$ and $^2P_{3/2}$ in the rules for the Wigner 3j and 6j symbols, the selection rules for possible transitions are determined. Rules derived from the Wigner 3j symbol:

$$\begin{array}{ll} \text{rule 1}: & M_J - M'_J = -q \\ \text{rule 2}: & J + 1 + J' \text{ has to be integer} \\ \text{rule 3}: & M_J \leq J \\ & q \leq 1 \\ & |-M'_J| \leq J' \\ \text{rule 4}: & |J-1| \leq J' \leq J+1 \end{array} \tag{3.27}$$

rules derived from the Wigner 6j symbol:

$$\begin{array}{ll} \text{rule 1} & |L'-J'| \leq S \leq L'+J' \\ & |L'-L| \leq 1 \leq L'+L \\ & |J-J'| \leq 1 \leq J+J' \\ & |J-L| \leq S \leq J+L \\ \text{rule 2} & \text{sum over the elements in a triad has to be an integer} \end{array} \tag{3.28}$$

Possible transitions derived from the Wigner symbols for different polarizations q are drawn in figure 3.4. The result for different polarizations and propagation directions of an incoming beam are given in table 3.3.

3.3.2 Selection rules including hyperfine interaction

When the atomic states are described in the basis $|F, m_F\rangle$, the selection rules are determined like before, by looking at the non-zero transition rates. The transition rates in this new basis is calculated as follows

$$\mu_{fi} = \langle F', m'_F | \, \hat{e} \cdot \vec{r} | F, m_F \rangle \tag{3.29}$$

Like in the previous paragraphs the easiest way to evaluate the transition rates is by first write every term in Y_l^m's. To be able to write the eigenstates $|F, m_F\rangle$ a basis transformation to $|Lm_L\rangle \, |Sm_S\rangle$ results in [23].

$$\begin{aligned} \mu_{fi} &= e(-1)^{1+L'+S+J+J'+I-M_F} \sqrt{(2J+1)(2J'+1)(2F+1)(2F'+1)} \\ &\times \begin{Bmatrix} L' & J' & S \\ J & L & 1 \end{Bmatrix} \begin{Bmatrix} J' & F' & I \\ F & J & 1 \end{Bmatrix} \begin{pmatrix} F & 1 & F' \\ M_F & q & -M'_F \end{pmatrix} \langle \alpha' L' | \, |r| \, | \alpha L \rangle \end{aligned} \tag{3.30}$$

where the last part the radial integral which will give an extra constant factor like equation 3.10. The Wigner 3j matrix here is in the same form as the one in the basis transformation in equation

Polarization	q	Δl	ΔJ	Δm_l	Δ_{m_J}	$^2S_{1/2} \Leftrightarrow ^2P_{3/2}$
$\Pi^z_{k_x,k_y}$	0	± 1	0,± 1	0	0	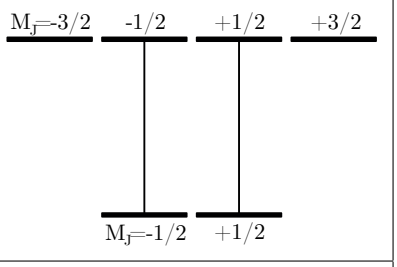
$\Pi^x_{k_z,k_y}$,$\Pi^y_{k_x,k_z}$	± 1	± 1	0,± 1	± 1	± 1	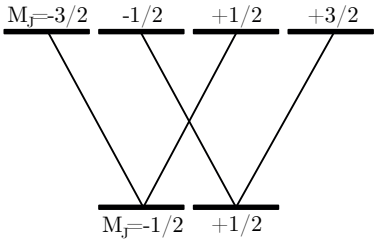
$\sigma^-_{k_z}$	-1	± 1	0,± 1	-1	-1	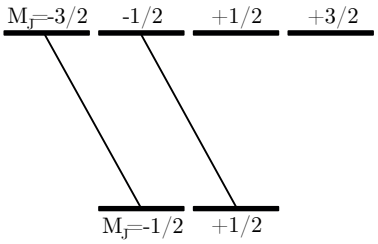
$\sigma^+_{k_z}$	$+1$	± 1	0,± 1	$+1$	$+1$	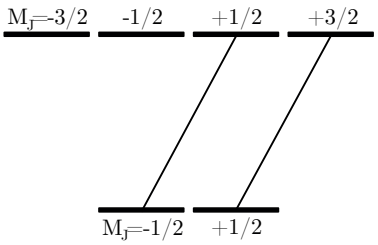
$\sigma^-_{k_y}$,$\sigma^+_{k_y}$,$\sigma^-_{k_x}$,$\sigma^+_{k_x}$	$0, \pm 1$	± 1	0,± 1	$0, \pm 1$	$0, \pm 1$	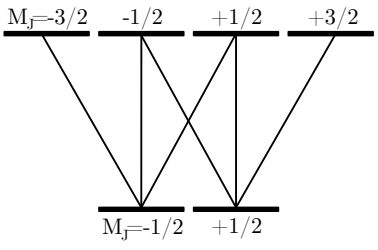

Table 3.3: Summary of all possible transitions, excitations and emissions for all different polarizations and propagation directions including spin-orbit coupling. The dipole coupling term operators are the same as summed in table 3.2. The diagrams are a combination of the diagrams in figure 3.3.

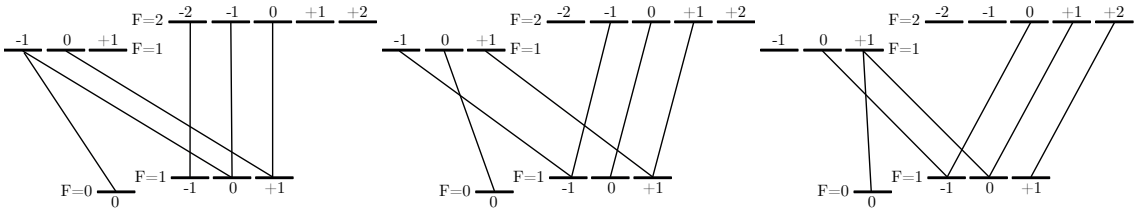

(a) Allowed transitions for q=-1 (b) Allowed transitions for q=0 (c) Allowed transitions for q=+1

Figure 3.4: Possible transitions between the energy states of ${}^2S_{1/2}$ and ${}^2P_{3/2}$. The lines connecting the energy states represent the allowed transitions for both excitation and stimulated emission for an incoming beam with a polarization q. These schemes are made for the simple case where $I = 1/2$. For the ground state the total angular momentum F can take two values, namely $F = |I - S| = 0$ and $F = I + S = 1$. For the excited state the possible values for F are $|I - J| = 1$ and $I + J = 2$. For each F there are $2F + 1$ degenerate states.

3.22, so the rules are also in the same form

$$\begin{aligned}
&\text{rule 1}: && M_F - M'_F = -q \\
&\text{rule 2}: && F + 1 + F' \text{ has to be integer} \\
& && \text{but when } M_F = M'_F = q = 0,\ F + 1 + F' \text{ has to be an even integer} \\
&\text{rule 3}: && M_F \leq F \\
& && q \leq 1 \\
& && |-M'_F| \leq F' \\
&\text{rule 4}: && |F - 1| \leq F' \leq F + 1
\end{aligned} \tag{3.31}$$

The first of the two Wigner 6j matrices is exactly the same as the one in the basis transformation from JM_J to SM_S in equation 3.22. The rules that apply are the same

$$\begin{aligned}
&\text{rule 1}: && |L' - J'| \leq S \leq L' + J' \\
& && |L' - L| \leq 1 \leq L' + L \\
& && |J - J'| \leq 1 \leq J + J' \\
& && |J - L| \leq S \leq J + L \\
&\text{rule 2}: && \text{sum over the elements in a triad has to be an integer}
\end{aligned} \tag{3.32}$$

The rules for the second Wigner 6j matrix can be found by replacing the elements from the first matrix. The triads and rules can be found by replacing the elements $L, L'J, J', S$ with respectively J, J', F, F', I. The triads become (L', J', S), $(J', J, 1)$, $(F, F', 1)$ and (F, J, I) the rules for getting nonzero values become

$$\begin{aligned}
&\text{rule 1}: && |J' - F'| \leq I \leq J' + F' \\
& && |J' - J| \leq 1 \leq J' + J \\
& && |F - F'| \leq 1 \leq F + F' \\
& && |F - J| \leq I \leq F + J \\
&\text{rule 2}: && \text{sum over the elements in a triad has to be an integer}
\end{aligned} \tag{3.33}$$

Possible transitions for different q's are drawn in figure 3.4. There are some interesting forbidden transitions to note. The transitions between $F = 0$ and $F = 2$ states are not possible because of the rule 2 and 4 for the Wigner 3j matrix. In diagram 3.4b, the transition from $F = 1$, $M_F = 0$ to $F' = 1$, $M'_F = 0$ is not possible, because of rule 2 for the Wigner 3j. The result of all possible transitions for different polarizations and propagation directions are summed in 3.4. For the simple system coupled to one nucleus with spin 1/2, all polarizations and propagation directions the selection rules are summarized in table 3.4, the schemes are combinations of the schemes in figure 3.4.

Polarization	q	ΔJ	ΔF	ΔM_F	$^2S_{1/2} \Leftrightarrow ^2 P_{3/2}$
$\Pi^z_{k_x,k_y}$	0	0,±1	$0,\pm1$	0	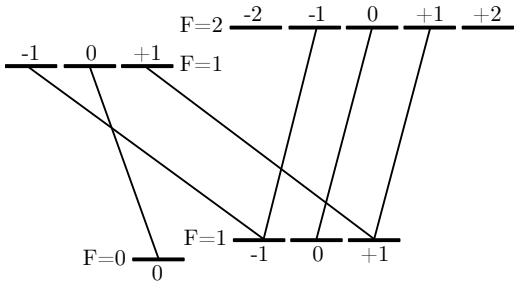
$\Pi^x_{k_z,k_y}$,$\Pi^y_{k_x,k_z}$	±1	$0,\pm1$	$0,\pm1$	±1	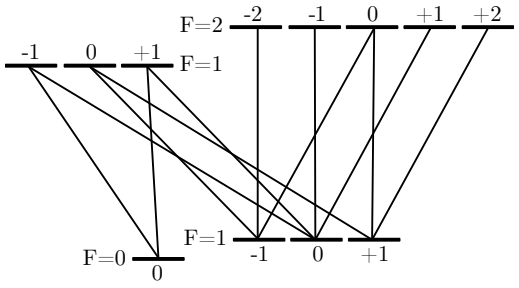
$\sigma^-_{k_z}$	-1	$0,\pm1$	$0,\pm1$	-1	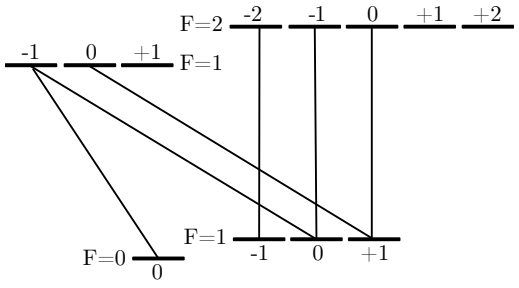
$\sigma^+_{k_z}$	$+1$	$0,\pm1$	$0,\pm1$	$+1$	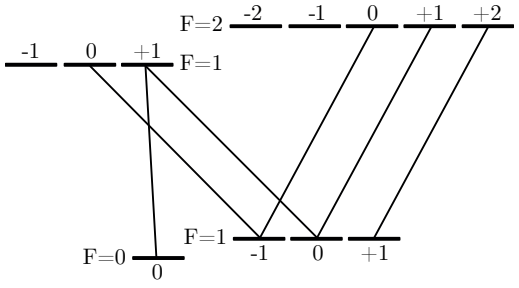
$\sigma^-_{k_y}$,$\sigma^+_{k_y}$,$\sigma^-_{k_x}$,$\sigma^+_{k_x}$	$0,\pm1$	$0,\pm1$	$0,\pm1$	$0,\pm1$	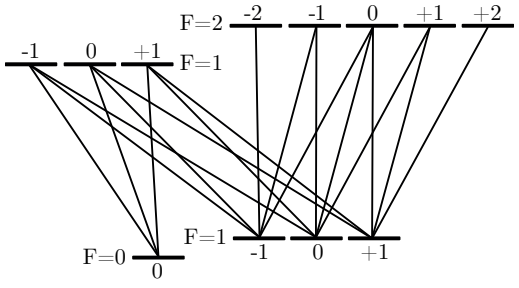

Table 3.4: Summary of all possible transitions, excitations and emissions for all different polarizations and propagation directions including Hyperfine structure. The dipole coupling operators are the same as summed in table 3.2. The diagrams are combinations of the diagrams in figure 3.4.

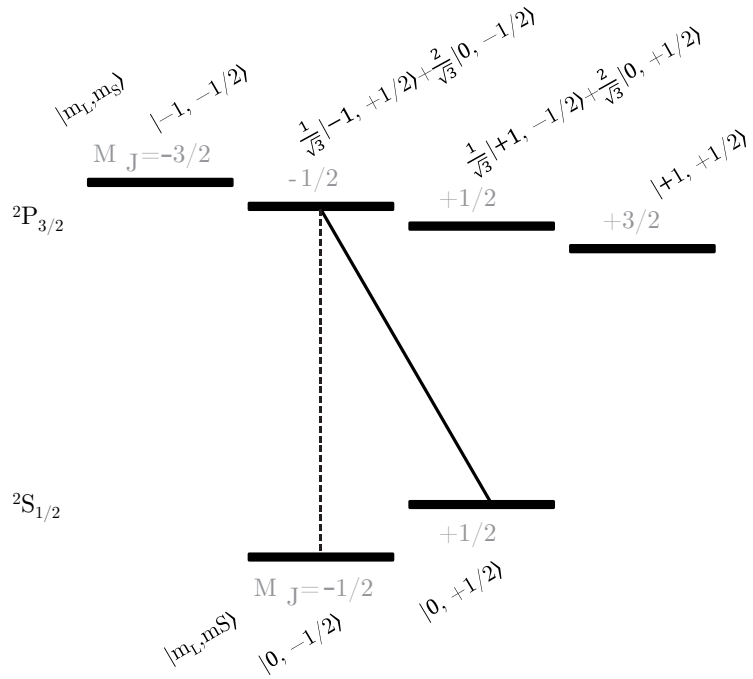

Figure 3.5: Demonstration of electron spin flip, by optically pumping electron population to the excited state, due to spontaneous emission, here indicated with a dashed line, the electron population will fall back to the ground state with electron spin down. Excitation happens in this diagram with a $q = -1$-polarization.

3.4 Conclusion

In figure 3.5 the states m_J are with the help of equation 3.21 written in the individual projections m_L and m_S. With the help of this figure it can be illustrated in what way an electron spin can be flipped by pumping electron population to the excited state. Transitions can be made between energy levels where the spin state is unchanged. Looking at figure 3.5 allowed transitions are sketched for a $q = -1$-polarization. When applying an external magnetic field the different spin states will be split relative to each other, and is possible to selectively couple to the to state from the ground state level with electron spin up and the excited state with projection $m_J = -1/2$. The coupling between the ground state $m_J = -1/2$ and the excited state $m_J = -3/2$ is also allowed, but because of the Zeeman splitting these levels have a bigger energy separation and are off resonance. The coupling between the $m_J = +1/2$ and $m_J = -1/2$ is allowed because the excited state is a superposition of two electron spin projections, spin up and spin down with a certain amplitude given by the Clebsch-Gordan constant, here $\frac{1}{\sqrt{3}}|-1, +1/2\rangle + \frac{2}{\sqrt{3}}|0, -1/2\rangle$, so because of the fraction with spin up there is a coupling possible where the spin is unchanged. The population can decay via spontaneous emission to the ground state level which contains the electron spin down state. So although a coupled electric field only couples with the electric charge of the electrons, the electron spin can be changed indirectly with the help of spontaneous emission. Electron spins can also be flipped without spontaneous emission, by coupling a second laser to the system between the two ground states and the same excited state $m_J = -1/2$. This technique is called Coherent Population Trapping CPT, which make use of the so called dark state (see reference [25] for a nice introduction). Flipping an nuclear spin with the help of optical pumping will be worked out in detail in chapter 6.

Chapter 4

Mixing of spin states

4.1 Introduction

At zero field states are well described with the quantum numbers F, m_F, they are in pure $|F, m_F\rangle$ states. At zero field these states can with the help of Clebsch-Gordan coefficients be described in basis factors $|m_J, m_I\rangle$ (see equation 2.5). At the high field limit the states are in pure $|m_J, m_I\rangle$ states. In intermediate fields there is a continues transition between the two descriptions. States cannot be described with pure $|F, m_F\rangle$ or $|m_J, m_I\rangle$ states, but they can be described with those states with field depending Clebsch-Gordan coefficients in front. In this chapter an example is worked out for a donor-bound electron coupled with hyperfine coupling to one nuclear spin 1/2. The concepts from chapter 2 are combined to construct an magnetic field depending energy diagram. With this example the field dependent mixing of states will be illustrated.

4.2 Construction of field depending energy diagrams

The expectation values for the Hamiltonian for the ground state D^0 coupled with one nuclear spin 1/2 are worked out. For the electron in the ground state D^0 coupled to one nucleus with spin $I = 1/2$, the orbital angular momentum $L = 0$, the total angular momentum $F = |I-J|, ..., I+J = 0, 1$ and $J = S = 1/2$. The possible eigenstates in the $|F, m_F\rangle$ basis are $|0, 0\rangle$, $|1, -1\rangle$, $|1, 0\rangle$ and $|1, +1\rangle$. The possible eigenstates of this system in the $|m_I, m_J\rangle$ basis are $|-1/2, -1/2\rangle$, $|-1/2, +1/2\rangle$, $|+1/2, -1/2\rangle$ and $|+1/2, +1/2\rangle$.

Including the Zeeman term and the hyperfine interaction term in the Hamiltonian from equations 2.36 and 2.21.

$$H_{hf} + H_Z = \mathcal{A}\vec{I} \cdot \vec{J} - \omega_0 \left(g_J J_z + g_I I_z\right) \tag{4.1}$$

The operators in the Zeeman term are diagonal in the $|J, m_J\rangle$ basis and the Hyperfine interaction operator is diagonal in the $|F, m_F\rangle$ basis. The eigenvalues of these operators can be expressed in either one of these bases, which results in diagonal elements from the operators with eigenvalues diagonal in that basis and off diagonal elements from the operators with eigenvalues diagonal in the other basis. To diagonalize this Hamiltonian a new basis has to be constructed from the excising basis states.

First the expectation values will be worked out in one of the two bases, where after the terms will be diagonalized with the help of defining a new basis. The eigenstates from different bases are related with the help of Clebsch-Gordan constants. The eigenstates from one basis can be transformed in the other. All basis vectors can now easily be transformed into each other.

$$\left(|m_I, m_J\rangle\right)_m = M \left(|F, m_F\rangle\right)_n \tag{4.2}$$

where M is a $m \times n$ matrix, containing the Clebsch-Gordan constants and $\left(|m_I, m_J\rangle\right)_m$ and $\left(|F, m_F\rangle\right)_n$ are respectively vectors containing m and n elements of the basisvectors $|m_I, m_J\rangle$ and $|F, m_F\rangle$.

For the example in this chapter the transformation for the ground states coupled to one nuclear spin 1/2 looks like

$$\begin{pmatrix} \left|-\frac{1}{2} \quad -\frac{1}{2}\right\rangle \\ \left|-\frac{1}{2} \quad +\frac{1}{2}\right\rangle \\ \left|+\frac{1}{2} \quad -\frac{1}{2}\right\rangle \\ \left|+\frac{1}{2} \quad +\frac{1}{2}\right\rangle \end{pmatrix} = \begin{pmatrix} 0 & 1 & 0 & 0 \\ -\frac{1}{\sqrt{2}} & 0 & \frac{1}{\sqrt{2}} & 0 \\ \frac{1}{\sqrt{2}} & 0 & \frac{1}{\sqrt{2}} & 0 \\ 0 & 0 & 0 & 1 \end{pmatrix} \begin{pmatrix} |0 \quad 0\rangle \\ |1 \quad -1\rangle \\ |1 \quad 0\rangle \\ |1 \quad 1\rangle \end{pmatrix} \tag{4.3}$$

This transformation is needed for calculating the expectation value of the operators which are not diagonal in the basis where is worked in. Working in the basis $|m_J, m_I\rangle$ the Zeeman operators are diagonal. So the eigenvalues of the Zeeman operator are easily found

$$-\omega_0 \left(g_J \hat{J}_z + g_I \hat{I}_z\right) \begin{pmatrix} \left|-\frac{1}{2} \quad -\frac{1}{2}\right\rangle \\ \left|-\frac{1}{2} \quad +\frac{1}{2}\right\rangle \\ \left|+\frac{1}{2} \quad -\frac{1}{2}\right\rangle \\ \left|+\frac{1}{2} \quad +\frac{1}{2}\right\rangle \end{pmatrix} = \begin{pmatrix} -\frac{\hbar\omega_0}{2}\left(-g_J - g_I\right)\left|-\frac{1}{2} \quad -\frac{1}{2}\right\rangle \\ -\frac{\hbar\omega_0}{2}\left(-g_J + g_I\right)\left|-\frac{1}{2} \quad +\frac{1}{2}\right\rangle \\ -\frac{\hbar\omega_0}{2}\left(+g_J - g_I\right)\left|+\frac{1}{2} \quad -\frac{1}{2}\right\rangle \\ -\frac{\hbar\omega_0}{2}\left(+g_J + g_I\right)\left|+\frac{1}{2} \quad +\frac{1}{2}\right\rangle \end{pmatrix} \tag{4.4}$$

To calculate the eigenvalues of the hyperfine interaction operators, the basis transformation worked out in equation 4.3, is needed. With the help of equation 2.25 the eigenvalues of the hyperfineinteraction can be calculated.

$$\begin{aligned} \mathcal{A}\hat{I}\cdot\hat{J} \begin{pmatrix} \left|-\frac{1}{2} \quad -\frac{1}{2}\right\rangle \\ \left|-\frac{1}{2} \quad +\frac{1}{2}\right\rangle \\ \left|+\frac{1}{2} \quad -\frac{1}{2}\right\rangle \\ \left|+\frac{1}{2} \quad +\frac{1}{2}\right\rangle \end{pmatrix} &= \mathcal{A}\hat{I}\cdot\hat{J} \begin{pmatrix} |0 \quad -1\rangle & & \\ -\frac{1}{\sqrt{2}}|0 \quad 0\rangle & +\frac{1}{\sqrt{2}}|1 \quad 0\rangle & \\ +\frac{1}{\sqrt{2}}|0 \quad 0\rangle & +\frac{1}{\sqrt{2}}|1 \quad 0\rangle & \\ |1 \quad +1\rangle & & \end{pmatrix} \\ &= \begin{pmatrix} +\frac{1}{4}\mathcal{A}\hbar^2|0 \quad -1\rangle & & \\ +\frac{3}{4\sqrt{2}}\mathcal{A}\hbar^2|0 \quad 0\rangle & +\frac{1}{4\sqrt{2}}\mathcal{A}\hbar^2|1 \quad 0\rangle & \\ -\frac{3}{4\sqrt{2}}\mathcal{A}\hbar^2|0 \quad 0\rangle & +\frac{1}{4\sqrt{2}}\mathcal{A}\hbar^2|1 \quad 0\rangle & \\ +\frac{1}{4}\mathcal{A}\hbar^2|1 \quad +1\rangle & & \end{pmatrix} \end{aligned} \tag{4.5}$$

To express these eigenvalues in $|m_J, m_I\rangle$ the inverse transformation from equation 4.3 is needed. After applying the inverse transformation the end result will be

$$\mathcal{A}\hat{I}\cdot\hat{J} \begin{pmatrix} \left|-\frac{1}{2} \quad -\frac{1}{2}\right\rangle \\ \left|-\frac{1}{2} \quad +\frac{1}{2}\right\rangle \\ \left|+\frac{1}{2} \quad -\frac{1}{2}\right\rangle \\ \left|+\frac{1}{2} \quad +\frac{1}{2}\right\rangle \end{pmatrix} = \begin{pmatrix} +\frac{1}{4}\mathcal{A}\hbar^2\left|-\frac{1}{2} \quad -\frac{1}{2}\right\rangle \\ +\frac{1}{4}\mathcal{A}\hbar^2\left[-1\left|-\frac{1}{2} \quad +\frac{1}{2}\right\rangle + 2\left|+\frac{1}{2} \quad -\frac{1}{2}\right\rangle\right] \\ +\frac{1}{4}\mathcal{A}\hbar^2\left[+2\left|-\frac{1}{2} \quad +\frac{1}{2}\right\rangle - 1\left|+\frac{1}{2} \quad -\frac{1}{2}\right\rangle\right] \\ +\frac{1}{4}\mathcal{A}\hbar^2|+1/2 \quad +1/2\rangle \end{pmatrix} \tag{4.6}$$

The eigenvalues for both the Zeeman and the hyperfine interaction operators are now calculated in the $|m_J, m_I\rangle$ basis. Calculating the expectation values of these two terms in the Hamiltonian is now possible

$$\langle m_J, m_I| \left(-\omega_0 \left(g_J \hat{J}_z + g_I \hat{I}_z\right) + \mathcal{A}\hat{I}\cdot\hat{J}\right) |m_J, m_I\rangle \tag{4.7}$$

When putting the expectation values in a matrix with the bra's $\langle m_J, m_I|$ put horizontal and the kets $|m_J, m_I\rangle$ vertical in the order $\left|-\frac{1}{2} \quad -\frac{1}{2}\right\rangle$, $\left|-\frac{1}{2} \quad +\frac{1}{2}\right\rangle$, $\left|+\frac{1}{2} \quad -\frac{1}{2}\right\rangle$, $\left|+\frac{1}{2} \quad +\frac{1}{2}\right\rangle$, this

is nicely illustrated.

$$\begin{pmatrix} -\frac{\hbar\omega_0}{2}(-g_J-g_I)+\frac{1}{4}\mathcal{A}\hbar^2 & 0 \\ 0 & -\frac{\hbar\omega_0}{2}(-g_J+g_I)-\frac{1}{4}\mathcal{A}\hbar^2 \\ 0 & +\frac{2}{4}\mathcal{A}\hbar^2 \\ 0 & 0 \end{pmatrix}$$

$$\begin{pmatrix} 0 & 0 \\ +\frac{2}{4}\mathcal{A}\hbar^2 & 0 \\ -\frac{\hbar\omega_0}{2}(+g_J-g_I)-\frac{1}{4}\mathcal{A}\hbar^2 & 0 \\ 0 & -\frac{\hbar\omega_0}{2}(+g_J+g_I)+\frac{1}{4}\mathcal{A}\hbar^2 \end{pmatrix} \tag{4.8}$$

Because the hyperfine interaction operator changes the state when working on the $|J, m_J\rangle$ states, as can seen in equation 4.6, the matrix from equation 4.8 containing the expectation values, has off-diagonal elements. The expectation values of the Zeeman terms only appear on the diagonal. This matrix can be diagonalized by defining a new basis $|\Psi_{new}\rangle = \left(\alpha\left|-\frac{1}{2}+\frac{1}{2}\right\rangle + \beta\left|+\frac{1}{2}-\frac{1}{2}\right\rangle\right)$. Diagonalizing this matrix by determining the eigenvalues of the matrix by solving $det\left[Matrix(4x4) - \lambda I_4\right] = 0$ for the eigenvalues lambda. The diagonalized matrix with expectation values looks like

$$\begin{pmatrix} -\frac{\hbar\omega_0}{2}(-g_J-g_I)+\frac{1}{4}\mathcal{A}\hbar^2 & 0 \\ 0 & -\frac{\hbar\omega_0}{2}(+g_J+g_I)+\frac{1}{4}\mathcal{A}\hbar^2 \\ 0 & 0 \\ 0 & 0 \end{pmatrix}$$

$$\begin{pmatrix} 0 & 0 \\ 0 & 0 \\ \frac{1}{4}\left(-\mathcal{A}\hbar^2 - 2\sqrt{\mathcal{A}^2\hbar^4 + \left[(g_I-g_J)\hbar\omega_0\right]^2}\right) & 0 \\ 0 & \frac{1}{4}\left(-\mathcal{A}\hbar^2 + 2\sqrt{\mathcal{A}^2\hbar^4 + \left[(g_I-g_J)\hbar\omega_0\right]^2}\right) \end{pmatrix} \tag{4.9}$$

Plotting these eigenvalues gives the field dependent energy diagram in figure 4.1. At zero field the offset is due to hyperfine interaction. With increasing external magnetic field the energy levels converge into two bundles. These two bundles are the Zeeman split projections of the electron spin $m_J = m_S$ up and down. The splitting between the two sub levels in the two overall bundles is due to the different nuclear spin projections. This energy splitting is given by equation 2.43. The two straight lines are from the two diagonal terms in the matrix from equation 4.8 the two hyperbola functions are from the coupled states due to off diagonal elements. In paragraph 4.3 is explained that these hyperbola functions are due to field dependent mixing of the two coupled spin states.

4.3 Field dependent mixing of spin states

For explaining the field dependent mixing of states, a closer look at the diagonalization process is needed. When the Hamiltonian operates on the new defined basis state, the eigenvalue equation is in the from

$$\begin{aligned} \hat{H}\left|\Psi_{new}\right\rangle &= \lambda\left|\Psi_{new}\right\rangle \\ \hat{H}\left(\alpha\left|-\tfrac{1}{2}+\tfrac{1}{2}\right\rangle + \beta\left|+\tfrac{1}{2}-\tfrac{1}{2}\right\rangle\right) &= \lambda\left(\alpha\left|-\tfrac{1}{2}+\tfrac{1}{2}\right\rangle + \beta\left|+\tfrac{1}{2}-\tfrac{1}{2}\right\rangle\right) \end{aligned} \tag{4.10}$$

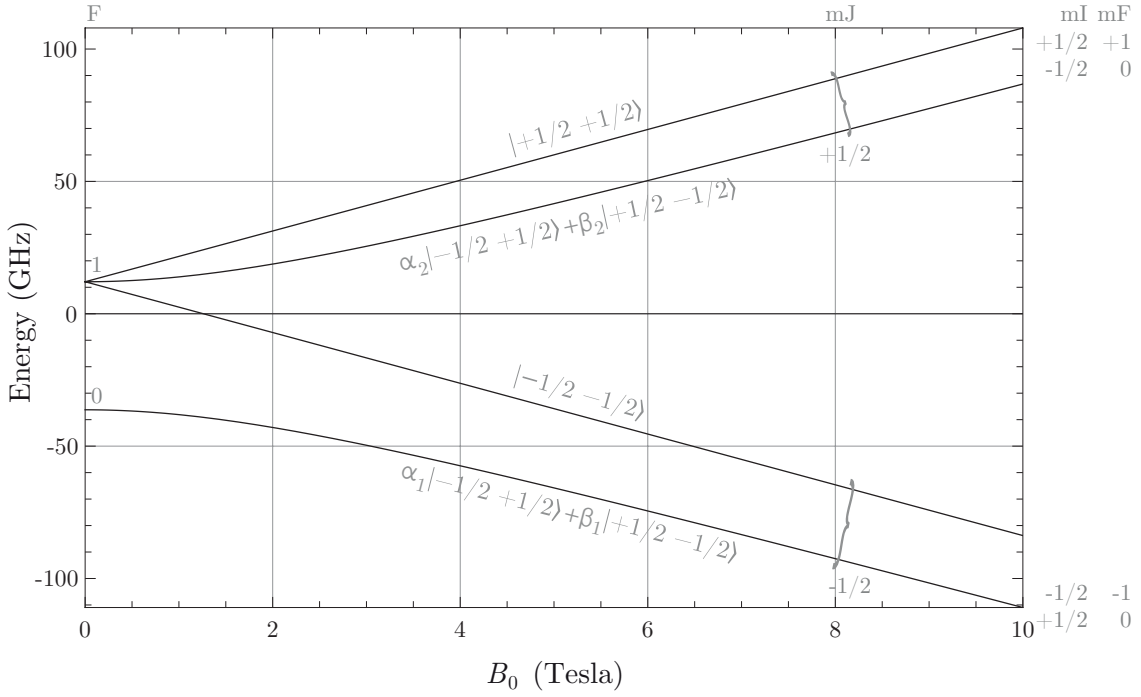

Figure 4.1: Field dependent energy diagram of the ground state D^0 coupled to one nucleus with spin 1/2. Parameters for ZnSe from section 5.3.1 are used. Further explanation about these energy diagrams can be found in chapter 5

The eigenvalues are given by the equations 4.4 and 4.5. Filling these eigenvalues for the Hamiltonian operator acting on the new basis eigenstates in equation 4.10

$$\begin{aligned}\hat{H}\left|\Psi_{new}\right\rangle &= \alpha\left[\ \left(-\tfrac{\hbar\omega_0}{2}\left(-g_J+g_I\right)-\tfrac{1}{4}\mathcal{A}\hbar^2\right)\left|-\tfrac{1}{2}\quad+\tfrac{1}{2}\right\rangle+\tfrac{2}{4}\mathcal{A}\hbar^2\left|+\tfrac{1}{2}\quad-\tfrac{1}{2}\right\rangle\ \right]\\ &+\beta\left[\ \left(+\tfrac{2}{4}\mathcal{A}\hbar^2\right)\left|-\tfrac{1}{2}\quad+\tfrac{1}{2}\right\rangle+\left(-\tfrac{\hbar\omega_0}{2}\left(+g_J-g_I\right)-\tfrac{1}{4}\mathcal{A}\hbar^2\right)\left|+\tfrac{1}{2}\quad-\tfrac{1}{2}\right\rangle\ \right]\end{aligned} \tag{4.11}$$

The constants alpha and beta will be the field dependent mixing amplitudes. Alpha is the measure for the amount of spin state $\left|-\frac{1}{2}+\frac{1}{2}\right\rangle$. Grouping the terms for each state from equation 4.11

$$\begin{aligned}\hat{H}\left|\Psi_{new}\right\rangle &= \left[-\tfrac{\hbar\omega_0}{2}\left(-g_J+g_I\right)-\tfrac{1}{4}\mathcal{A}\hbar^2+\tfrac{2\beta}{4\alpha}\mathcal{A}\hbar^2\right]\alpha\left|-\tfrac{1}{2}\quad+\tfrac{1}{2}\right\rangle\\ &+\left[-\tfrac{\hbar\omega_0}{2}\left(+g_J-g_I\right)-\tfrac{1}{4}\mathcal{A}\hbar^2+\tfrac{2\alpha}{4\beta}\mathcal{A}\hbar^2\right]\beta\left|+\tfrac{1}{2}\quad-\tfrac{1}{2}\right\rangle\\ &=\lambda\left(\alpha\left|-\tfrac{1}{2}+\tfrac{1}{2}\right\rangle+\beta\left|+\tfrac{1}{2}-\tfrac{1}{2}\right\rangle\right)\end{aligned} \tag{4.12}$$

Here both terms in front of alpha and beta equals lambda and thus equals each other

$$\left[-\frac{\hbar\omega_0}{2}\left(-g_J+g_I\right)-\frac{1}{4}\mathcal{A}\hbar^2+\frac{2\beta}{4\alpha}\mathcal{A}\hbar^2\right]=\left[-\frac{\hbar\omega_0}{2}\left(+g_J-g_I\right)-\frac{1}{4}\mathcal{A}\hbar^2+\frac{2\alpha}{4\beta}\mathcal{A}\hbar^2\right] \tag{4.13}$$

Solving this for alpha gives two solutions for α

$$\begin{aligned}\alpha_1 &= \tfrac{-\hbar\omega_0(g_I-g_J)-\sqrt{\mathcal{A}\hbar^4+\hbar^2\omega_0^2(g_I-g_J)^2}}{\mathcal{A}\hbar}\beta_1\\ \alpha_2 &= \tfrac{-\hbar\omega_0(g_I-g_J)+\sqrt{\mathcal{A}\hbar^4+\hbar^2\omega_0^2(g_I-g_J)^2}}{\mathcal{A}\hbar}\beta_2\end{aligned} \tag{4.14}$$

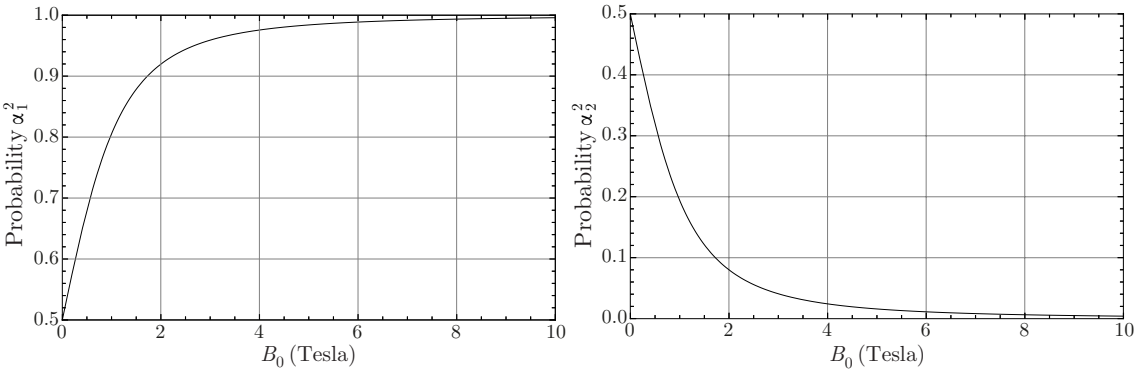

(a) α_1^2 plotted against external magnetic field.

(b) α_2^2 plotted against external magnetic field.

Figure 4.2: The field depending expectation values of the state $|-1/2,+1/2\rangle$ are here plotted. There are two solutions, representing the two different expectation values of the spin state $|-1/2,+1/2\rangle$ in the two mixed energy states in figure 4.1. The hyperfine coupling constant here taken is the total average coupling constant, explained in paragraph 5.2.1.

With the help of the restriction that the probability amplitudes are normalized alpha can be expressed in terms of the ratio $R_i(\omega_0) = \alpha_i/\beta_i$ determined from equation 4.14.

$$\begin{aligned} 1 &= \sqrt{\alpha_i^2 + \beta_i^2} \\ 1 &= \frac{1}{\alpha_i\sqrt{1+\frac{\beta_i^2}{\alpha_i^2}}} \\ \alpha_i &= \frac{1}{\sqrt{1+R_i^{-2}(\omega_0)}} \end{aligned} \tag{4.15}$$

When plotting α_i^2 against the magnetic field B_0, the field dependent percentage of the state $|-1/2,+1/2\rangle$ is visualized in figure 4.2. The hyperbola function indicate the portion of the spin state $|-1/2,+1/2\rangle$. At zero field the mixing is fifty fifty. This is also what is expected, because at zero field the state is described in pure $|F,m_F\rangle$ states. At zero field $|0,0\rangle = \frac{1}{\sqrt{2}}\left|-\frac{1}{2}+\frac{1}{2}\right\rangle - \frac{1}{\sqrt{2}}\left|+\frac{1}{2}-\frac{1}{2}\right\rangle$ and $|1,0\rangle = \frac{1}{\sqrt{2}}\left|-\frac{1}{2}+\frac{1}{2}\right\rangle + \frac{1}{\sqrt{2}}\left|+\frac{1}{2}-\frac{1}{2}\right\rangle$, thus the energy levels described by the two hyperbola in figure 4.1 contain at zero field both an equal amount of the spin states $\left|-\frac{1}{2}+\frac{1}{2}\right\rangle$ and $\left|+\frac{1}{2}-\frac{1}{2}\right\rangle$. For example at 7 Tesla $\alpha_1^2 = 0.991669$ and $\alpha_2^2 = 0.008331$. With increasing field the mixing of states converge to one of the pure $|m_J,m_I\rangle$.

Chapter 5

Calculated levels

5.1 Introduction

In this chapter the energy levels for an electron coupled to different number of nuclei are calculated. Field dependent energy diagrams are constructed, with the help of the Mathematica code in Appendix E. The first system that is worked out is a system where the donor-bound electron couples to nuclei with nuclear spin 3/2. Therefor the values of the g-factors, nuclear spin and hyperfine splitting are taken from a GaAs semiconductor. The second system that is described is a system where the electron couples to nuclei with spin 1/2. Here the g-factors and hyperfine coupling constant of ZnSe are used. Both systems are worked out for different number of nuclei. The diagrams in this thesis uses the total hyperfine coupling, when evaluating the coupling to one or two nuclei, this assumes that all nuclei are coupled, but only the coupling with one or two nuclei are evaluated. Transition schemes with possible transitions between the ground and excited states are constructed, with the help of the Mathematica code in Appendix F. The strongly allowed transitions at low field are weakly allowed at high field and vice versa. These transition diagrams are needed for constructing possible DNP diagrams, which will be constructed in chapter 6.

5.2 Donor electron coupled to nuclei with spin 3/2

5.2.1 Parameters for Si:GaAs

Before starting with the calculations, a short summary of the parameters that are used for the model with nuclear spins 3/2. Parameters of bandstructure GaAs: $E_{SO} \approx 0.34eV \approx 82.2 \cdot 10^3 GHz$ [26], $E_g \approx 1.51eV$ [27].

Hyperfine coupling constants: $A_{hole}\hbar^2 \approx -15\mu eV$ [12], $A_{electron}\hbar^2 \approx +90\mu eV$ [12], [28]. These values for the hyperfine coupling constants are the average over the hyperfine coupling constants for the three nuclear isotopes ^{69}Ga, ^{71}Ga and ^{75}As weighted by theire relative abundances [15]. These values are used for the construction of the field dependent energy diagrams in this chapter. This value is the total hyperfine coupling between the electron and all nuclei. This constant still has to be multiplied with the electron density function squared, as showed in equation 2.20. When dealing with more nuclei coupled the expression in equation 2.20 also needs to be multiplied by the number of nuclei, which is explained in section 2.6.

g-factors GaAs: nuclear g-factor $g_n = \approx 1.3$ [28], electron g-factor $g_e = +0.44$ [29] (free electron $g_e \approx -2$, sign convention used from reference [14]), hole g-factor $g_h = +0.2$[[30], [31]] (Zeeman splitting of the hole energy levels is half that of the electron and the signs of the g-factor are equal).

5.2.2 Donor electron coupled to one nuclear spin 3/2

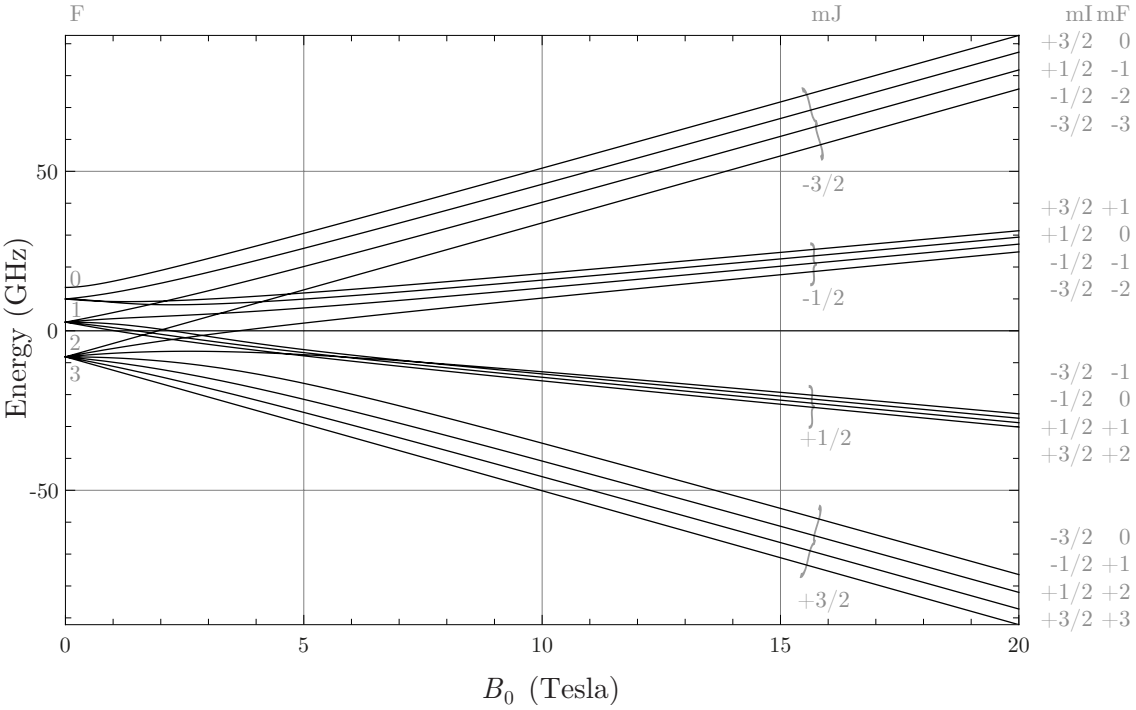

(a) D^0X state of the donor system coupled with one nucleus with spin 3/2

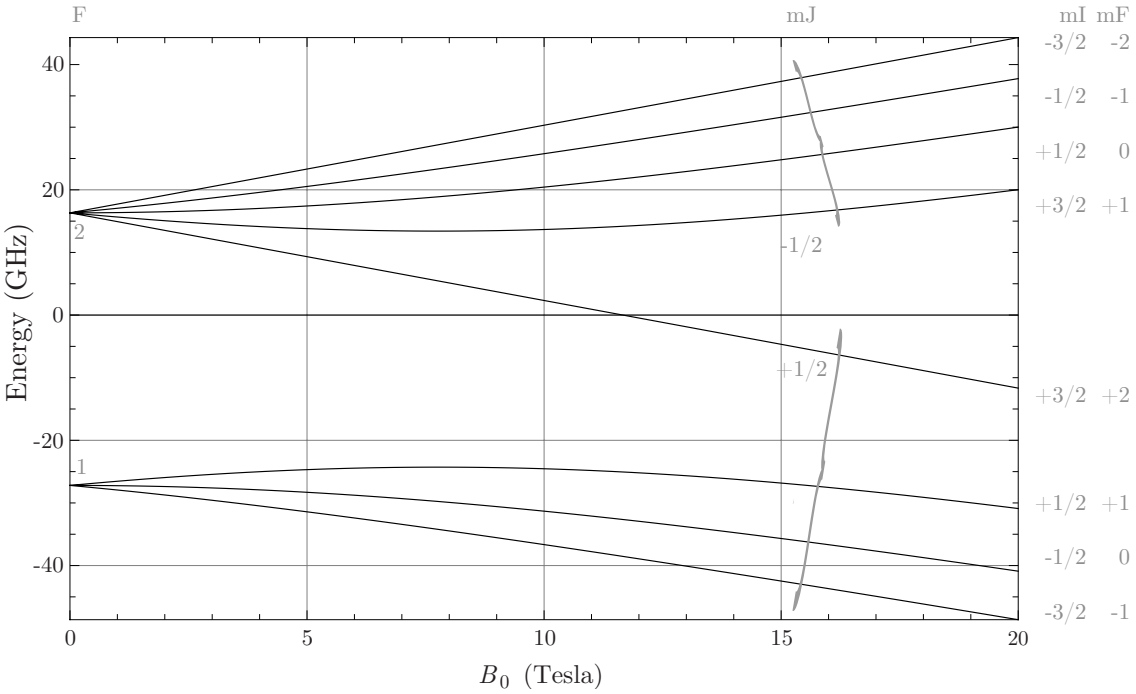

(b) D^0 state of the donor system coupled with one nucleus with spin 3/2

Figure 5.1: System coupled with one nuclear spin 3/2, with the parameters defined in paragraph 5.2.1. For the hyperfine coupling constant, the total average hyperfine coupling constant is taken, which result in bigger splittings in the diagram, than the hyperfine coupling to just 1 nucleus (see discussion in paragraph 5.2.1). The F values for the excited state D^0X are $|I-J|$,...,$I+J$, respectively 0,1,2 and 3. For the ground state D^0 the F values are $I+S$ and $|I-S|$, respectively 2 and 1. The values for m_F are placed at the right side of the diagram, although these numbers are only well defined at zero field. the quantum numbers mJ and m_I are well defined only at the high field limit. See chapter 4 for more details.

Energy diagram in external magnetic field In figures 5.1a and 5.1b the energy levels of the D^0X and D^0 coupled with one nucleus with nuclear spin 3/2 are shown. At zero field the levels are split due to Hyperfine interaction. Each level is $2F+1$ degenerate. When increasing the external magnetic field, the degenerate levels split up. When increasing the field the lines converge into overall bundles. These bundles are due to the Zeeman splitting of the electron/hole projection. With increasing magnetic field the sub levels inside these bundles converge to parallel lines with equal spacing. This holds only if the Zeeman term of the nucleus which is a factor $M_n/m_e \approx 10^5$ smaller than that of an electron is neglected. When the Zeeman term of the nucleus is included these parallel sub levels will at very high fields diverge again. These sub levels are due to the Zeeman splitting of the possible nuclear spin projections.

Energy diagram of the ground level $\mathbf{D_0}$ In the ground state D^0, the hyperfine coupling due to the bound electron is $A_e \approx +90\mu eV \approx +21.7$ GHz. This value is the average hyperfine coupling constant and represents the total coupling with all nuclei, so for determining the value for one nucleus this would be $\mathcal{A}/(10^5)$, also the amount of contact with the electron density should be included as explained in paragraph 5.2.1. For the D^0 in figure 5.1b the offset is correlated to the hyperfine coupling constant and the size of the total angular momentum F. The F values here are $I+S$ and $|I-S|$, respectively 2 and 1. The offsets from zero are respectively $-\frac{5\mathcal{A}_e\hbar^2}{4}$ and $\frac{3\mathcal{A}_e\hbar^2}{4}$ derived from equation 2.24. With increasing external magnetic field the degenerate levels split up due to Zeeman splitting. Each projection F_z gets an extra term $-g_F\omega_0 F_z$, which is explained in section 2.7. At high fields where the Zeeman term of the electron is more dominant than the hyperfine splitting (i.e. $\hbar\omega_0 >> \mathcal{A}\hbar^2$), the energy splittings are dominated by the overall splitting of the electron spin projection. Energy splittings inside these overall bundles are due to the projection of the nuclear spin. Here the system couples with one nuclear spin 3/2, so there are four possible projections per bundle, namely $I_z = -3/2, -1/2, +1/2, +3/2$. The splitting can be calculated with the equation derived in section 2.7

$$\langle m_J m_I | \, \mathcal{A} I_z J_z \, | m_J m_I \rangle = \mathcal{A}\hbar^2 m_J m_I \tag{5.1}$$

If the Zeeman splitting of the nucleus is neglected the sub levels converge to parallel lines with equal spacing. The spacing between the sub levels in the ground state is $\mathcal{A}\hbar^2 \cdot 1/2 \cdot 3/2 - \mathcal{A}\hbar^2 \cdot 1/2 \cdot 1/2 = 21.7 \cdot (3/4 - 1/4) = 10.85$ GHz. It is possible to check if the result plotted in figure 5.1 are in agreement with this high field description. Looking at the analytical solution of the two lowest lines of the D^0 states gives

$$\begin{matrix} \frac{1}{4}(3\mathcal{A}\hbar^2 - 2g_J\hbar\omega_0) \\ \frac{1}{4}\left(-\mathcal{A}\hbar^2 + 2\sqrt{3\mathcal{A}^2\hbar^4 + (\mathcal{A}\hbar^2 - g_J\hbar\omega_0)^2}\right) \end{matrix} \tag{5.2}$$

For large magnetic field $\omega_0 >> 1$ the term $3\mathcal{A}^2\hbar^4$ inside the square root can be neglected. The difference between the two lines becomes

$$\frac{1}{4}(3\mathcal{A}\hbar^2 - 2g_J\hbar\omega_0) - \frac{1}{4}\left(-\mathcal{A}\hbar^2 + 2\sqrt{(\mathcal{A}\hbar^2 - g_J\hbar\omega_0)^2}\right) \tag{5.3}$$

The Zeeman terms cancel, the remaining term is $\frac{\mathcal{A}\hbar^2}{2} = 10.85$ GHz. So the high field description from equation 5.1 are in agreement with the derived analytical solution. To give more feeling for the analytical expression in equation 5.2, at zero magnetic field ($\omega_0 = 0$) both expressions equals the offset for $F=1$: $\frac{3\mathcal{A}_e\hbar^2}{4}$. The analytical solutions are derived with the help of the model build in Mathematica given in Appendix E.

Energy diagram of the excited level D^0X Here $A_h\hbar^2 \approx -15\mu eV \approx 21.7$ GHz For the D^0X in figure 5.1b the F values are $|I-J|$,...,$I+J$, respectively 0,1,2 and 3. The offsets from zero are respectively $-\frac{15\mathcal{A}}{4}, -\frac{11\mathcal{A}}{4}, -\frac{3\mathcal{A}}{4}$ and $+\frac{9\mathcal{A}}{4}$ which are derived from equation 2.24, where $\mathcal{A}_h$ is the

hyperfine coupling constant for the hole. Because the hyperfine coupling constant of the hole is negative, there are three offsets above zero and one beneath. The spacings inside the bundles differ between bundles. The spacings inside the outer two bundles are larger than the spacings in the inner two bundles. The nucleus experiences a higher local field in the outer bundles because the nucleus couple to a larger local field of the hole, namely $\pm 3/2$ and to $\pm 1/2$ in the inner bundle. For the D^0X the hyperfine splitting is $A_h\hbar^2 \approx -15\mu eV \approx -3.6$ GHz. The energy splitting between the sub levels at high field is $\mathcal{A}\hbar^2 \cdot 3/2 \cdot 3/2 - \mathcal{A}\hbar^2 \cdot 3/2 \cdot 1/2 = 3.6 \cdot (9/4 - 3/4) = 5.4$ GHz for the outer bundles. The spacing between the sub levels in the inner bundles is $\mathcal{A}\hbar^2 \cdot 1/2 \cdot 3/2 - \mathcal{A}\hbar^2 \cdot 1/2 \cdot 1/2 = 3.6 \cdot (3/4 - 1/4) = 1.8$ GHz. It seems like that the lower inner bundle corresponding to $m_J = +1/2$ has less spacing between its sub levels than the upper inner bundle $m_J = -1/2$. However when increasing external magnetic field these spacings become equal.

Identifying states in the energy diagrams At low field the degenerate states the Zeeman splitting of the projection of total angular momentum F_z looks like

$$H_z = -g_F \hbar \omega_0 F_z \tag{5.4}$$

which was derived in section 2.7. The factor g_F is defined in equation 2.39. With the help of the sign of g_F, the energy levels can be labeled with quantum numbers m_F. When the g_F is positive, the highest line corresponds with the most negative projection m_F. For the energy levels in the D^0X energy diagram figure 5.1b, the F values and their corresponding g_F factors at low field from up to down are

$$\begin{array}{ll} \text{For } F = 0: & g_F = 0 \\ \text{For } F = 1, 2 \text{ and } 3: & g_F \approx +0.1 \end{array} \tag{5.5}$$

So the ordering in low external field of m_F projections from up to down is from most negative to most positive. For the energy levels in the D^0 energy diagram in figure 5.1a the F values and theire corresponding g_F factors are

$$\begin{array}{ll} \text{For } F = 1: & g_F \approx -0.05 \\ \text{For } F = 2: & g_F \approx +0.05 \end{array} \tag{5.6}$$

So the order of the projections of the $F = 1$ states are opposite. The labels for m_F are placed right from the diagram, but these hold only for low magnetic field. At high field the states are described with the quantum numbers m_J, m_I. In the diagrams in figure 5.1 the energy levels are labeled with the quantum numbers m_J and m_I. With the help of the sign of the electron/hole g-factor the ordering of labeling m_J can be derived. When the g-factor g_J is negative, the projections m_J run from most positive to most negative. The ordering of the projections m_I can be obtained in two ways. One is looking at the energy splitting between the sub levels, described in equation 2.26. The sign of the product of m_J m_I and the hyperfine couplings constant, determines the order of m_I. The second way is looking at the sum $m_J + m_I = m_F$.

Possible transitions In figure 5.2 the energy levels with theire quantum numbers are derived from the field dependent energy diagrams. The energy levels per bundle are grouped and placed alongside at the same height, because the energy splittings between the sub levels in the overall bundles are small, they are optically unresolvable. So all states on the same height belong to the same electron/hole projection. The strongly allowed transitions between the ground and excited states are indicated with lines. These represent both excitations and stimulated emissions with $q = 0$-polarized light. In figure 5.2a the strongly allowed transitions at low external magnetic field are given. The lines indicate both excitation and emission. The selection rules are determined by equation 3.30. The dominating rule is the restriction on the change of m_F. For $q = 0$-transitions $\Delta m_F = 0$. Almost all transitions that satisfies this condition are drawn. There are a few exceptions, most of them are not allowed because the change in F can be either $0, \pm 1$. Besides these two conditions there is still one unexplained not allowed transition. The transition from state $|2, 0\rangle$ to $|2, 0\rangle$ is not allowed, because of the second rule derived from the Wigner 3j matrix

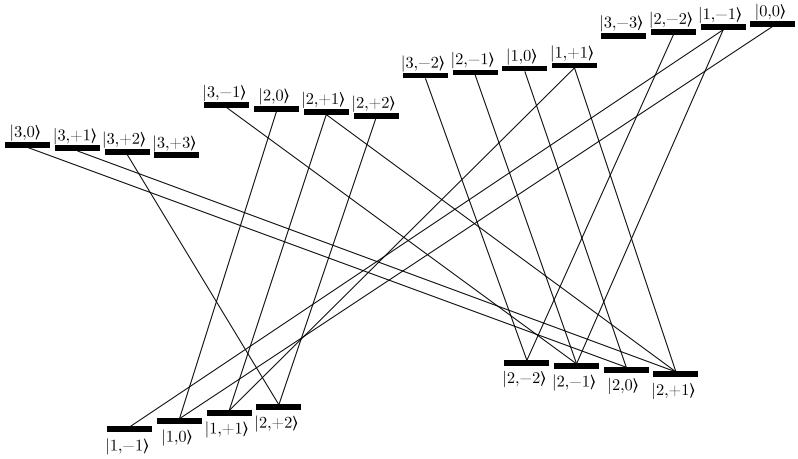

(a) Weakly allowed $q = 0$-transitions at high fields.

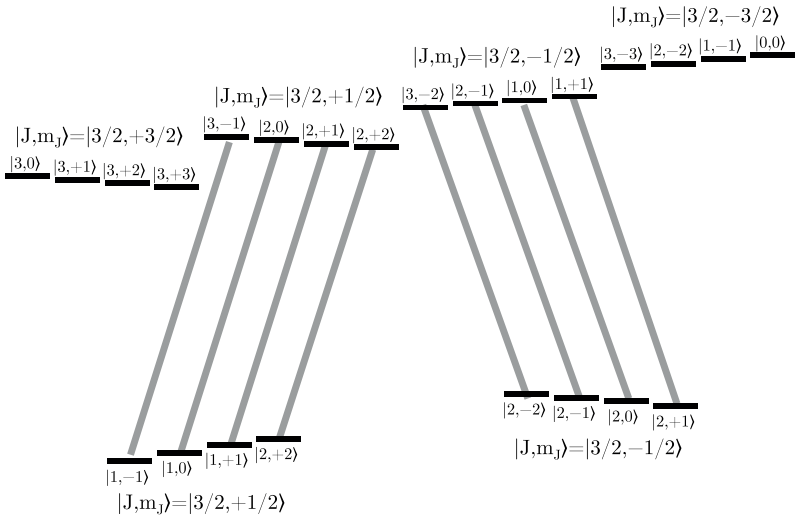

(b) Strongly allowed $q = 0$-transitions at the high field.

Figure 5.2: $q = 0$-transitions between the ground level D^0 and the excited state D^0X for a system coupled to one nuclear spin 3/2. Figure a) are the strongly allowed transitions at low external magnetic field, which are weakly allowed at high fields. In figure b) are the strongly allowed transitions at high magnetic field, these are weakly allowed at low magnetic fields. The selection rules for transition at high field are given in equation 5.8. The quantum number that are not important for the strongly allowed transitions at high field are grayed out, here the quantum numbers I, m_I, J, m_J are needed to calculate the transition strengths. Transition schemes for other polarizations are given in Appendix B.2.

in equation 3.31. When both m_F and m'_F are zero than $F + 1 + F'$ has to be an even integer, which is not the case here.

In 5.2b the strongly allowed transitions at high field are given. The states at high field are described by $|J, m_J\rangle |I, m_I\rangle$ so the matrix element of with the interaction term

$$\langle I', m'_I| \langle J', m'_J| \hat{e} \cdot \hat{r} |J, m_J\rangle |I, m_I\rangle \tag{5.7}$$

because the interaction operator only acts on radial parts and not on the spin part, this term can be rewritten as

$$\langle I', m'_I \, |I, m_I\rangle \langle J', m'_J| \hat{e} \cdot \hat{r} |J, m_J\rangle = \delta_{I',I}\delta_{m'_I,m_I} \langle J', m'_J| \hat{e} \cdot \hat{r} |J, m_J\rangle \tag{5.8}$$

The rules from paragraph 3.3.1 apply, with the extra restriction that there is no change in spin angular momentum I and projection m_I.

At intermediate fields there will be a mixture of two the possible transition schemes. As explained in chapter 4 the energy levels at low field are purely described with the quantum numbers F and m_F and at high field purely with the quantum numbers J and m_J. At intermediate field the energy levels are described as a mixture of states, with field depending probabilities. Because of this mixture of states the possible transitions are also effected. So in intermediate field the transitions that are possible are both the transitions at low and high field with a field depending amplitude. These amplitudes are described in chapter 4.

5.2.3 Donor electron coupled to two nuclear spins 3/2

Energy diagram in external magnetic field In figures 5.3a and 5.3b the energy levels of the ground state D^0 and the excited state D^0X are shown. Because there are now two nuclei coupled to the system, the electron couples to a total nuclear spin I_{tot}, which can take the values $|I_1 - I_2| = 0$ to $I_1 + I_2 = 3$ with integer steps. The assumption made is that the coupling between electron and nuclear spin is equal for both nuclei. Because the total nuclear spin can take multiple values, the number of hyperfine splittings at low field increases. For each total nuclear spin there are total angular momenta F which determines the energy offset. For all values of total nuclear spin I_{tot}, F runs from $|I - J|$ to $I + J$ in integer steps. In table 5.1 the possibilities for F values are given. At zero external magnetic field the hyperfine structure levels have an offset due to

	D^0X	D^0X	D^0	D^0
I_{tot}	F	offsets	F	offsets
0	$\frac{3}{2}$	0	$\frac{1}{2}$	0
1	$\frac{1}{2}$, $\frac{3}{2}$, $\frac{5}{2}$	$-\frac{5\mathcal{A}_h\hbar^2}{2}$, $-\mathcal{A}_h\hbar^2$, $\frac{3\mathcal{A}_h\hbar^2}{2}$	$\frac{1}{2}$, $\frac{3}{2}$	$-\mathcal{A}_e\hbar^2$, $\frac{\mathcal{A}_e\hbar^2}{2}$
2	$\frac{1}{2}$, $\frac{3}{2}$, $\frac{5}{2}$, $\frac{7}{2}$	$-\frac{9\mathcal{A}_h\hbar^2}{2}$, $-3\mathcal{A}_h\hbar^2$, $-\frac{\mathcal{A}_h\hbar^2}{2}$, $3\mathcal{A}_h\hbar^2$	$\frac{3}{2}$, $\frac{5}{2}$	$-\frac{3\mathcal{A}_e\hbar^2}{2}$, $\mathcal{A}_e\hbar^2$
3	$\frac{3}{2}$, $\frac{5}{2}$, $\frac{7}{2}$, $\frac{9}{2}$	$-6\mathcal{A}_h\hbar^2$, $-\frac{7\mathcal{A}_h\hbar^2}{2}$, 0, $\frac{9\mathcal{A}_h\hbar^2}{2}$	$\frac{5}{2}$, $\frac{7}{2}$	$-2\mathcal{A}_e\hbar^2$, $\frac{3\mathcal{A}_e\hbar^2}{2}$

Table 5.1: Quantum numbers corresponding to coupling to two nuclear spins. Here I_{tot} is defined in equation 2.29.

the hyperfine interaction. These values for the offsets corresponding to the different values of F are summed in table 5.1, these are calculated with equation 2.26. With increasing field the degenerate levels split up due to Zeeman splitting. The overall bundles are due to the Zeeman splitting of the electron/hole, just the same as in the case with one nuclear spin coupled. With two nuclei coupled to the electron, inside the overall bundles there are more sub levels. At high field the splitting inside the overall bundles is due the different projections of the total nuclear spin, described with equation $\mathcal{A}\hbar^2 m_I m_J$. In this case the total nuclear spin $I_{tot} = 3$, there are

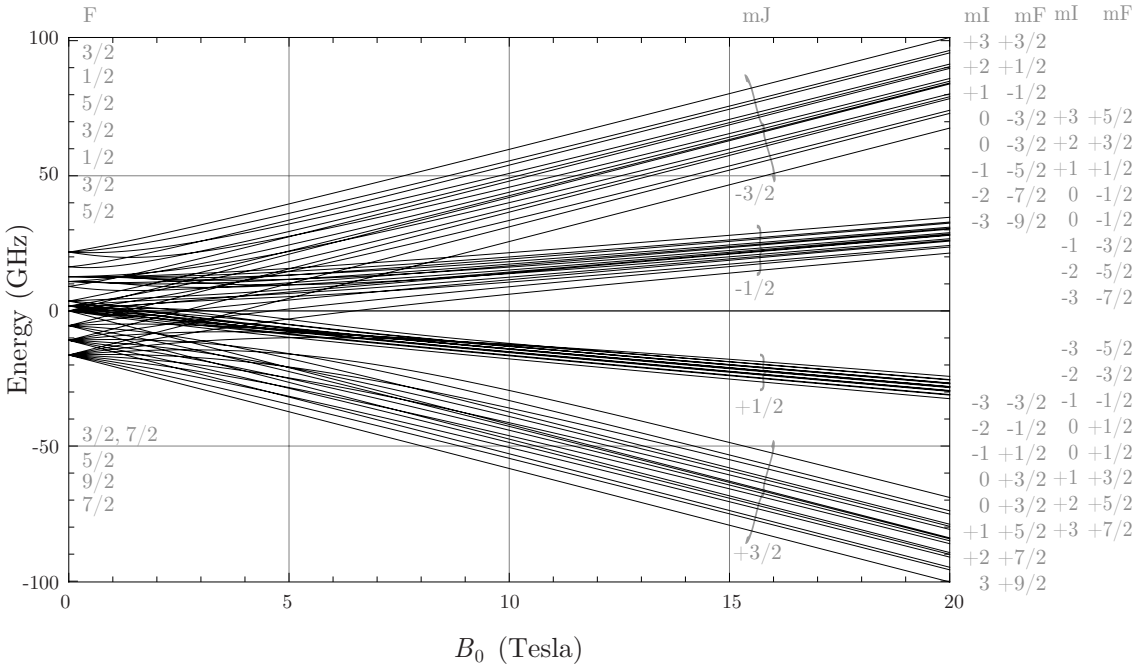

(a) Excited state of a system coupled with two nuclei with spin 3/2

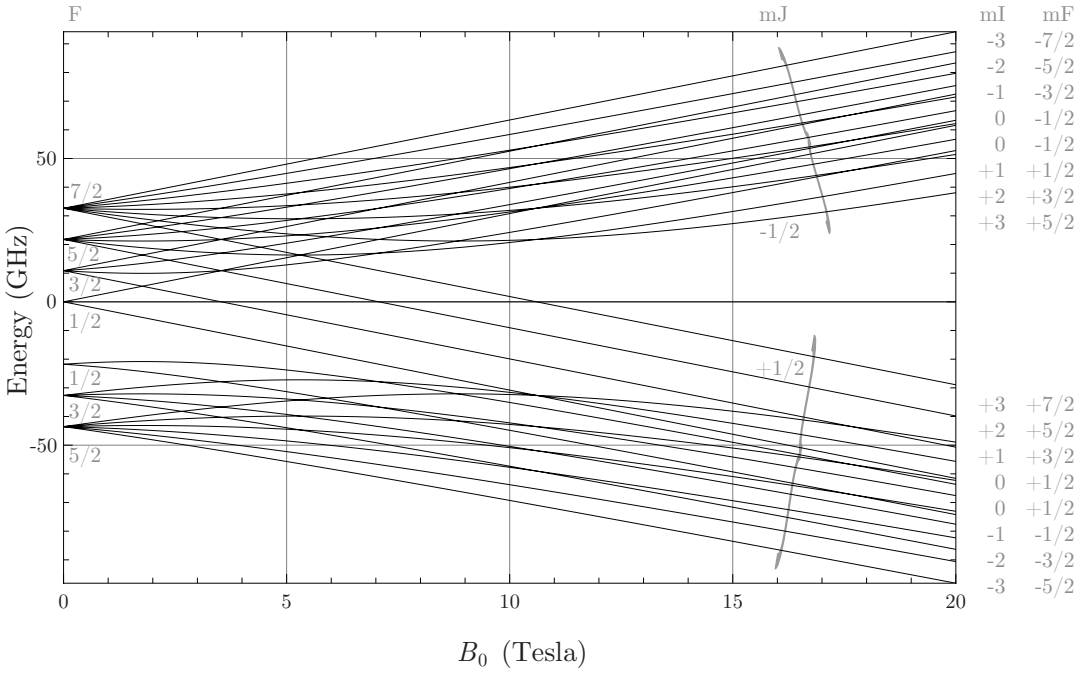

(b) Ground state of a system coupled with two nuclei with spin 3/2

Figure 5.3: System coupled with two nuclei with spin 3/2, with the parameters of GaAs.

$2I+1$ possible projections in an external magnetic field. In the case $I_{tot}=0$ the only projection in an external magnetic field is $m_I=0$. With increasing field the zero projections from the total nuclear spin $I_{tot}=0,1,2,3$ converge, as can seen in figure 5.3.

Identifying states in the energy diagrams Like in paragraph 5.2.2, with the help of the g_F factors the states can be identified. But another way, much easier is using the signs of the g_J and of the hyperfine coupling $\mathcal{A}$ to determine the ordering of m_I projections. For example the highest bundle of D^0X has a projection $m_J=-3/2$ because the hole g-factor is positive (+0.2). The hyperfine coupling constant is negative (-0.15μeV) so due to the energy shift $\mathcal{A}\hbar^2 m_J m_I$, the ordering m_I from up to down runs from +3 to −3. The labeling of m_F values can easily obtained from the relation $m_F=m_I+m_J$. Labeling the values F at zero field, needs the calculated offsets given in table 5.1 (the sign inside the hyperfine coupling constant must be taken into account. For example for the excited state an offset $+\mathcal{A}$ gives a negative offset).

5.3 Donor electron coupled to nuclei with spin 1/2

5.3.1 Parameters for F:ZnSe

The model of systems coupled to nuclei with spin 1/2, the parameters for F:ZnSe are used. The composition for F:ZnSe: the natural abundance of ^{67}Zn with nuclear spin I=5/2 is 4.11%. ^{77}Se with nuclear spin I=1/2, has a natural abundance of 7.58%. ^{19}F with spin 1/2, has a natural abundance of 100%. The hyperfine coupling constants are: $A_{Se}\hbar^2=33.6\mu eV$,$A_{Zn}\hbar^2=3.7\mu eV$ and $A_F\hbar^2=200\mu eV$ [32]. Like in the discussion for the parameters of GaAs in paragraph 5.2.1 the hyperfine coupling constants given are the average over the coupling constants of all coupled nuclei. This constant is the total coupling with all nuclei and still has to be multiplied with the electron density function squared, as showed in equation 2.20.

The g-factors of importance for ZnSe are: for the electron $g_e=-1.37$ [33], for the hole g_h=+0.21 [33], the nuclear g-factors: for Selenium the g-factor can be derived from the gyro magnetic factor given in reference [34], for Zinc the g-factor can be found in reference [35]. Fluorine nuclear g-factor is $g_n=+5.3$ [36]. In this model the values for the nuclear g-factor and hyperfine coupling of Fluorine are taken.

5.3.2 Donor electron coupled to one nuclear spin 1/2

Energy diagram in external magnetic field In figure 5.4 the field dependent diagrams are given for a system coupled with one nucleus with nuclear spin 1/2. The difference with the coupling to nuclei with spin 3/2 is that the number of splittings in the overall bundle is less. The possible projections of the nuclear spin here are only $m_I=\pm 1/2$. Also the number of levels at zero field is less, because the number of possible values that F can take is less. For the ground state D^0 the values for F are $|I-S|=1/2-1/2=0$ and $I+S=1/2+1/2=1$ with respectively offsets $-\frac{3\mathcal{A}_e\hbar^2}{4}$ and $+\frac{\mathcal{A}_e\hbar^2}{4}$. For the excited state the possible F values are $|I-J|=|1/2-3/2|=1$ and $I+J=1/2+3/2=2$, with respectively theire offsets at zero field $-\frac{5\mathcal{A}_h\hbar^2}{4}$ and $+\frac{3\mathcal{A}_h\hbar^2}{4}$. The ordering of electron spin projection is here the other way around, because the g-factor for the electron is here $g_e=-1.37$ and for the diagrams for nuclear spins 3/2 $g_e=+0.44$.

Possible transitions In figure 5.5 the possible transitions between the energy levels of a system coupled with one nucleus 1/2 are shown.

5.3.3 Donor electron coupled to two nuclear spins 1/2

Energy diagram in external magnetic field The energy dependent diagrams for a system coupled with two nuclei with spin 1/2 are shown in figure 5.6. For the ground state D^0 the possible values for F run from $|I_{tot}-S|$ to $I_{tot}+S$, where I_{tot} has two possible values $I_1-I_2=0$ and

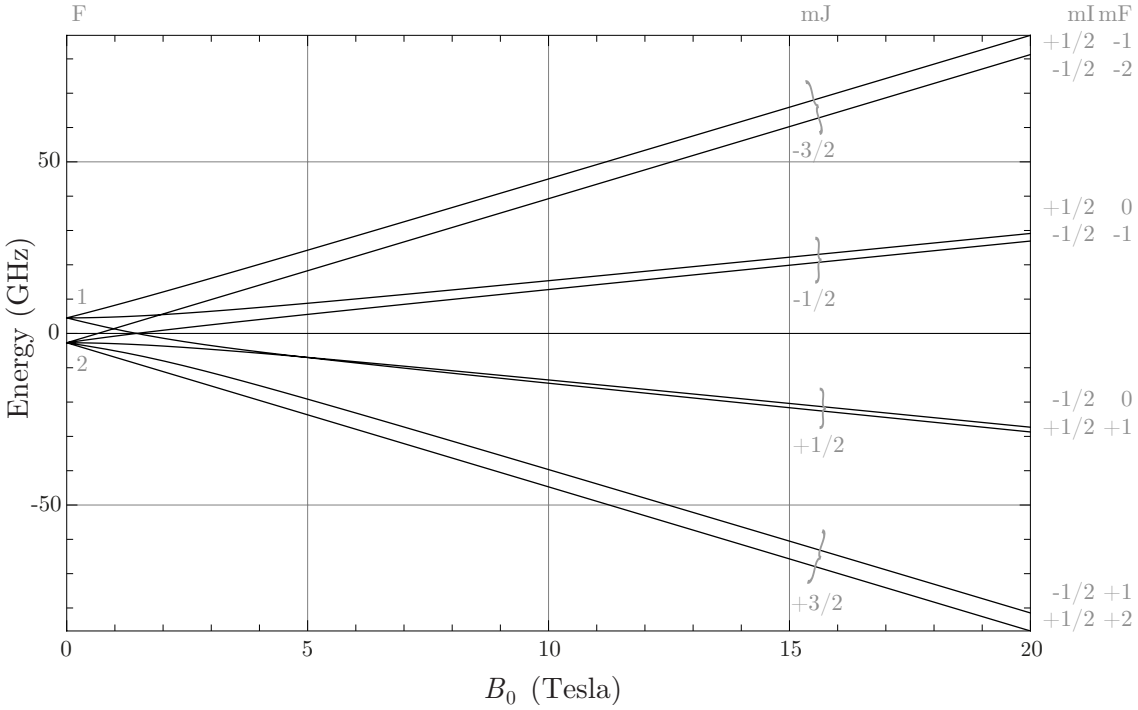

(a) D^0X state of a system coupled with one nucleus with spin 1/2.

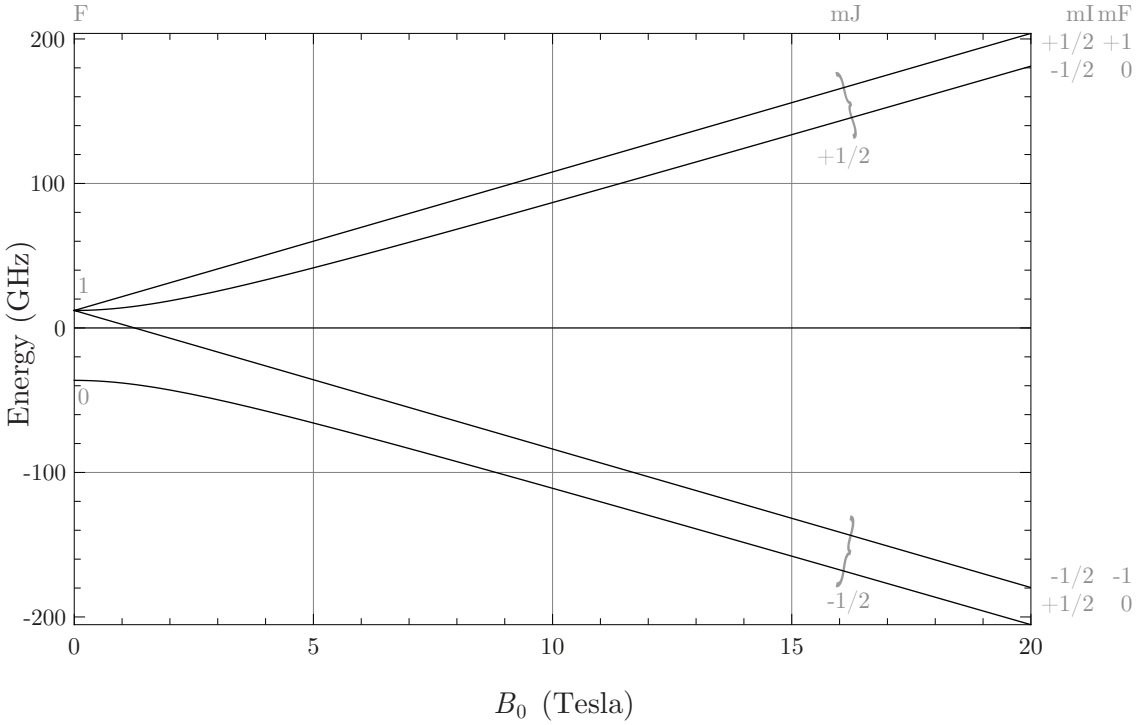

(b) D^0 state of the donor system coupled with one nucleus with spin 1/2.

Figure 5.4: System coupled with with one nucleus with spin 1/2, with the parameters defined in paragraph 5.3.1. The total coupling constant is taken and still has to be multiplied with the electron density function of the electron. So because of this, the energy splittings in this energy diagram are in reality smaller. The F values for the excited state D^0X are $|I-J|$,...,$I+J$, respectively 1 and2. For the ground state D^0 the F values are $I+S$ and $|I-S|$, respectively 1 and 0.

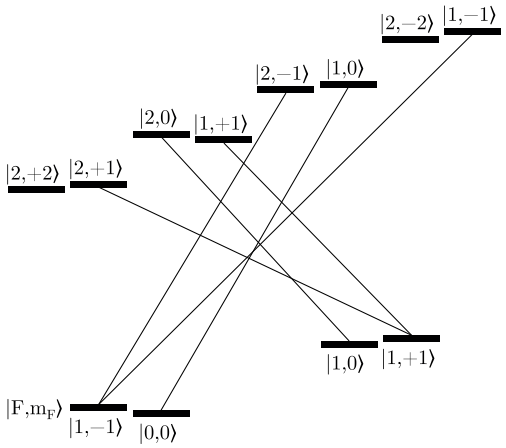

(a) Weakly allowed $q = 0$-transitions at the high field.

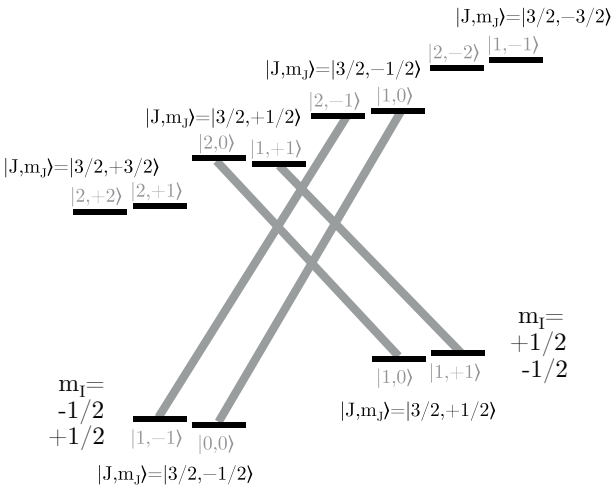

(b) Strongly allowed $q = 0$-transitions at the high field.

Figure 5.5: $q = 0$-transitions between the ground level D^0 and the excited state D^0X, which are strongly allowed in low and high external magnetic field. Selection rules in high field are given by equation 5.8. Here the system is coupled to one nucleus with spin 1/2. The quantum number that are not important for the strongly allowed transitions at high field are grayed out, here the quantum numbers I, m_I, J, m_J are needed to calculate the transition strengths. Transition schemes for other polarizations are given in the Appendix B.3.

$I_1 + I_2 = 1$ as explained in paragraph 2.6. The possible values for F in the ground state become thus 1/2, 1/2 and 3/2. Here the value $F = 1/2$ can be obtained in two ways, one for the total nuclear spin $I_{tot} = 0$ and one for the $I_{tot} = 1$. Therefor the offsets for the two levels with quantum number $F = 1/2$ are different. The offsets can be calculated with equation 2.26, where for I in both cases the value of I_{tot} is taken. For the excited state D^0X the possible F values run from $|I_{tot} - J|$ to $I_{tot} + J$: 1/2, 3/2, 3/2 and 5/2. At high field the $m_I = 0$ projections of the two different total nuclear spin I_{tot} vectors will converge, because at high field the spacings inside the bundles are due to Zeeman splitting of the nuclear spin projection, which are the same for both I_{tot}.

Possible transitions Possible transitions between these ground and excited states are given in figure 5.7. Transition schemes for different polarizations are given in Appendix B.4.

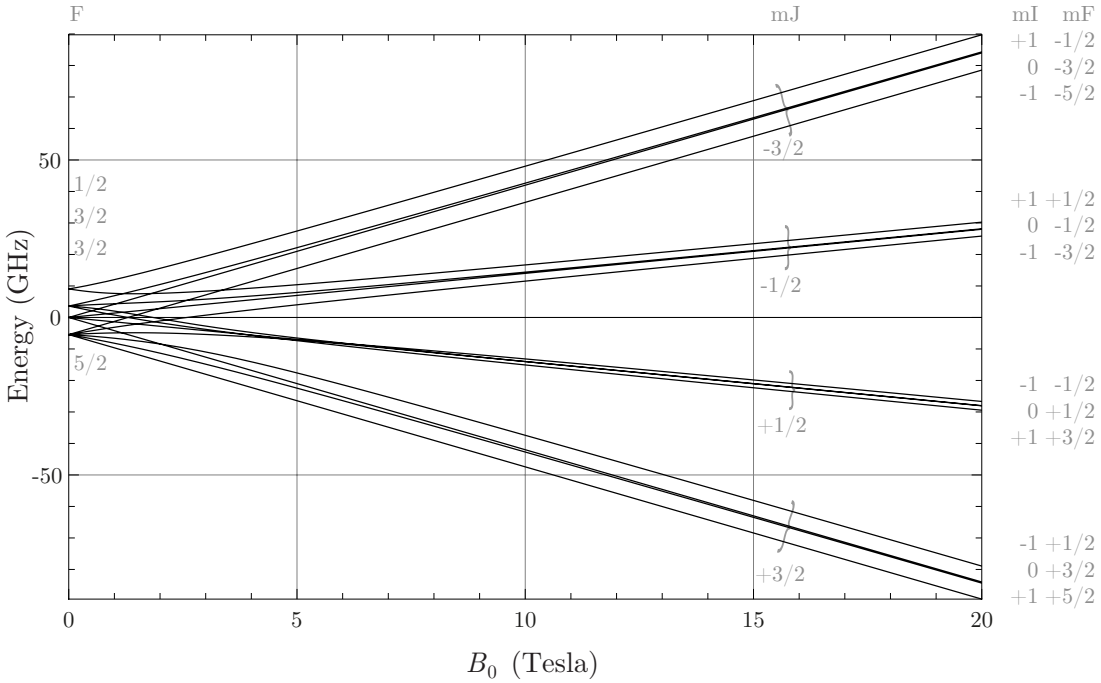

(a) D^0X state of a system coupled with two nuclei with spin 1/2.

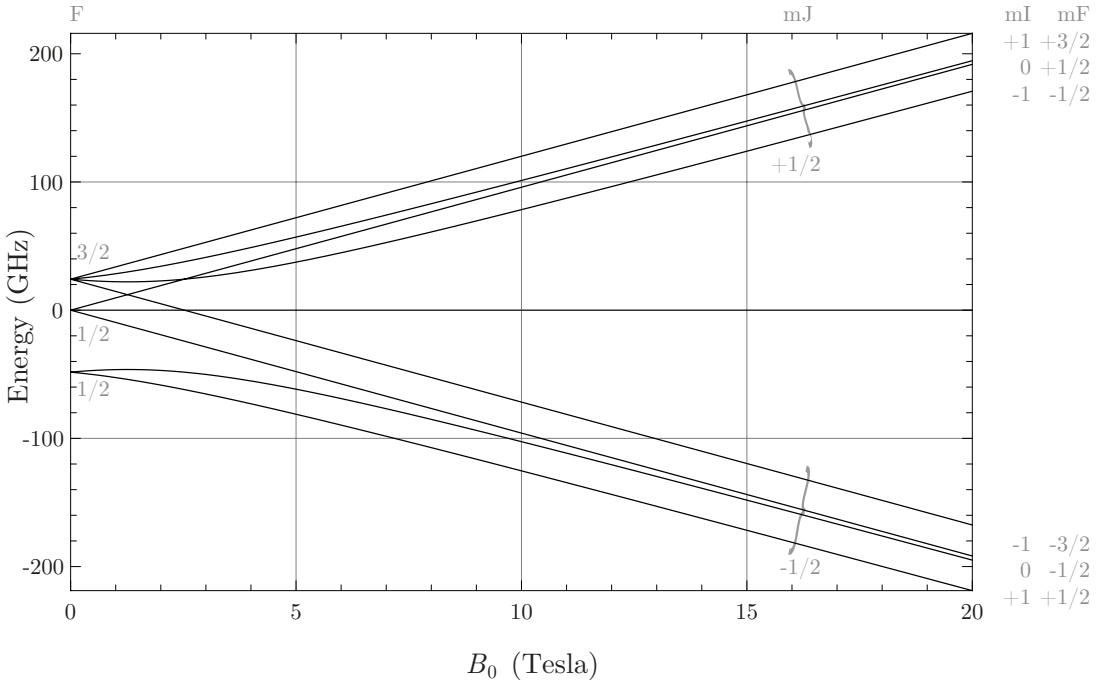

(b) D^0 state of the donor system coupled with two nuclei with spin 1/2.

Figure 5.6: A system coupled with two nuclei with spin 1/2, with the parameters of ZnSe. The F values for the excited state D^0X are $|I-J|$,...,$I+J$, respectively 1 and2. For the ground state D^0 the F values are $I+S$ and $|I-S|$, respectively 1 and 0.

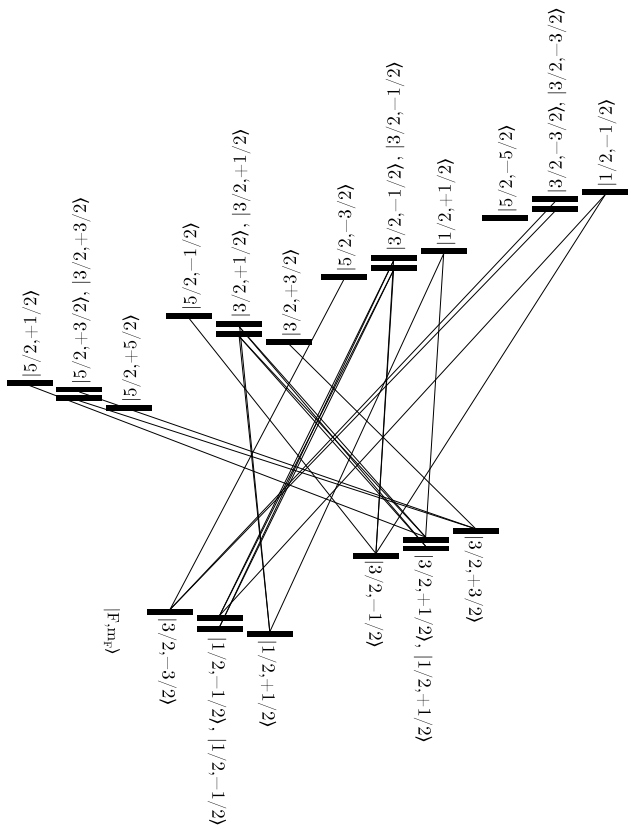

(a) Weakly allowed $q = 0$-transitions at the high field.

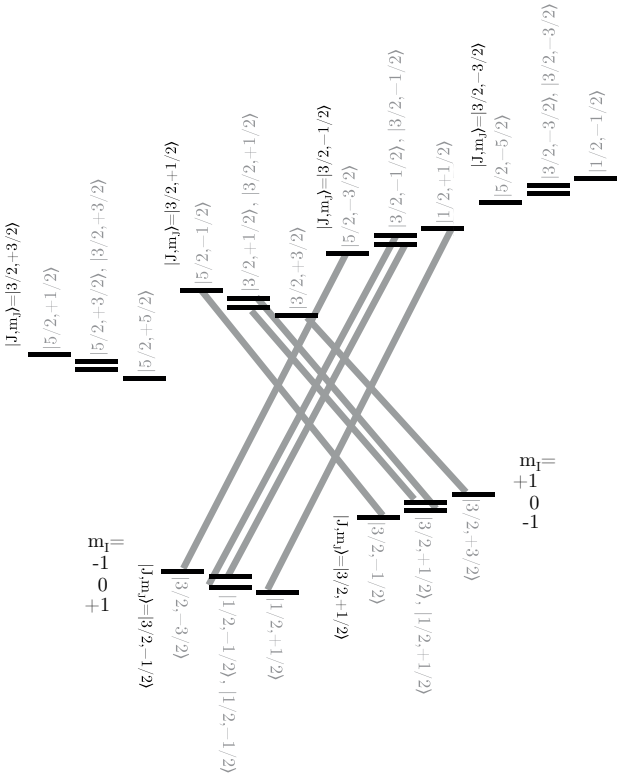

(b) Strongly allowed $q = 0$-transitions at the high field.

Figure 5.7: $q = 0$-transitions between the ground level D^0 and the excited state D^0X, which are strongly allowed in low and high external magnetic field. Here the system is coupled to two nuclei with spin 1/2. The quantum number that are not important for the strongly allowed transitions at high field are grayed out, here the quantum numbers I, m_I, J, m_J are needed to calculate the transition strengths. Transition schemes for other polarizations are given in the Appendix B.4.

Chapter 6

Optical processes that could cause nuclear polarization

6.1 Introduction

With the help of the transition diagrams derived in chapter 5, the schemes for possibilities for inducing DNP can be constructed. In these schemes the excitations can be selectively chosen by choosing the photon energy and polarization of the light that couples to the system. When constructing a DNP scheme the excitation transitions and the stimulated emissions are determined by the polarization of the light that couples to the system. The transitions for spontaneous emissions take place for the allowed transitions for all possible polarizations. The transition schemes for all polarizations and theire transition strengths are worked out in Appendix B.

6.2 Possible scheme to induce DNP in a system coupled to one nuclear spin 3/2

To be able to induce DNP an external magnetic field is needed to be able to couple selectively to electron/hole spin states. When the field is high enough the energy levels for the different electron/hole spin states get optically resolvable, because of Zeeman splitting. Now it is possible to couple for example a laser on resonance between the electron spin down state $m_J = -1/2$ of the ground level D^0 and the $m_J = +3/2$ spin projection of the hole state in the excited state D^0X. For building the diagram, which can induce DNP, all spontaneous emissions should be collected. In figure 6.1 the emissions allowed at high field are taken from the diagram C.1 in Appendix C. Emission from the state $m_J = +3/2$ to $m_J = -1/2$ exceeds the limitation of $\Delta m_J = 0, \pm 1$ determined in paragraph 3.3.1. In figure 6.2 are the strongly allowed emissions at low field, thus weakly allowed at high field, drawn. The diagram contains emissions with all three polarizations, namely with $q = -1$ which are given in figure B.3, $q = +1$ which are given in figure B.2 and $q = 0$ which are given in figure 5.2.

In figure 6.3 the weakly allowed transitions at high field are drawn which are coupled to a laser with a $q = +1$-polarization. A $q = +1$-polarization can be obtained by applying an beam with a $\sigma^+_{k_z}$ polarization, in other words a σ^+-polarization in the Faraday configuration (In paragraph 3.2 and in table 3.2 is explained how a certain q-polarization is obtained).

In figure 6.4 all these transitions are combined and form a diagram to induce DNP. The solid lines are the transitions that are coupled with a laser with a polarization $q = +1$, these are weakly allowed transitions at higher fields. The thin black dashed lines are all weakly allowed transitions corresponding to spontaneous emission. The thick gray dashed lines are strongly allowed transitions corresponding to spontaneous emission. When the laser is coupled to the system, population will be pumped from three of the four levels corresponding to the electron spin

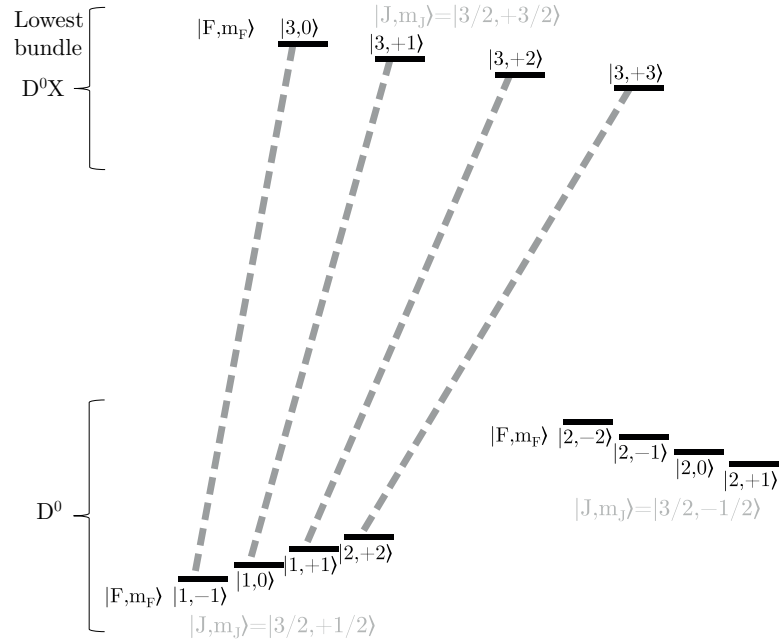

Figure 6.1: The strongly allowed transitions at high field, between the ground levels and the lowest bundle of the excited state D^0X of a system coupled with one nuclear spin 3/2 are sketched.

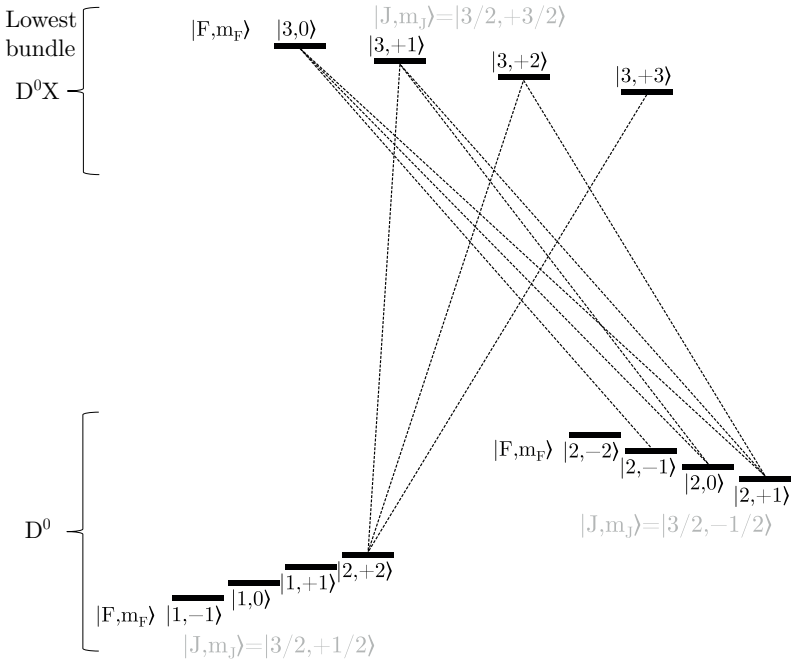

Figure 6.2: The strongly allowed transitions at low field. These are at high fields weakly allowed.

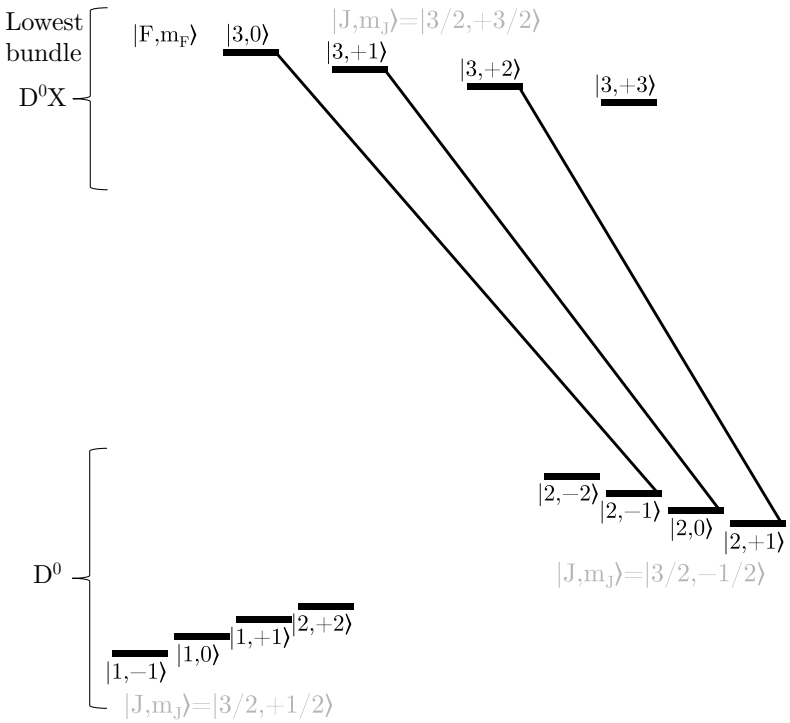

Figure 6.3: Allowed absorption transitions with an incoming beam with polarization $q = +1$.

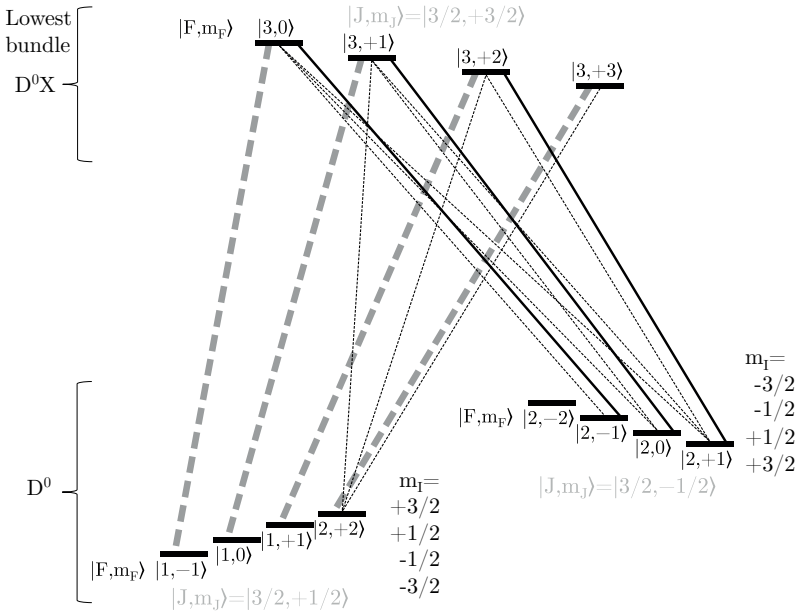

Figure 6.4: Possible scheme to induce DNP in a system coupled to one nuclear spin 3/2. The transitions combined, where the thick gray dashed lines are the strongly allowed emission at high field, the black dashed lines the weakly allowed emissions at high field and the solid black lines are the weakly allowed transitions at high fields, which are coupled with the laser with a polarization $q = +1$ (σ^+ in Faraday configuration (see paragraph 3.2)).

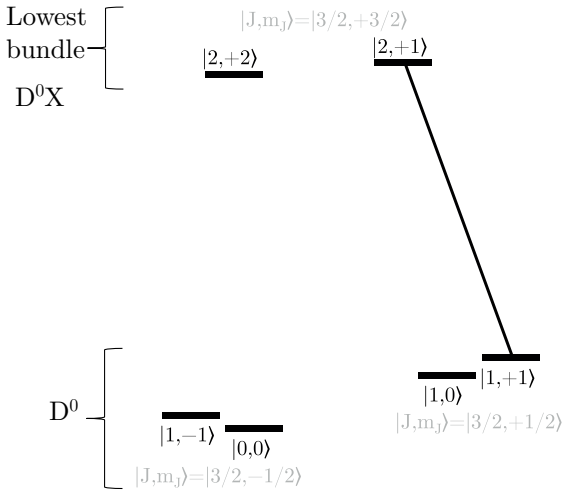

Figure 6.5: Weakly allowed transitions at high field with $q = 0$-polarization, between two ground level D^0 and the lowest bundle of the excited state D^0X. For a system coupled with one nuclear spin 1/2.

down to the four levels corresponding to the electron spin up. During pumping, the population in the four electron spin up levels will decay back to the four electron spin down levels to retain thermal equalibrium. Only three of the four levels will be repumped, so one would expect the level $|2, -2\rangle$ to be filled, which corresponds with a nuclear spin projection $m_I = -3/2$. Which is the same as saying the nuclear spins are beeing polarized. To quantitatively say something about the nuclear polarization, the rate equations should be solved with the help of the density matrix formalism, explained in Appendix A.

6.3 Possible scheme to induce DNP in a system coupled to one nuclear spin 1/2

In figure 6.5 the weakly allowed transitions at high field, with $q = 0$-polarization are sketched. These transitions are taken from figure B.4 in Appendix B. The transitions in figure 6.6 are the weakly allowed transitions in high field, with polarization $q = +1$ taken from figure B.5. In diagram B.9 can be seen that there are no weakly allowed transitions with a polarization $q = -1$. In figure 6.7 are the strongly allowed transitions shown. These are taken from diagram C.2 in the appendix. Pumping with a $q = 0$ polarization can be achieved by applying a beam with an polarization $\Pi^z_{k_x}$ or $\Pi^z_{k_y}$, in other words vertical polarization in the Voight configuration (see paragraph 3.2). Population will end up in the state $|1, +1\rangle$, which corresponds with nuclear spin up.

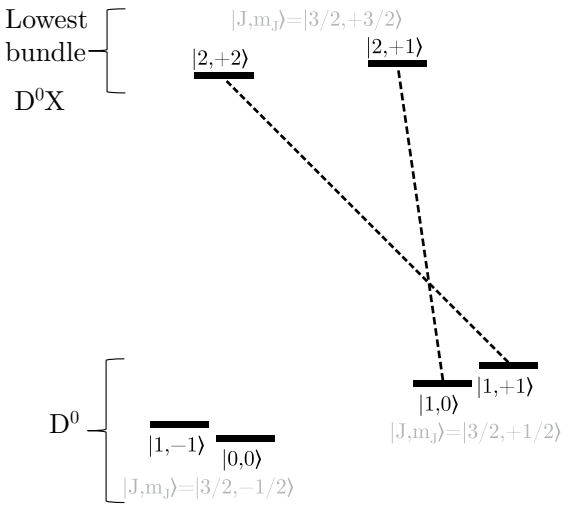

Figure 6.6: Weakly allowed transitions at high field with $q = +1$-polarization.

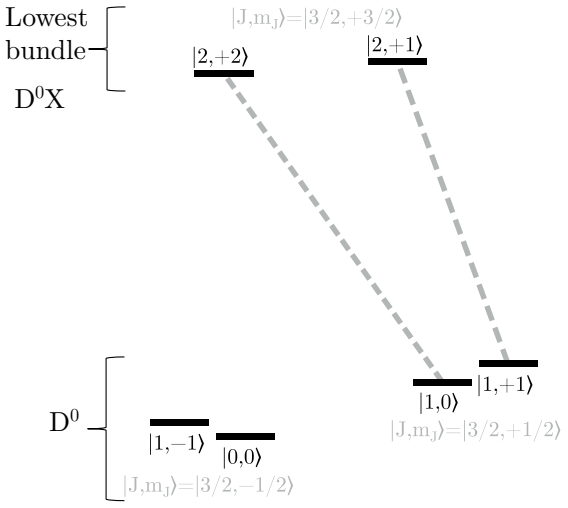

Figure 6.7: Strongly allowed transitions at high field with.

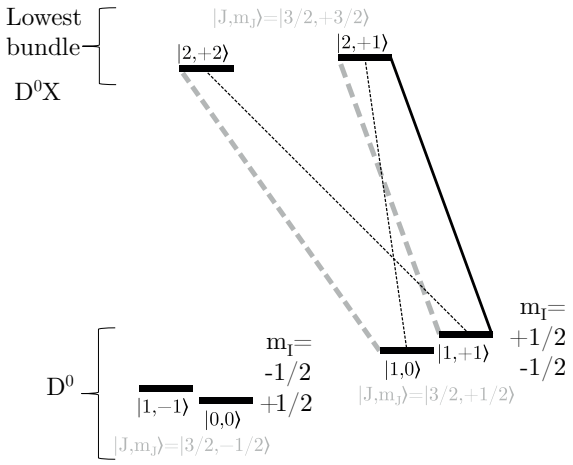

Figure 6.8: Possible scheme to induce DNP in a system coupled to one nuclear spin 1/2. The transitions between two ground levels and the lowest bundle of the excited state D^0X are sketched. The thick gray dashed lines are strongly allowed transitions, representing spontaneous emission. The thin black dashed lines indicate the weakly allowed emissions. The black solid lines represent weakly allowed transitions that are coupled with the laser with a $q = 0$-polarization (vertical polarized light in the Voight configuration (see 3.2)).

Chapter 7

Conclusion and outlook

Inducing Dynamic Nuclear Polarization by selectively addressing transitions between nuclear spin states should be possible. Essential for inducing DNP in this way is the concept of field dependent mixing of states. The external magnetic field should be strong enough to be able to couple selectively to the different electron/hole states. At low magnetic fields the different spin projections of the electron are optically non resolvable. The strongly allowed transitions cannot induce transitions involving nuclear spin flips. With increasing field the allowed transitions that play a role in changing nuclear spin projections become weaker, but can still play a big role when concerning large number of oscillations. The amount of mixing determines the amplitude of the weakly allowed transitions at higher field. The strength of the hyperfine coupling will determine the decline of mixing. The bigger the hyperfine coupling, the slower the decline of mixing with increasing magnetic field. The size of the total hyperfine coupling constant scales with the number of nuclei that are coupled to the donor system, so using the mixing of states to induce DNP, the amount of nuclei plays a role.

Looking at the DNP schemes in chapter 6 only qualitatively arguments are given why it should be possible to induce nuclear polarization by optically pump the system. What would be a nice next step in further research for directly induce DNP, is to construct rate equations with the help of density matrix formalism. With this formalism the steady state amount of population in each energy level can be calculated. The amount of nuclear polarization possible in the different DNP schemes can be determined. In appendix A an introduction of setting up rate equations is given. Also an example with four levels is worked out.

The computer model to produce the field dependent energy diagrams in this thesis has no limitation on the number of nuclei which can be coupled to the system, or the value of the nuclear spin. The only limitation on adding a large number of nuclei, or large values for the nuclear spins is the amount of Random Access Memory (RAM) of the computer. Depending on the size of the nuclear spin and the amount of RAM the system can be coupled with around 5 nuclei (with 4GB RAM). For case were the electron in the ground state is coupled to nuclear spins 1/2, there is the smallest amount of RAM needed to calculate the energy diagrams. A system in the ground state coupled with a nuclear spin 1/2 can easily be coupled with 50 nuclei. In figure 7.1 the energy dependent diagram for a system coupled with 50 nuclear spins is shown.

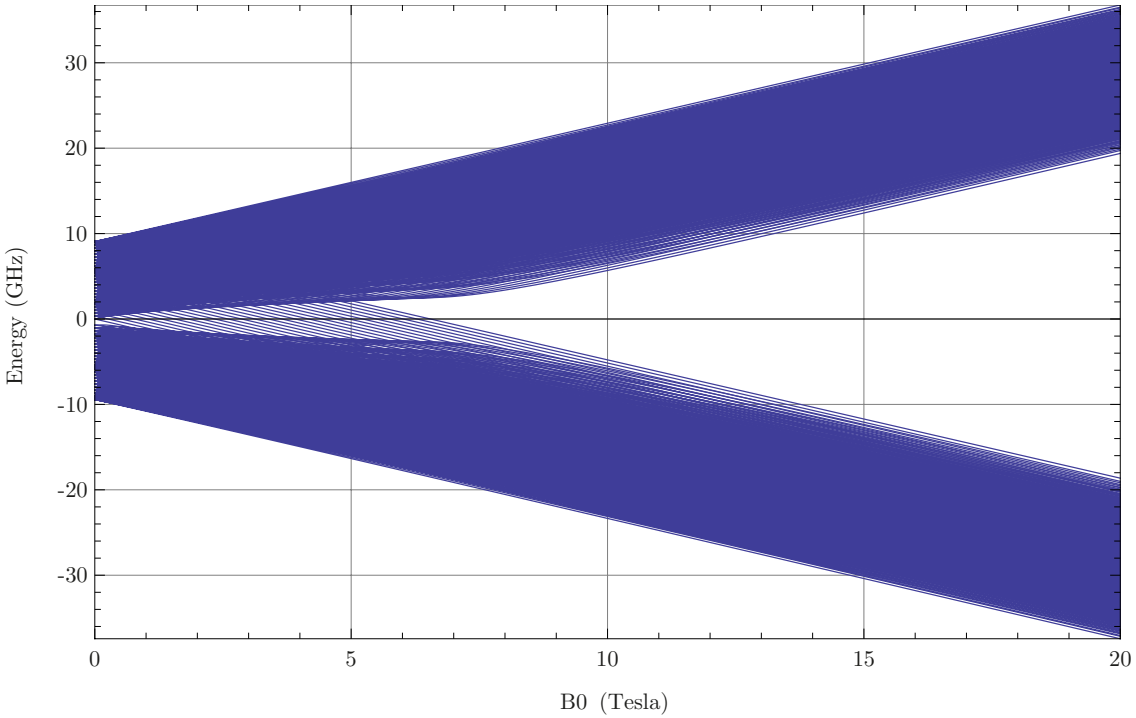

Figure 7.1: Ground state of a system coupled with 50 nuclei with spin 1/2.

Bibliography

[1] Hendrik Bluhm, Sandra Foletti, Izhar Neder, Mark Rudner, Diana Mahalu, Vladimir Umansky, and Amir Yacoby. Dephasing time of GaAs electron-spin qubits coupled to a nuclear bath exceeding 200μs. *Nature Physics*, 7(2):109–113, December 2010.

[2] Alexander V. Khaetskii, Daniel Loss, and Leonid Glazman. Electron Spin Decoherence in Quantum Dots due to Interaction with Nuclei. *Phys. Rev. Lett.*, 88:186802, Apr 2002.

[3] A. Imamoglu, E. Knill, L. Tian, and P. Zoller. Optical Pumping of Quantum-Dot Nuclear Spins. *Physical Review Letters*, 91(1), July 2003.

[4] Dimitrije Stepanenko, Guido Burkard, Geza Giedke, and Atac Imamoglu. Enhancement of Electron Spin Coherence by Optical Preparation of Nuclear Spins. *Phys. Rev. Lett.*, 96:136401, Apr 2006.

[5] R. Oulton, A. Greilich, S. Yu. Verbin, R. V. Cherbunin, T. Auer, D. R. Yakovlev, M. Bayer, I. A. Merkulov, V. Stavarache, D. Reuter, and A. D. Wieck. Subsecond Spin Relaxation Times in Quantum Dots at Zero Applied Magnetic Field Due to a Strong Electron-Nuclear Interaction. *Phys. Rev. Lett.*, 98:107401, Mar 2007.

[6] C. Latta, A. Hgele, Y. Zhao, A. N. Vamivakas, P. Maletinsky, M. Kroner, J. Dreiser, I. Carusotto, A. Badolato, D. Schuh, W. Wegscheider, M. Atature, and A. Imamoglu. Confluence of resonant laser excitation and bidirectional quantum-dot nuclear-spin polarization. *Nature Physics*, 5(10):758–763, August 2009.

[7] A. Greilich, A. Pawlis, F. Liu, O. A. Yugov, D. R. Yakovlev, K. Lischka, Y. Yamamoto, and M. Bayer. Spin dephasing of fluorine-bound electrons in ZnSe. *Phys. Rev. B*, 85:121303, Mar 2012.

[8] Maksym Sladkov, A. U. Chaubal, M. P. Bakker, A. R. Onur, D. Reuter, A. D. Wieck, and C. H. van der Wal. Electromagnetically induced transparency with an ensemble of donor-bound electron spins in a semiconductor. *Phys. Rev. B*, 82:121308, Sep 2010.

[9] T. Wang, R. Rajapakse, and S.F. Yelin. Electromagnetically induced transparency and slow light with n-doped GaAs. *Optics Communications*, 272(1):154–160, April 2007.

[10] G.H. Kudlek, U.W. Pohl, Ch. Fricke, R. Heitz, A. Hoffmann, J. Gutowski, and I. Broser. Electronic structure and dynamical behaviour of different bound-exciton complexes in ZnSe bulk crystals. *Physica B: Condensed Matter*, 185(1-4):325–331, April 1993.

[11] New semiconductor materials. characteristics and properties. http://www.ioffe.ru/SVA/.

[12] Jan Fischer, W. A. Coish, D. V. Bulaev, and Daniel Loss. Spin decoherence of a heavy hole coupled to nuclear spins in a quantum dot. *Phys. Rev. B*, 78:155329, Oct 2008.

[13] John David Jackson. *Classical electrodynamics*. Wiley, New York, 1999.

[14] J. M. Brown, R. J. Buenker, A. Carrington, C. Di Lauro, R. N. Dixon, R. W. Field, J. T. Hougen, W. Huttner, K. Kuchitsu, M. Mehring, A. J. Merer, T. A. Miller, M. Quack, D. A. Ramsay, L. Veseth, and R. N. Zare. Remarks on the signs of g factors in atomic and molecular Zeeman spectroscopy. *Molecular Physics*, 98(20):1597–1601, October 2000.

[15] W. A. Coish. *Spins in quantum dots: Hyperfine interaction, transport, and coherent control*. PhD thesis, Philosophisch-Naturwissenschaftlichen Fakultat der Universitat Basel, 2008.

[16] E. A. Chekhovich, A. B. Krysa, M. S. Skolnick, and A. I. Tartakovskii. Direct Measurement of the Hole-Nuclear Spin Interaction in Single InP/GaInP Quantum Dots Using Photoluminescence Spectroscopy. *Phys. Rev. Lett.*, 106:027402, Jan 2011.

[17] Jan Fischer, W. A. Coish, D. V. Bulaev, and Daniel Loss. Spin decoherence of a heavy hole coupled to nuclear spins in a quantum dot. *Phys. Rev. B*, 78:155329, Oct 2008.

[18] Richard Fitzpatrick. Quantum Mechanics, The University of Texas at Austin, http://farside.ph.utexas.edu/teaching/qmech/qmech.pdf.

[19] C Foot. *Atomic physics*. Oxford University Press, Oxford, 2005.

[20] Claude Cohen-Tannoudji. *Quantum mechanics*. Wiley, New York, 1977.

[21] Eric W. Weisstein. "clebsch-gordan coefficient." from mathworld–a wolfram web resource. `http://mathworld.wolfram.com/Clebsch-GordanCoefficient.html`. Last visited on 13/4/2012.

[22] Eric W. Weisstein. "wigner 3j-symbol.", from mathworld–a wolfram web resource. `http://mathworld.wolfram.com/Wigner3j-Symbol.html`. Last visited on 13/4/2012.

[23] H Metcalf. *Laser cooling and trapping*. Springer, New York, 1999.

[24] Eric W. Weisstein. "wigner 6j-symbol." from mathworld–a wolfram web resource. `http://mathworld.wolfram.com/Wigner6j-Symbol.html`. Last visited on 13/4/2012.

[25] Xiaodong Xu, Bo Sun, Paul R. Berman, Duncan G. Steel, Allan S. Bracker, Dan Gammon, and L. J. Sham. Coherent population trapping of an electron spin in a single negatively charged quantum dot. *Nature Physics*, 4(9):692–695, August 2008.

[26] M. Reine, R. L. Aggarwal, B. Lax, and C. M. Wolfe. Split-Off Valence-Band Parameters for GaAs from Stress-Modulated Magnetoreflectivity. *Phys. Rev. B*, 2:458–463, Jul 1970.

[27] J. L. Shay. Temperature Dependence of the Energy Gap in GaAs. *Phys. Rev. B*, 4:1385–1386, Aug 1971.

[28] D. Gammon, Al. L. Efros, T. A. Kennedy, M. Rosen, D. S. Katzer, D. Park, S. W. Brown, V. L. Korenev, and I. A. Merkulov. Electron and Nuclear Spin Interactions in the Optical Spectra of Single GaAs Quantum Dots. *Phys. Rev. Lett.*, 86:5176–5179, May 2001.

[29] I. A. Yugova, A. Greilich, D. R. Yakovlev, A. A. Kiselev, M. Bayer, V. V. Petrov, Yu. K. Dolgikh, D. Reuter, and A. D. Wieck. Universal behavior of the electron g factor in $GaAsAl_xGa_{1-x}As$ quantum wells. *Phys. Rev. B*, 75:245302, Jun 2007.

[30] S. Glasberg, H. Shtrikman, I. Bar-Joseph, and P. C. Klipstein. Exciton exchange splitting in wide GaAs quantum wells. *Phys. Rev. B*, 60:R16295–R16298, Dec 1999.

[31] M. J. Snelling, E. Blackwood, C. J. McDonagh, R. T. Harley, and C. T. B. Foxon. Exciton, heavy-hole, and electron g factors in type-I $GaAs/Al_xGa_{1-x}As$ quantum wells. *Phys. Rev. B*, 45:3922–3925, Feb 1992.

[32] A. Greilich, A. Pawlis, F. Liu, O. A. Yugov, D. R. Yakovlev, K. Lischka, Y. Yamamoto, and M. Bayer. pin dephasing of fluorine-bound electrons in ZnSe. *Phys. Rev. B*, 85:121303, Mar 2012.

[33] H. Venghaus. Valence-band parameters and g factors of cubic zinc selenide derived from free-exciton magnetoreflectance. *Phys. Rev. B*, 19:3071–3082, Mar 1979.

[34] L L Lumata, K Y Choi, J S Brooks, A P Reyes, P L Kuhns, G Wu, and X H Chen. 77 Se and 63 Cu NMR studies of the electronic correlations in Cu x TiSe 2 (x = 0.05, 0.07). *Journal of Physics: Condensed Matter*, 22(29):295601, July 2010.

[35] Pavel G. Baranov, Sergei B. Orlinskii, Celso de Mello Donega, Andries Meijerink, Hubert Blok, and Jan Schmidt. Dynamical nuclear polarization by means of shallow donors in ZnO quantum dots. *Physica B: Condensed Matter*, 404(2324):4779 – 4782, 2009. Proceedings of the 25th International Conference on Defects in Semiconductors.

[36] Nuclear magnetic and electron spin resonance objectives. http://astro.physics.calpoly.edu/jodi/W11Phys341/NmrEsrW11.pdf.

Appendix A

density matrix formalism

Introduction In this appendix an example for a system with three energy levels coupled with two lasers is worked out with the help of the density matrix formalism. Two lasers are included in this model, as a first step towards setting up a so called lambda scheme. Which coherently couples two electron spin states. This model is extend to four levels to illustrate the difference between coherent coupling between energy levels and energy levels that are not coherently coupled with a laser. The levels which are not coherently coupled to the system with a laser, are involved due to population decay.

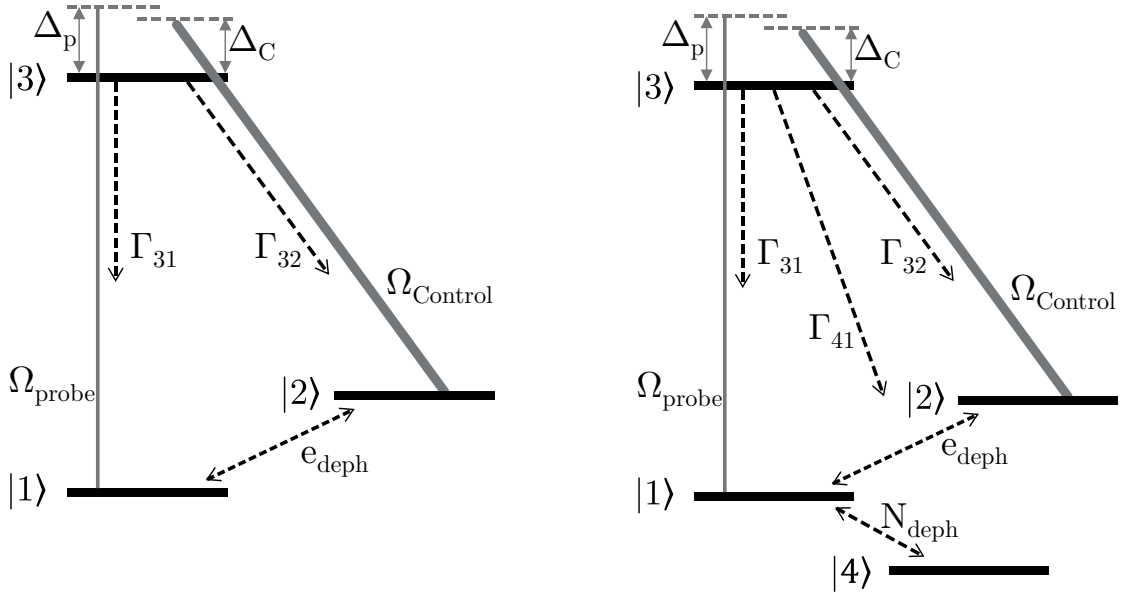

(a) Three level scheme

(b) Four level scheme

Figure A.1: Coherent coupling with two lasers, one control and one probe laser. Decay rates are indicated for a system with three and four levels. The system with four levels is an extension to the system with three levels.

Short introduction to the concept of the density matrix Beginning with the time-dependent Schödinger equation

$$i\hbar\frac{\partial\Psi_s(\mathbf{r},t)}{\partial t} = \hat{H}\psi_s(\mathbf{r},t)$$

and split the Hamiltonian in such a way that there is the part for a free atom and a part for the interaction energy.

$$\hat{H} = \hat{H}_0 + \hat{V}(t)$$

The wave function of state s can be defined in this way

$$\psi_s(\mathbf{r}, t) = \sum_n C_n^s(t) u_n(\mathbf{r})$$

Here $C_n^s(t)$ gives the probability amplitude that the atom in state s, is in the eigenstate n at time t. The $u_n(\mathbf{r})$'s are the energy eigenfunctions. The density operator is defined as follows

$$\rho_{nm} = \sum_s p(s) C_m^{s*} C_n^s$$

Where $p(s)$ is the probability that the system is in state s. or in shorter notation

$$\rho_{nm} = \overline{C_m^* C_n}$$

The over line denotes an ensemble average. The density matrix ρ_{nm} is defined in such a way that the diagonal components describes the probability of the system being in state n and the off diagonal elements in the matrix can be interpreted as the coherence between the levels n and m. The time evolution of ρ_{nm} can be evaluated by the commutation of ρ_{nm} with the Hamiltonian.

$$\dot{\rho}_{nm} = -\frac{i}{\hbar} \left[\hat{H}, \hat{\rho}\right]_{nm} \tag{A.1}$$

Model density matrix formalism Consider a system with four energy levels, with two coupled lasers. Assume electric dipole transitions are allowed between the levels 1 and 3, 2 and 3, 3 and 4, other transitions are not allowed by an electric dipole transition. The transition between level 1 and 2 are not allowed by dipole transitions but can take place by a so called cross relaxation process, where at the same time the electron spin and nuclear spin changes orientation. The transition between 1 and 4 happens because of Nuclear spin dephasing.

The system can be split into two different parts, one part with the first three energy levels, see figure A.1a, where population is coherent controlled with the two applied lasers, and a fourth level that is only coupled to the other three levels with decay rates in figure A.1b.

three level system The three level part can be described with the density matrix formalism described earlier. First the Hamiltonian must be specified.

$$\hat{H}(t) = \hat{H}_{atom} + \hat{V}_{int}(t) \tag{A.2}$$

where

$$\hat{H}_{atom} = \hbar \begin{pmatrix} \omega_1 & 0 & 0 \\ 0 & \omega_2 & 0 \\ 0 & 0 & \omega_3 \end{pmatrix} \tag{A.3}$$

The interaction part of the Hamiltonian V_{int} is described with the dipole coupling with the electric field of the applied lasers. $V_{int} = -\hat{\mu}\tilde{E}(t)$, where

$$\begin{aligned} \tilde{E}_c(t) &= E_c e^{-\omega_c t} + c.c. \\ \tilde{E}_p(t) &= E_p e^{-\omega_p t} + c.c. \end{aligned} \tag{A.4}$$

and the electric dipole operator can be represented by

$$\hat{\mu}(t) = \begin{pmatrix} 0 & 0 & \mu_{31}^* \\ 0 & 0 & \mu_{32}^* \\ \mu_{31} & \mu_{32} & 0 \end{pmatrix} \tag{A.5}$$

The diagonal elements are zero, because all three energy levels have distinct parity. The of diagonal element which are zero, are zero because these represent the forbidden dipole transitions. The relation $\mu_{ab} = \mu_{ba}^*$ is also used. $V_{int} = -\hat{\mu}\tilde{E}()$ becomes now

$$\hat{V}_{int} = -\begin{pmatrix} 0 & 0 & \mu_{31}^*\tilde{E}_p(t) \\ 0 & 0 & \mu_{32}^*\tilde{E}_c(t) \\ \mu_{31}\tilde{E}_p(t) & \mu_{32}\tilde{E}_c(t) & 0 \end{pmatrix} \tag{A.6}$$

$$\hat{H} = \hbar\begin{pmatrix} \omega_1 & 0 & -\mu_{31}^*\tilde{E}_p/\hbar \\ 0 & \omega_2 & -\mu_{32}^*\tilde{E}_c/\hbar \\ -\mu_{31}\tilde{E}_p/\hbar & -\mu_{32}\tilde{E}_c/\hbar & \omega_3 \end{pmatrix} = \hbar\begin{pmatrix} \omega_1 & 0 & -\frac{1}{2}\Omega_p^*(t) \\ 0 & \omega_2 & -\frac{1}{2}\Omega_c^*(t) \\ -\frac{1}{2}\Omega_p(t) & -\frac{1}{2}\Omega_c(t) & \omega_3 \end{pmatrix} \tag{A.7}$$

where the Rabi frequency Ω is defined as

$$\Omega = 2|\mu_{nm}||E|/\hbar \tag{A.8}$$

By the use of equation A.1 and the just derived Hamiltonian in equation A.7 the rate equations can be derived

$$\begin{aligned}
\dot{\rho}_{11} &= \tfrac{1}{2}\Omega_p(t)\rho_{13} - \tfrac{1}{2}\Omega_p^*(t)\rho_{31} \\
\dot{\rho}_{22} &= \tfrac{1}{2}\Omega_c(t)\rho_{23} - \tfrac{1}{2}\Omega_c^*(t)\rho_{32} \\
\dot{\rho}_{33} &= -\tfrac{1}{2}\Omega_p(t)\rho_{13} - \tfrac{1}{2}\Omega_c(t)\rho_{23} + \tfrac{1}{2}\Omega_p^*(t)\rho_{31} + \tfrac{1}{2}\Omega_c^*(t)\rho_{32} \\
\dot{\rho}_{21} &= -i\omega_{21}\rho_{21} + \tfrac{1}{2}i\Omega_c^*(t)\rho_{31} - \tfrac{1}{2}i\Omega_p(t)\rho_{23} \\
\dot{\rho}_{31} &= -i\omega_{31}\rho_{31} - \tfrac{1}{2}i\Omega_p(t)(\rho_{33} - \rho_{11}) + \tfrac{1}{2}i\Omega_c(t)\rho_{21} \\
\dot{\rho}_{32} &= -i\omega_{32}\rho_{32} - \tfrac{1}{2}i\Omega_c(t)(\rho_{33} - \rho_{22}) + \tfrac{1}{2}i\Omega_p(t)\rho_{12}
\end{aligned} \tag{A.9}$$

In a rotating wave approximation the system is described with the components as a product of a slow and a fast varying part in time.

$$\begin{aligned}
\rho_{31} &= \sigma_{31}e^{-i\omega_p t} \\
\rho_{32} &= \sigma_{32}e^{-i\omega_c t} \\
\rho_{21} &= \sigma_{21}e^{-i(\omega_p - \omega_c)t}
\end{aligned} \tag{A.10}$$

plugging these into equation A.9

$$\begin{aligned}
\dot{\rho}_{11} &= \tfrac{1}{2}\Omega_p\sigma_{13} - \tfrac{1}{2}\Omega_p^*\sigma_{31} \\
\dot{\rho}_{22} &= \tfrac{1}{2}\Omega_c\sigma_{23} - \tfrac{1}{2}\Omega_c^*\sigma_{32} \\
\dot{\rho}_{33} &= -\tfrac{1}{2}\Omega_p\sigma_{13} - \tfrac{1}{2}\Omega_c\sigma_{23} + \tfrac{1}{2}\Omega_p^*\sigma_{31} + \tfrac{1}{2}\Omega_c^*\sigma_{32} \\
\dot{\sigma}_{21} &= i\delta\sigma_{21} + \tfrac{1}{2}i\Omega_c^*\sigma_{31} - \tfrac{1}{2}i\Omega_p\sigma_{23} \\
\dot{\sigma}_{31} &= i\Delta_p\sigma_{31} - \tfrac{1}{2}i\Omega_p(\rho_{33} - \rho_{11}) + \tfrac{1}{2}i\Omega_c\sigma_{21} \\
\dot{\sigma}_{32} &= i\Delta_c\sigma_{32} - \tfrac{1}{2}i\Omega_c(\rho_{33} - \rho_{22}) + \tfrac{1}{2}i\Omega_p\sigma_{12}
\end{aligned} \tag{A.11}$$

In all equations the fast oscillating terms $e^{\pm 2\omega_{p,c}}$ are neglected. For example the derivation of the first row

$$\frac{1}{2}\Omega_p(e^{-i\omega_p t} + e^{+i\omega_p t})\sigma_{13}e^{-i\omega_p t} = \frac{1}{2}\Omega_p(e^{-i2\omega_p t} + 1)\sigma_{13} \approx \frac{1}{2}\Omega_p\sigma_{13} \tag{A.12}$$

here the term $e^{-i2\omega_p t}$ can be neglected, because the oscillation is to fast for the system to respond. This is called the Rotating Wave Equation RWA. The derivation of the fourth row for example

$$\begin{aligned}
&\dot{\sigma}_{21}e^{-i(\omega_p-\omega_c)t} + \sigma_{21}(-i(\omega_p-\omega_c))e^{-i(\omega_p-\omega_c)t} \\
&= -i\omega_{21}\sigma_{21}e^{-i(\omega_p-\omega_c)t} + \tfrac{1}{2}i\Omega_c^*(t)\sigma_{31}e^{-i\omega_p t} - \tfrac{1}{2}i\Omega_p(t)\sigma_{23}e^{+i\omega_c t} \\
&\dot{\sigma}_{21} = i(-\omega_{21}+\omega_p-\omega_c)\sigma_{21} + \tfrac{1}{2}i\Omega_c^*(t)\sigma_{31}e^{+i\omega_c t} - \tfrac{1}{2}i\Omega_p(t)\sigma_{23}e^{+i\omega_p t} \\
&\dot{\sigma}_{21} \approx i\delta\sigma_{21} + \tfrac{1}{2}i\Omega_c^*\sigma_{31} - \tfrac{1}{2}i\Omega_p\sigma_{23}
\end{aligned} \tag{A.13}$$

Where $\delta = \Delta_p - \Delta_c = (\omega_p - \omega_{31}) - (\omega_c - \omega_{32}) = -\omega_{21} + \omega_p - \omega_c$ and in the last step the fast oscillating terms are neglected(RWA). The RWA applied on these rate equations can also be put in a RWA Hamiltonian, which will give the same result when using this to derive the time dependence from equation A.1

$$\hat{H} = \hbar \begin{pmatrix} 0 & 0 & -\frac{1}{2}\Omega_p^* \\ 0 & -(\Delta_p - \Delta_c) & -\frac{1}{2}\Omega_c^* \\ -\frac{1}{2}\Omega_p & -\frac{1}{2}\Omega_c & -\Delta_p \end{pmatrix} \tag{A.14}$$

To make the rate equations complete all decay and dephasing rates have to be added. Looking at figure A.1b the decay rates per level can be summed and afterwards be added in the rate equations. In some literature the relaxation terms are a result of a relaxation operator, a so called Liouville operator $\hat{L}$, but here is chosen to explicitly write out all the relaxation terms and implement them in the rate equations. The longitudinal and transverse decay rates respectively $\Gamma_{nn} = T_{1,n}^{-1}$ and $\gamma_{nm} = T_{2,nm}^{-1}$ are defined as followed. Population in state $|m\rangle$ $\rho_{mm} \equiv \overline{C_m C_m^*}$ decays with $e^{-\Gamma_{mm}t}$. The decay rate from a certain level is the net result of the sum of outwards and inwards decay rates from other levels. The longitudinal decay rates Γ_{mm}, are defined as $\Gamma_{mm}\rho_{mm} = \sum_{p,k}(\Gamma_{mp}\rho_{mm} - \Gamma_{km}\rho_{kk})$. Where Γ_{mm} is the rate of population from level m outwards. Γ_{nm} is the rate of population from level n to m. The transverse decay rates γ_{nm}, the so called dephasings, can be derived from the longitudinal decay rates. The probability amplitude C_m decays with $e^{-\Gamma_{mm}t/2}$, so the coherence $\rho_{nm} \equiv \overline{C_n C_m^*}$ decays with $e^{-\gamma_{nm}t}$, where $\gamma_{nm} = (\Gamma_{nn} + \Gamma_{mm})/2$.

Including decay rates Level four can now also be included by simply adding as the decay rates of level four

$$\begin{aligned}
\Gamma_{11}\rho_{11} &= -\Gamma_{31}\rho_{33} - \Gamma_{21}\rho_{22} + \Gamma_{12}\rho_{11} - \Gamma_{41}\rho_{44} + \Gamma_{14}\rho_{11} \\
\Gamma_{22}\rho_{22} &= -\Gamma_{32}\rho_{33} - \Gamma_{12}\rho_{11} + \Gamma_{21}\rho_{22} \\
\Gamma_{33}\rho_{33} &= +\Gamma_{31}\rho_{33} + \Gamma_{32}\rho_{33} + \Gamma_{34}\rho_{33} \\
\Gamma_{44}\rho_{44} &= -\Gamma_{34}\rho_{33} + \Gamma_{41}\rho_{44} - \Gamma_{14}\rho_{11}
\end{aligned} \tag{A.15}$$

The dephasings are defined like

$$\begin{aligned}
\gamma_{12} &= \tfrac{1}{2}(\Gamma_{11} + \Gamma_{22}) + \gamma_{1,deph} + \gamma_{2,deph} \\
\gamma_{13} &= \tfrac{1}{2}(\Gamma_{11} + \Gamma_{33}) + \gamma_{1,deph} + \gamma_{3,deph} \\
\gamma_{23} &= \tfrac{1}{2}(\Gamma_{22} + \Gamma_{33}) + \gamma_{2,deph} + \gamma_{3,deph} \\
\gamma_{21} &= \tfrac{1}{2}(\Gamma_{22} + \Gamma_{11}) + \gamma_{2,deph} + \gamma_{1,deph} \\
\gamma_{31} &= \tfrac{1}{2}(\Gamma_{33} + \Gamma_{11}) + \gamma_{3,deph} + \gamma_{1,deph} \\
\gamma_{32} &= \tfrac{1}{2}(\Gamma_{33} + \Gamma_{22}) + \gamma_{3,deph} + \gamma_{2,deph}
\end{aligned} \tag{A.16}$$

Where $\gamma_{n,deph}$ are the proper/pure dephasing rates due to energy-conservative decoherence processes such as collisions. Implementing all decay and dephasing rates in the rate equations the

rate equations become

$$\begin{aligned}
\dot{\rho}_{11} &= \tfrac{1}{2}\Omega_p\sigma_{13} - \tfrac{1}{2}\Omega_p^*\sigma_{31} - \Gamma_{11}\rho_{11} \\
\dot{\rho}_{22} &= \tfrac{1}{2}\Omega_c\sigma_{23} - \tfrac{1}{2}\Omega_c^*\sigma_{32} - \Gamma_{22}\rho_{22} \\
\dot{\rho}_{33} &= -\tfrac{1}{2}\Omega_p\sigma_{13} - \tfrac{1}{2}\Omega_c\sigma_{23} + \tfrac{1}{2}\Omega_p^*\sigma_{31} + \tfrac{1}{2}\Omega_c^*\sigma_{32} - \Gamma_{33}\rho_{33} \\
\dot{\rho}_{44} &= -\Gamma_{44}\rho_{44} \\
\dot{\sigma}_{21} &= i\delta\sigma_{21} + \tfrac{1}{2}i\Omega_c^*\sigma_{31} - \tfrac{1}{2}i\Omega_p\sigma_{23} - \gamma_{21}\sigma_{21} \\
\dot{\sigma}_{31} &= i\Delta_p\sigma_{31} - \tfrac{1}{2}i\Omega_p(\rho_{33} - \rho_{11}) + \tfrac{1}{2}i\Omega_c\sigma_{21} - \gamma_{31}\sigma_{31} \\
\dot{\sigma}_{32} &= i\Delta_c\sigma_{32} - \tfrac{1}{2}i\Omega_c(\rho_{33} - \rho_{22}) + \tfrac{1}{2}i\Omega_p\sigma_{12} - \gamma_{32}\sigma_{32}
\end{aligned} \tag{A.17}$$

Steady state solutions for this 4 energy level model are given with all the equations set to be equal to zero. To calculate the susceptibility $\chi(\omega_p)$ of this model to the incoming probe bundle, the expectation value of the dipole moment is needed. The susceptibility of a medium is defined like

$$P = \epsilon_0 \chi E \tag{A.18}$$

$$P(t) = N\left\langle\hat{\mu}(t)\right\rangle = N \cdot Tr[\hat{\rho}(t)\hat{\mu}(t)] = N\left[(\rho_{31}(t)\mu_{13} + \rho_{32}(t)\mu_{23} + c.c.)\right] \tag{A.19}$$

Looking at the response of the system to the probe laser, only the terms that are on resonance with the probe are considered, so the term with μ_{23} can be neglected.

$$\chi(\omega_p) = \frac{N\langle\hat{\mu}(t)\rangle}{\epsilon_0 E(\omega_p)} \approx \frac{N(\sigma_{31}e^{-i\omega_p t}\mu_{13} + \sigma_{13}e^{+i\omega_p t}\mu_{31})}{\epsilon_0(E_p e^{-i\omega_p t})} \approx \frac{\mu_{13}\sigma_{31}}{\epsilon_0 E_p} = \frac{2|\mu_{13}|^2\sigma_{31}}{\epsilon_0\hbar\Omega p} \tag{A.20}$$

In the first approximation, the complex part of the applied probe field can be neglected because of RWA, because ρ_{31} tends to evolve in time as $e^{-i\omega_{31}t}$. In the second approximation, the fast oscillating term $+2i\omega_p t$ is neglected (RWA).

For an analytically solution, replace σ_{31} with the steady state solution for σ_{31} from equation A.17, neglecting the term depending on the control field. Remind that in the steady state solution from equation A.17, due to the RWA, the fast oscillating terms $\pm i2\omega_p t$ are neglected. Then we end up with the expression for $\chi(\omega_p)$

$$\chi(\omega_p) = \frac{N[(\frac{1}{(\Delta_p - i\gamma_{31})}\mu_{31}E_p(\rho_{33}-\rho_{11})/\hbar)e^{-i\omega_p t}\mu_{13} + c.c.]}{\epsilon_0(E_p e^{-i\omega_p t} + c.c.)} = \frac{N|\mu_{13}|^2(\rho_{33}-\rho_{11})}{\hbar(\Delta_p - i\gamma_{31})\epsilon_0} \tag{A.21}$$

Results of Matlab simulation

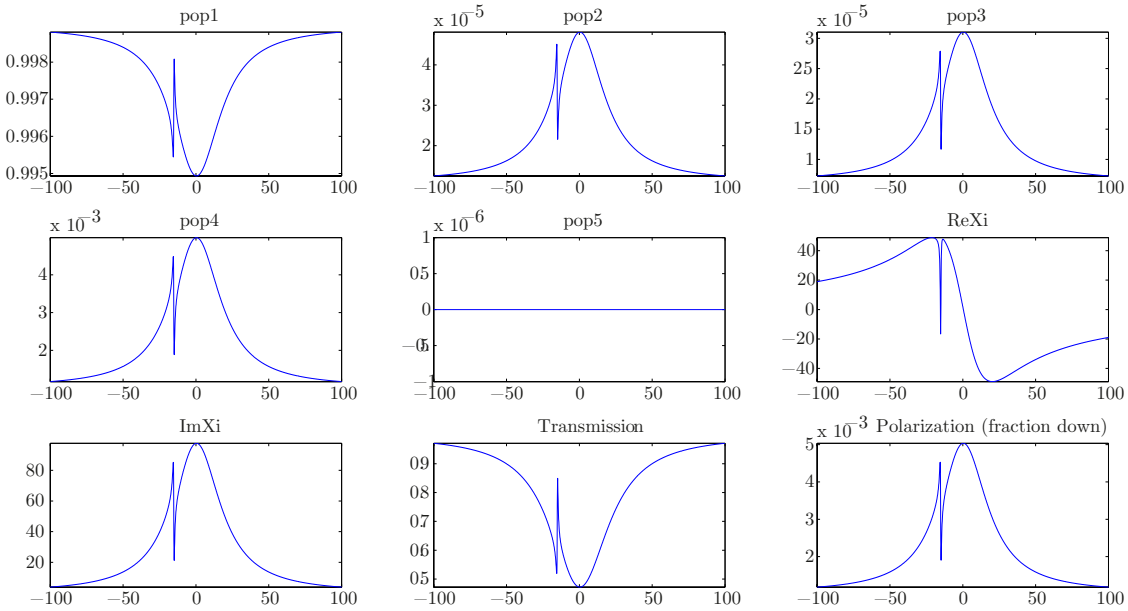

Figure A.2: Steady state solutions. Horizontally the detuning of the probe laser, which is scanning over the transition $|1\rangle - |3\rangle$. Steady state populations are plotted for the four levels, depending on the detuning of the probe laser. There is also a fifth level plotted, but the decays to this level is put to zero. This is an extension already for including more levels. The Matlab code can be found in appendix D. The overall peak is due to absorption of the probe laser at resonance between level 1 and 3 in figure A.1. The small peak inside the overall peak is due to destructive interference of the probe and control laser, this phenomena is called Electronically Induced Transparency, shortly EIT. Where population is trapped in the lower to states 1 and 2, and absorption of the prope laser is reduced. This is the so called dark state.

Appendix B

Transition schemes Low Fields

B.1 Introduction

In this Appendix chapter the remaining transition diagrams for the different systems coupled to different number of nuclear spins are summed. The transition strengths for each diagram are summed in a matrix. The matrices contain the dipole coupling strengths for each combination of states between the ground level and excited level. The ground states are ordered as shown in the diagram from left to right horizontal in the matrix. The excited states are ordered vertical in the matrix in the order as shown in the diagram. So for example the transition strength between the first ground level and the sixth excited level shown in the transition diagram 5.2, the ground state $|1,-1\rangle$ and the excited state $|2,0\rangle$, can be found in the first column and in the sixth row. The transition strength between these two states is thus 1/36. These transition strengths are calculated with the help of equation 3.30. The transition strengths for excitation and for emission are the same, this was derived in equation 3.7 where in both expressions for emission and absorption the same electric dipole moment appears.

B.2 GaAs coupled to one nucleus spin 3/2

$$\begin{pmatrix}
0 & 0 & 0 & 0 & 0 & 0 & \frac{1}{5} & 0 \\
0 & 0 & 0 & 0 & 0 & 0 & 0 & \frac{8}{45} \\
0 & 0 & 0 & \frac{1}{9} & 0 & 0 & 0 & 0 \\
0 & 0 & 0 & 0 & 0 & 0 & 0 & 0 \\
0 & 0 & 0 & 0 & 0 & \frac{8}{45} & 0 & 0 \\
0 & \frac{1}{9} & 0 & 0 & 0 & 0 & 0 & 0 \\
0 & 0 & \frac{1}{12} & 0 & 0 & 0 & 0 & \frac{1}{36} \\
0 & 0 & 0 & \frac{1}{9} & 0 & 0 & 0 & 0 \\
0 & 0 & 0 & 0 & \frac{1}{9} & 0 & 0 & 0 \\
0 & 0 & 0 & 0 & 0 & \frac{8}{45} & 0 & 0 \\
0 & 0 & 0 & 0 & 0 & 0 & \frac{1}{45} & 0 \\
0 & 0 & \frac{5}{36} & 0 & 0 & 0 & 0 & \frac{1}{60} \\
0 & 0 & 0 & 0 & 0 & 0 & 0 & 0 \\
0 & 0 & 0 & 0 & \frac{1}{9} & 0 & 0 & 0 \\
\frac{5}{36} & 0 & 0 & 0 & 0 & \frac{1}{60} & 0 & 0 \\
0 & \frac{1}{9} & 0 & 0 & 0 & 0 & 0 & 0
\end{pmatrix} \tag{B.1}$$

Excitation and emission transition strengths at zero field, for q=0-polarization, for a system coupled to one nuclear spin 3/2. The transition diagram was already given in figure 5.2*a*

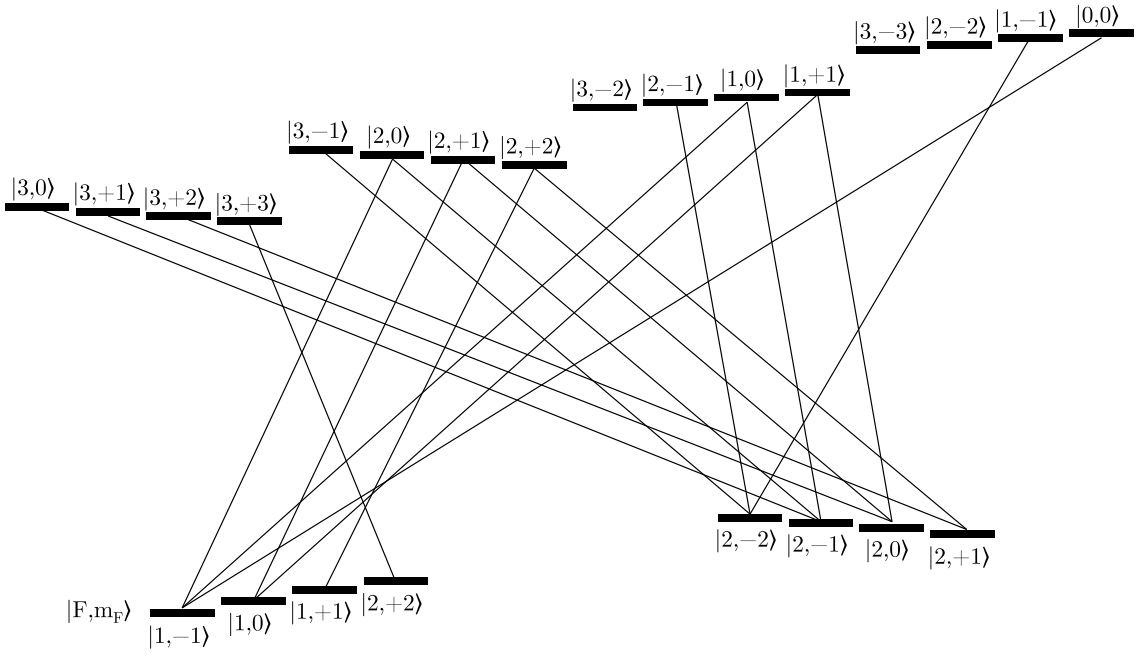

$$\begin{pmatrix}
0 & 0 & 0 & 0 & 0 & \frac{1}{15} & 0 & 0 \\
0 & 0 & 0 & 0 & 0 & 0 & \frac{2}{15} & 0 \\
0 & 0 & 0 & 0 & 0 & 0 & 0 & \frac{2}{9} \\
0 & 0 & 0 & \frac{1}{3} & 0 & 0 & 0 & 0 \\
0 & 0 & 0 & 0 & \frac{1}{45} & 0 & 0 & 0 \\
\frac{1}{36} & 0 & 0 & 0 & 0 & \frac{1}{12} & 0 & 0 \\
0 & \frac{1}{12} & 0 & 0 & 0 & 0 & \frac{1}{12} & 0 \\
0 & 0 & \frac{1}{6} & 0 & 0 & 0 & 0 & \frac{1}{18} \\
0 & 0 & 0 & 0 & 0 & 0 & 0 & 0 \\
0 & 0 & 0 & 0 & \frac{1}{45} & 0 & 0 & 0 \\
\frac{5}{36} & 0 & 0 & 0 & 0 & \frac{1}{60} & 0 & 0 \\
0 & \frac{5}{36} & 0 & 0 & 0 & 0 & \frac{1}{180} & 0 \\
0 & 0 & 0 & 0 & 0 & 0 & 0 & 0 \\
0 & 0 & 0 & 0 & 0 & 0 & 0 & 0 \\
0 & 0 & 0 & 0 & \frac{1}{30} & 0 & 0 & 0 \\
\frac{1}{9} & 0 & 0 & 0 & 0 & 0 & 0 & 0
\end{pmatrix}$$

Transition diagram including strongly allowed excitations and emissions for $q = +1$-polarization at the low field. Its corresponding matrix, containing the transition strengths at zero field. For a system coupled to one nuclear spin 3/2.

(B.2)

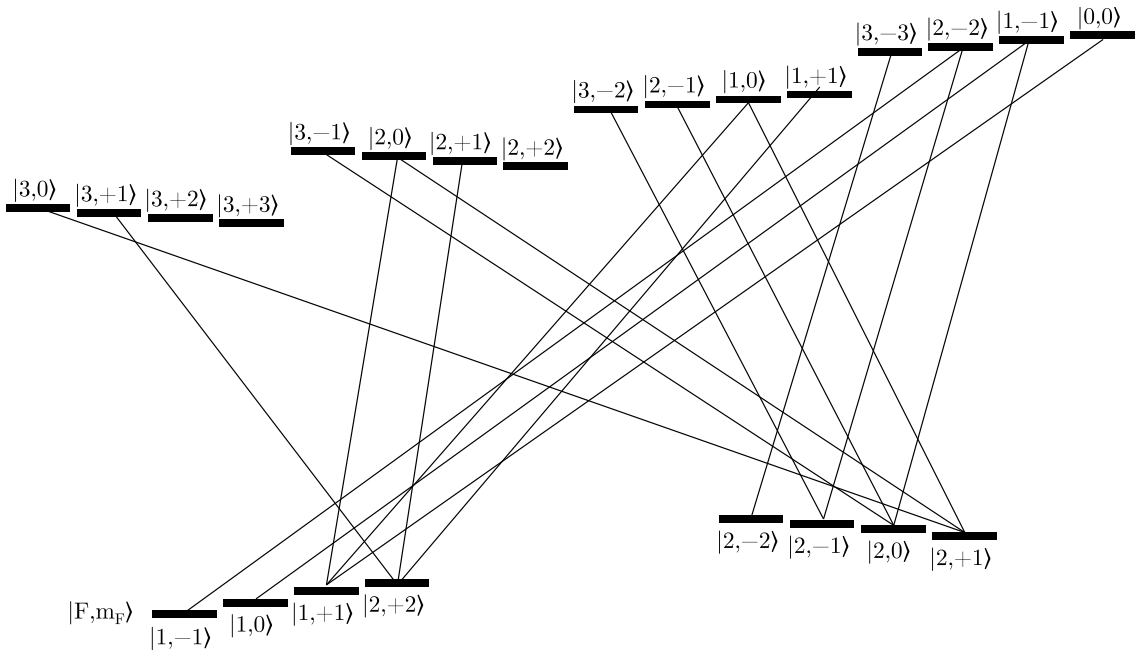

$$\begin{pmatrix}
0 & 0 & 0 & 0 & 0 & 0 & 0 & \frac{1}{15} \\
0 & 0 & 0 & \frac{1}{45} & 0 & 0 & 0 & 0 \\
0 & 0 & 0 & 0 & 0 & 0 & 0 & 0 \\
0 & 0 & 0 & 0 & 0 & 0 & 0 & 0 \\
0 & 0 & 0 & 0 & 0 & 0 & \frac{2}{15} & 0 \\
0 & 0 & \frac{1}{36} & 0 & 0 & 0 & 0 & \frac{1}{12} \\
0 & 0 & 0 & \frac{1}{18} & 0 & 0 & 0 & 0 \\
0 & 0 & 0 & 0 & 0 & 0 & 0 & 0 \\
0 & 0 & 0 & 0 & 0 & \frac{2}{9} & 0 & 0 \\
0 & 0 & 0 & 0 & 0 & 0 & \frac{2}{15} & 0 \\
0 & 0 & \frac{5}{36} & 0 & 0 & 0 & 0 & \frac{1}{60} \\
0 & 0 & 0 & \frac{1}{30} & 0 & 0 & 0 & 0 \\
0 & 0 & 0 & 0 & \frac{1}{3} & 0 & 0 & 0 \\
\frac{1}{6} & 0 & 0 & 0 & 0 & \frac{1}{18} & 0 & 0 \\
0 & \frac{5}{36} & 0 & 0 & 0 & 0 & \frac{1}{180} & 0 \\
0 & 0 & \frac{1}{9} & 0 & 0 & 0 & 0 & 0
\end{pmatrix}$$

Transition diagram including strongly allowed excitation and emission transitions for q=-1 polarization at the low field. Its corresponding matrix,
containing the transition strengths at zero field. For a system coupled to one nuclear spin 3/2.
(B.3)

B.3 ZnSe coupled to one nucleus spin 1/2

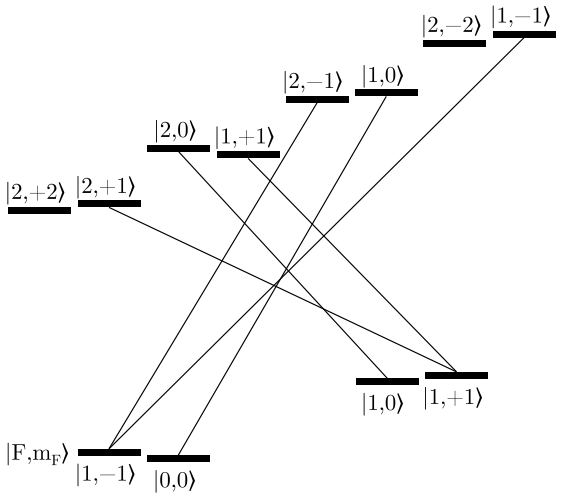

$$\begin{pmatrix} 0 & 0 & 0 & 0 \\ 0 & 0 & 0 & \frac{1}{6} \\ 0 & 0 & \frac{2}{9} & 0 \\ 0 & 0 & 0 & \frac{1}{18} \\ \frac{1}{6} & 0 & 0 & 0 \\ 0 & \frac{2}{9} & 0 & 0 \\ 0 & 0 & 0 & 0 \\ \frac{1}{18} & 0 & 0 & 0 \end{pmatrix}$$

Transition diagram including strongly allowed excitations and emissions for q=0 polarization at low field and its corresponding matrix, containing the transition strengths at zero field. For a system coupled to one nuclear spin 1/2.

(B.4)

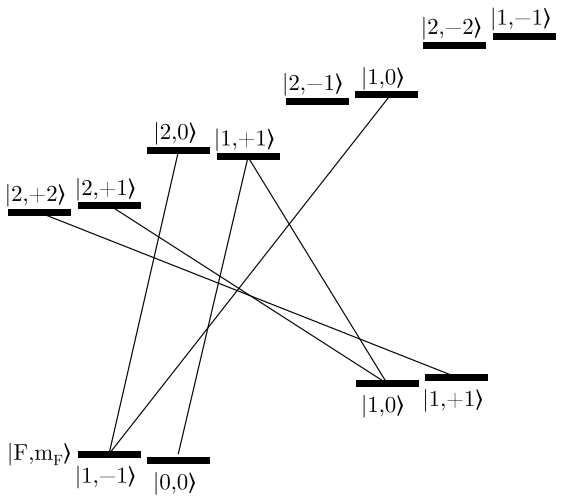

$$\begin{pmatrix} 0 & 0 & 0 & \frac{1}{3} \\ 0 & 0 & \frac{1}{6} & 0 \\ \frac{1}{18} & 0 & 0 & 0 \\ 0 & \frac{2}{9} & \frac{1}{18} & 0 \\ 0 & 0 & 0 & 0 \\ \frac{1}{18} & 0 & 0 & 0 \\ 0 & 0 & 0 & 0 \\ 0 & 0 & 0 & 0 \end{pmatrix}$$

Transition diagram including strongly allowed excitations and emissions for q=+1 polarization in low field and its corresponding matrix, containing the transition strengths at zero field. For a system coupled to one nuclear spin 1/2.

(B.5)

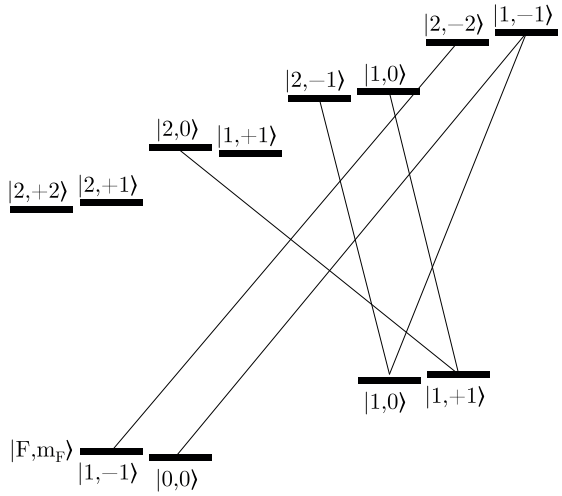

$$\begin{pmatrix} 0 & 0 & 0 & 0 \\ 0 & 0 & 0 & 0 \\ 0 & 0 & 0 & \frac{1}{18} \\ 0 & 0 & 0 & 0 \\ 0 & 0 & \frac{1}{6} & 0 \\ 0 & 0 & 0 & \frac{1}{18} \\ \frac{1}{3} & 0 & 0 & 0 \\ 0 & \frac{2}{9} & \frac{1}{18} & 0 \end{pmatrix}$$

Transition diagram including strongly allowed excitations and emissions for q=-1 polarization at low field. and its corresponding matrix, containing the transition strengths at zero field. For a system coupled to one nuclear spin 1/2.

(B.6)

B.4 ZnSe coupled to two nuclei spin 1/2

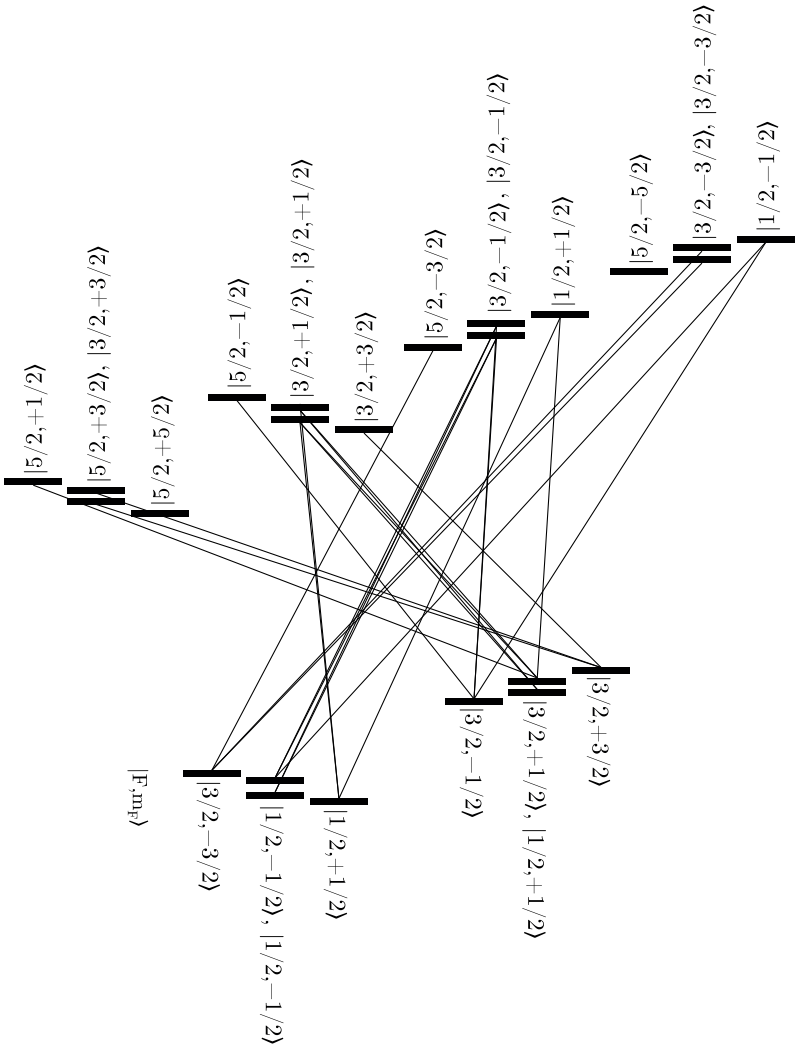

$$\begin{pmatrix}
0 & 0 & 0 & 0 & 0 & \frac{1}{5} & 0 & 0 \\
0 & 0 & 0 & 0 & 0 & 0 & 0 & \frac{2}{15} \\
0 & 0 & 0 & 0 & 0 & 0 & 0 & \frac{4}{45} \\
0 & 0 & 0 & 0 & 0 & 0 & 0 & 0 \\
0 & 0 & 0 & 0 & \frac{1}{5} & 0 & 0 & 0 \\
0 & 0 & 0 & \frac{10}{81} & 0 & \frac{4}{405} & \frac{2}{9} & 0 \\
0 & 0 & 0 & \frac{10}{81} & 0 & \frac{4}{405} & \frac{2}{9} & 0 \\
0 & 0 & 0 & 0 & 0 & 0 & 0 & \frac{4}{45} \\
\frac{2}{15} & 0 & 0 & 0 & 0 & 0 & 0 & 0 \\
0 & \frac{10}{81} & \frac{2}{9} & 0 & \frac{4}{405} & 0 & 0 & 0 \\
0 & \frac{10}{81} & \frac{2}{9} & 0 & \frac{4}{405} & 0 & 0 & 0 \\
0 & 0 & 0 & \frac{8}{81} & 0 & \frac{1}{81} & 0 & 0 \\
0 & 0 & 0 & 0 & 0 & 0 & 0 & 0 \\
\frac{4}{45} & 0 & 0 & 0 & 0 & 0 & 0 & 0 \\
\frac{4}{45} & 0 & 0 & 0 & 0 & 0 & 0 & 0 \\
0 & \frac{8}{81} & 0 & 0 & \frac{1}{81} & 0 & 0 & 0
\end{pmatrix}$$

Transition diagram including strongly allowed excitations and emissions for q=0 polarization at low field. and its corresponding matrix, containing the transition strengths at zero field. For a system coupled to two nuclear spins 1/2.

(B.7)

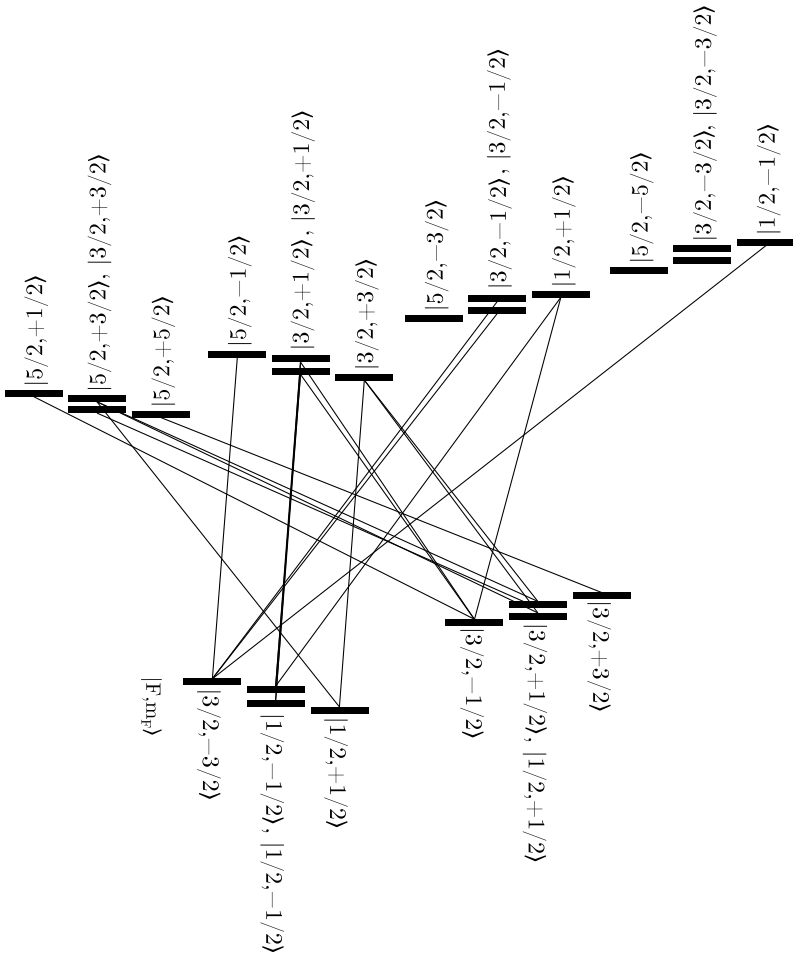

$$\begin{pmatrix}
0 & 0 & 0 & 0 & \frac{1}{10} & 0 & 0 & 0 \\
0 & 0 & 0 & 0 & 0 & \frac{1}{5} & 0 & 0 \\
0 & 0 & 0 & \frac{5}{27} & 0 & \frac{8}{135} & \frac{1}{3} & 0 \\
0 & 0 & 0 & 0 & 0 & 0 & 0 & \frac{1}{3} \\
\frac{1}{30} & 0 & 0 & 0 & 0 & 0 & 0 & 0 \\
0 & \frac{5}{81} & \frac{1}{9} & 0 & \frac{32}{405} & 0 & 0 & 0 \\
0 & \frac{5}{81} & \frac{1}{9} & 0 & \frac{32}{405} & 0 & 0 & 0 \\
0 & 0 & 0 & \frac{5}{27} & 0 & \frac{8}{135} & \frac{1}{3} & 0 \\
0 & 0 & 0 & 0 & 0 & 0 & 0 & 0 \\
\frac{8}{135} & 0 & 0 & 0 & 0 & 0 & 0 & 0 \\
\frac{8}{135} & 0 & 0 & 0 & 0 & 0 & 0 & 0 \\
0 & \frac{16}{81} & 0 & 0 & \frac{1}{162} & 0 & 0 & 0 \\
0 & 0 & 0 & 0 & 0 & 0 & 0 & 0 \\
0 & 0 & 0 & 0 & 0 & 0 & 0 & 0 \\
0 & 0 & 0 & 0 & 0 & 0 & 0 & 0 \\
\frac{1}{54} & 0 & 0 & 0 & 0 & 0 & 0 & 0
\end{pmatrix}$$

Transition diagram including strongly allowed excitations and emissions for q=+1 polarization at low field. and its corresponding matrix, containing the transition strengths at zero field. For a system coupled to two nuclear spins 1/2.

(B.8)

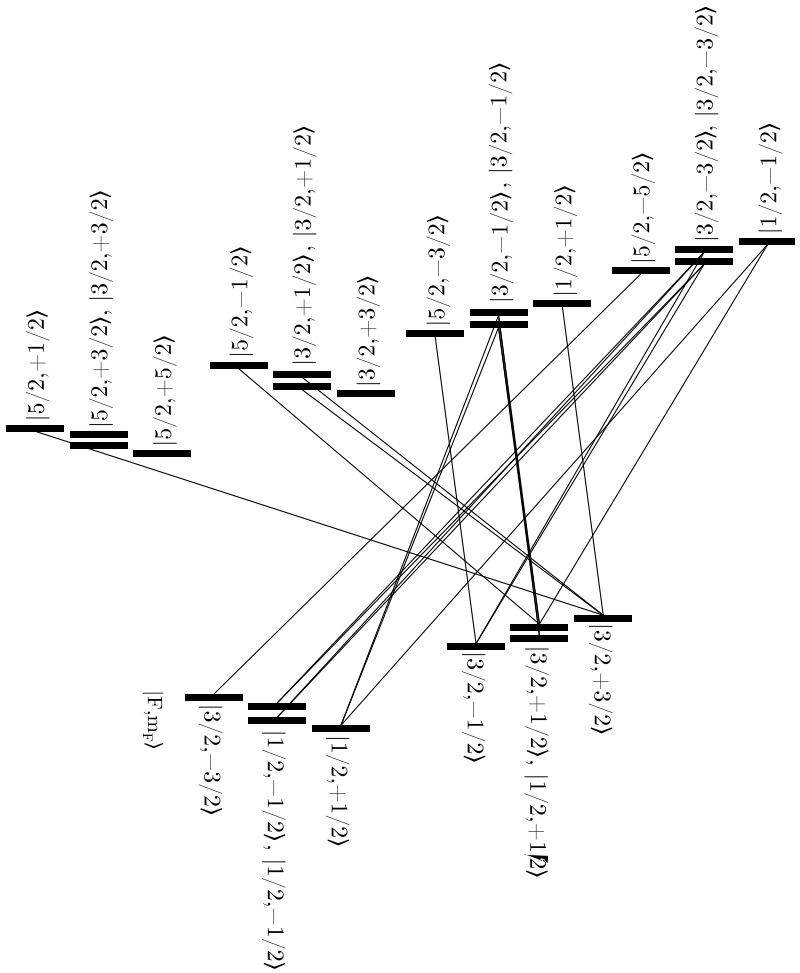

$$\begin{pmatrix}
0 & 0 & 0 & 0 & 0 & 0 & 0 & \frac{1}{30} \\
0 & 0 & 0 & 0 & 0 & 0 & 0 & 0 \\
0 & 0 & 0 & 0 & 0 & 0 & 0 & 0 \\
0 & 0 & 0 & 0 & 0 & 0 & 0 & 0 \\
0 & 0 & 0 & 0 & 0 & \frac{1}{10} & 0 & 0 \\
0 & 0 & 0 & 0 & 0 & 0 & 0 & \frac{8}{135} \\
0 & 0 & 0 & 0 & 0 & 0 & 0 & \frac{8}{135} \\
0 & 0 & 0 & 0 & 0 & 0 & 0 & 0 \\
0 & 0 & 0 & 0 & \frac{1}{5} & 0 & 0 & 0 \\
0 & 0 & 0 & \frac{5}{81} & 0 & \frac{32}{405} & \frac{1}{9} & 0 \\
0 & 0 & 0 & \frac{5}{81} & 0 & \frac{32}{405} & \frac{1}{9} & 0 \\
0 & 0 & 0 & 0 & 0 & 0 & 0 & \frac{1}{54} \\
\frac{1}{3} & 0 & 0 & 0 & 0 & 0 & 0 & 0 \\
0 & \frac{5}{27} & \frac{1}{3} & 0 & \frac{8}{135} & 0 & 0 & 0 \\
0 & \frac{5}{27} & \frac{1}{3} & 0 & \frac{8}{135} & 0 & 0 & 0 \\
0 & 0 & 0 & \frac{16}{81} & 0 & \frac{1}{162} & 0 & 0
\end{pmatrix}$$

Transition diagram including strongly allowed excitations and emissions for q=-1 at low field. and its corresponding matrix, containing the transition strengths at zero field. For a system coupled to two nuclear spins 1/2.

(B.9)

Appendix C

Transition schemes High field

C.1 Introduction

For the high field limit the transition schemes are less complicated. One can see that transitions are allowed between the sub levels, the restriction is that a transition is only allowed when no nuclear spin is changed. Only the diagrams are shown, which are of interest for chapter 6. In Appendix F the Mathematica code is given for calculating the transition strengths.

C.2 Transition Schemes at high field

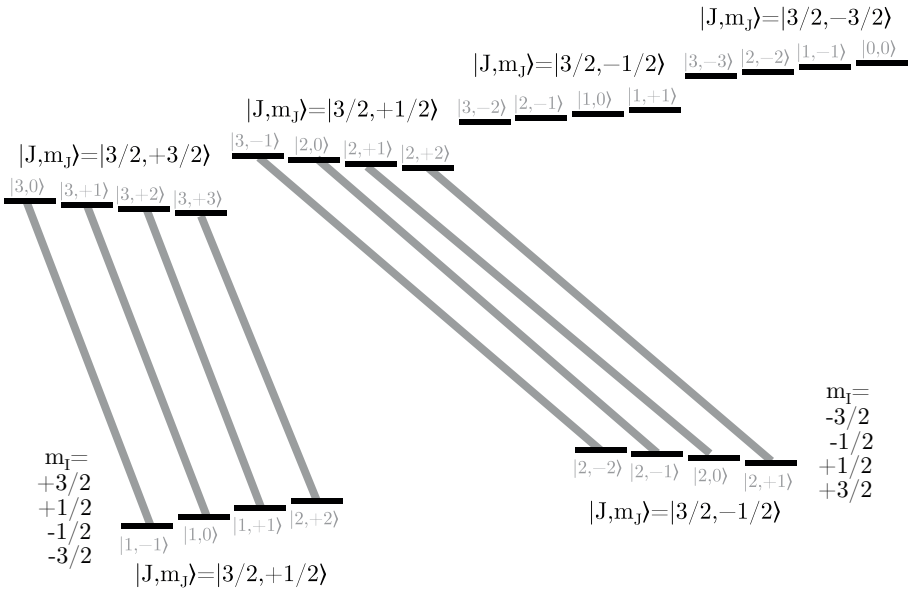

$$\begin{pmatrix}
\frac{2}{3} & 0 & 0 & 0 & 0 & 0 & 0 & 0 \\
0 & \frac{2}{3} & 0 & 0 & 0 & 0 & 0 & 0 \\
0 & 0 & \frac{2}{3} & 0 & 0 & 0 & 0 & 0 \\
0 & 0 & 0 & \frac{2}{3} & 0 & 0 & 0 & 0 \\
0 & 0 & 0 & 0 & 0 & 0 & 0 & \frac{2}{9} \\
0 & 0 & 0 & 0 & 0 & 0 & \frac{2}{9} & 0 \\
0 & 0 & 0 & 0 & 0 & \frac{2}{9} & 0 & 0 \\
0 & 0 & 0 & 0 & \frac{2}{9} & 0 & 0 & 0 \\
0 & 0 & 0 & 0 & 0 & 0 & 0 & 0 \\
0 & 0 & 0 & 0 & 0 & 0 & 0 & 0 \\
0 & 0 & 0 & 0 & 0 & 0 & 0 & 0 \\
0 & 0 & 0 & 0 & 0 & 0 & 0 & 0 \\
0 & 0 & 0 & 0 & 0 & 0 & 0 & 0 \\
0 & 0 & 0 & 0 & 0 & 0 & 0 & 0 \\
0 & 0 & 0 & 0 & 0 & 0 & 0 & 0 \\
0 & 0 & 0 & 0 & 0 & 0 & 0 & 0
\end{pmatrix}$$

transition strengths

Transition diagram including strongly allowed transitions for q=+1 polarization at high field. and its corresponding matrices, containing the transition strengths. For a system coupled to one nuclear spins 3/2.

(C.1)

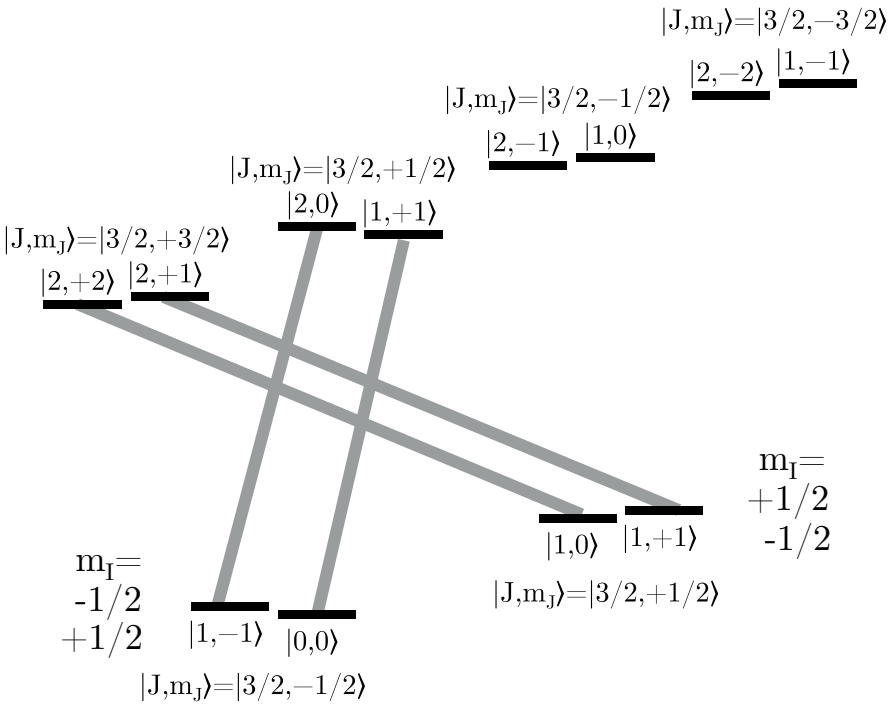

(C.2)

$$\begin{pmatrix} 0 & 0 & 0 & \frac{1}{6} \\ 0 & 0 & \frac{1}{6} & 0 \\ \frac{1}{18} & 0 & 0 & 0 \\ 0 & \frac{1}{18} & 0 & 0 \\ 0 & 0 & 0 & 0 \\ 0 & 0 & 0 & 0 \\ 0 & 0 & 0 & 0 \\ 0 & 0 & 0 & 0 \end{pmatrix}$$

transition strengths

Transition diagram including transitions for q=+1 polarization at high field. and its corresponding matrices, containing the transition strengths. For a system coupled to one nuclear spins 1/2.

Appendix D

Matlab code for the density matrix formalism

```
%%%%%%%%%%%%%%%%%%%%%%%%%%%%%%%% Labda-scheme %%%%%%%%%%%%%%%%%%%%%%%%%%%%%%%%%%%%

%                  .............w3
%      Δp |                      | Δc (negative detuning)
%                      *       *
%                     *         *
%                    *           *
%               wp  *              *wc
%                  *                *
%                 *                  *
%                *                    *
%              *              .............w2
%             *                                |
%           *                                  |Zeeman
%      .............w1                         |
%%%%%%%%%%%%%%%%%%%%%%%%%%%%%%%%%%%%%%%%%%%%%%%%%%%%%%%%%%%%%%%%%%%%%%%%%%%%%%%%%%
%%%%%%%%%%%%%%%%%%%%%%%% Decay rates in labda scheme %%%%%%%%%%%%%%%%%%%%%%%%%%%%

%                  .............w3      ------>
%                     |          |          G34
%                G31  |          |G32
%                     |          |
%                     <          >
%
%
%
%
%                               .............w2       G42
%                                                  ^----
%                                                  <---- .............w4
%      .............w1                             G41

%%%%%%%%%%%%%%%%%%%%%%%%%%%%%%%%%%%%%%%%%%%%%%%%%%%%%%%%%%%%%%%%%%%%%%%%%%%%%%%%%%

%begin code:
clear; clc;

%Adjustable>>>
%level on/or off
levelfour=1;%1 for on 0 for off
levelfive=0;%1 for on 0 for off

B=7;%tesla
P=0.01;%0.01;%probe beam intensity
```

```
C=1;%control beam intensity
Δc=−15;
T=4.2;%Kelvin

%%%%%%%%%%%%%%%%%%%%%%%%% Constants %%%%%%%%%%%%%%%%%%%%%%%%%%%%%%%%%%%%%%%%%%%%
hbar=1;%1.054571726E−34;%[J * sec]
muB=927.4E−26;%bohr magneton
muN=5.05078324E−27;%nuclear magneton
gN=5.4297;%g−factor nucleus fluor
ge=0.41;%g−factor electron
k=1.38E−23;
e0=8.854187817620E−12;%[C2N−1m−2]or[C2N−1]or[CV−1m− 1]
c=3E5;%m/ns
%Zeeman=g*muB*B/k;% Zeeman energy is ¬0.5 for 4.2K
u31=2*pi;
u32=2*pi;
mu=[0 0 conj(u31);0 0 conj(u32);u31 u32 0];
Wc=5;% Control field Rabi freq.
Wp=0.01;% Probe field Rabi freq.
N=50;%densityfactor

%%%%%%%%%%%%%%%%%%%%%%%%% Define decay rates %%%%%%%%%%%%%%%%%%%%%%%%%%%%%%%%%%
G31=0.1;%population decay from energy level w3 to w1
G32=0.1;%population decay from w3 to w2
G34=0.1*levelfour;%.1;%0.1;%2ns
G21=1/(1E6);%1millisec population decay from ws to wg, possible with nuclear flip flop
G12=G21*exp(−ge*muB*B/(T*k));%population decay from w1 to w2, possible with nuclear flip
     flop
G13=0;
G23=0;
G24=1/(1E3);%electric dipole forbidden, micro sec microwave transition
G42=G24*exp(−ge*muB*B/(T*k));%electric dipole forbidden, micro sec microwave transition
G43=0;
G41=1/(1E12)*levelfour;%1000sec Nuclear spin flip
G14=1/(1E12)*levelfour;%1000sec Nuclear spin flip or? G41*exp(−gN*muN*0.5*B/(T*k));
%decayrates concerning a fifth level
G51=1/(1E3)*levelfive;%electric dipole forbidden, micro sec microwave transition
G15=G51*exp(−ge*muB*B/(T*k))*levelfive;%electric dipole forbidden, micro sec microwave
    transition
G25=1/(1E12)*levelfive;%;%1000sec Nuclear spin flip
G52=1/(1E12)*levelfive;%1/(1E12);%1000sec Nuclear spin flip
G35=0*levelfive;
G53=0*levelfive;
G54=1/(1E6)*levelfive*levelfour;%1millisec Solid effect
G45=G54*exp(−ge*muB*B/(T*k))*levelfive*levelfour;

G11=G13+G12+G14−G31−G21−G41;
G22=G23+G21+G24−G12−G32−G42;
G33=G32+G31+G34−G23−G13−G43;
G44=G41+G43+G42−G14−G34−G24;

%%%%%%%%%%%%%%%%%%%%%%%%%%% Dephasing rates %%%%%%%%%%%%%%%%%%%%%%%%%%%%%%%%%%
sp=0;%adjust by hand to make plots in same plot with offset 0.5*sp above the first
supplot=sp*0.5;
g2deph=1/5;% 2 GHz 1/T2*
g3deph=20;% 22 GHz
g31=0.5*(G33+G11)+g3deph;
g21=0.5*(G22+G11)+g2deph;
g32=0.5*(G33+G22)+g3deph+g2deph;
g13=0.5*(G11+G33)+g3deph;
g23=0.5*(G22+G33)+g2deph+g3deph;
g12=0.5*(G11+G22)+g2deph;

k=1;%index
for Δp = −100:0.1:100

    Δptmp(k)=Δp;
```

```
    %%%%%%%%%%%%%%%%%%%%%%%% MatlabCodeRob %%%%%%%%%%%%%%%%%%%%%%%%%%%%%%%%%%
    H0 = hbar*[0 0 0; 0 (Δp-Δc) 0; 0 0 Δp];
    %Hint=-u*E
    Hint = 0.5*[0 0 conj(Wp);0 0 conj(Wc);Wp Wc 0];
    %H=H0+Hint
    H=H0+Hint;
    %elements   11  22  33  44  55  31  21  32  13  12  23
    RateEQ =      [   1 1   1   levelfour   levelfive   0   0   0   0   0   0;
                      -(G13+G12+G14+G15)    G21 G31 G41 G51 i*H(1,3)    i*H(1,2)    0
                          -i*H(3,1)   -i*H(2,1)   0;
                      G12   -(G23+G21+G24+G25)  G32 G42 G52 0   -i*H(1,2)   i*H(2,3)
                          0   i*H(2,1)    -i*H(3,2);
                      G13   G23 -(G32+G31+G34+G35)  G43 G53 -i*H(1,3)   0   -i*H(2,3)
                          i*H(3,1)    0   i*H(3,2);
                      G14   G24 G34 -(G41+G43+G42+G45)  G54 0   0   0   0   0   0;
                      G15   G25 G35 G45 -(G51+G53+G52+G54)  0   0   0   0   0   0;
                      i*H(3,1)  0   -i*H(3,1)   0   0   -g31-i*H(1,1)+i*H(3,3)  i*H(3,2)
                              -i*H(2,1)   0   0   0;
                      i*H(2,1)  -i*H(2,1)   0   0   0   i*H(2,3)    -g21+i*H(2,2)-i*H
                          (1,1)  0   0   0   -i*H(3,1);
                      0 i*H(3,2)    -i*H(3,2)   0   0   -i*H(1,2)   0   -g32+i*H(3,3)-i*
                          H(2,2)  0   i*H(3,1)    0;
                     -i*H(1,3)  0   i*H(1,3)    0   0   0   0   0   -g13+i*H(1,1)-i*H
                         (3,3)  -i*H(2,3)   i*H(1,2);
                     -i*H(1,2)  i*H(1,2)    0   0   0   0   0   i*H(1,3)    -i*H(3,2)
                         -g12-i*H(2,2)+i*H(1,1)  0;
                      0 -i*H(2,3)   i*H(2,3)    0   0   0   -i*H(1,3)   0   i*H(2,1)
                          0   -g23+i*H(2,2)-i*H(3,3)];

    BoundCond = [1 ; 0 ; 0 ; 0 ; 0 ; 0 ; 0 ; 0 ; 0 ; 0 ; 0];
    %density matrix is here column vector [totalpopulation
        ;11;22;33;44;55;31;21;32;13;12;23]

    rhoSteady  = RateEQ\BoundCond;  % solDensMatVec
    %%%%%%%%%%%%%%%%%%%%%%%%%%%%%%%%%%%%%%%%%%%%%%%%%%%%%%%%%%%%%%%%%%%%%%%%%%
    rho = [rhoSteady(1) rhoSteady(10) rhoSteady(9);rhoSteady(7) rhoSteady(2) rhoSteady
        (11);rhoSteady(6) rhoSteady(8) rhoSteady(3)]
    Xi= N*abs(u31)^2*rhoSteady(6)/(hbar*0.5*Wp)%removed e0 from expression
    ReXi(k) = real(Xi);%
    ImXi(k) = imag(Xi);%
    pop1(k) = real(rhoSteady(1));
    pop2(k) = real(rhoSteady(2));
    pop3(k) = real(rhoSteady(3));
    pop4(k) = real(rhoSteady(4));
    pop5(k) = real(rhoSteady(5));
    %total(k) = real(rhoSteady(1))+real(rhoSteady(2))+real(rhoSteady(3))+real(rhoSteady
        (4));
%     Absorb(k) = imag
    Transmission(k) = exp(-(2*pi/(817.35))*imag(Xi));%(2*pi/(817.35)+Δp)*imag(Xi)*10E-6)
        %wp=2*pi*frequency=2*pi*c/lambda=2*pi*c/(817.35E-9)+Δp
    Polarization(k) = (rhoSteady(2)+rhoSteady(4))/(rhoSteady(5)+rhoSteady(1)+rhoSteady
        (2)+rhoSteady(4));
    k=k+1;
end

variables = sprintf(' T= %0.1f  C=%0.2f P=%0.2f Δc=%0.1f  B=%0.1f Wc=%0.2f Wp=%0.3f G21
    =%0.6f G41=G14=%0.9f G32=G31=G34=%0.1f G12=%0.9f' ,T,C,P,Δc,B,Wc,Wp,G21,G41,G32,G12)

hold on
subplot(3,3,1),plot(Δptmp,pop1);
title('pop1');
maxX =  max(Δptmp);
minX = -maxX;
maxY =  max(pop1)%+0.000001;
minY =  min(pop1)%-0.000001;
axis([minX maxX minY maxY]);
```

```
subplot(3,3,2),plot(Δptmp,pop2);
title('pop2');
maxX =  max(Δptmp);
minX = -maxX;
maxY =  max(pop2);%+0.000001;
minY =  min(pop2);%-0.000001;
axis([minX maxX minY maxY]);

subplot(3,3,3),plot(Δptmp,pop3);
title('pop3');
maxX =  max(Δptmp);
minX = -maxX;
maxY =  max(pop3);%+0.000001;
minY =  min(pop3);%-0.000001;
axis([minX maxX minY maxY]);

subplot(3,3,4),plot(Δptmp,pop4);
title('pop4');
maxX =  max(Δptmp);
minX = -maxX;
maxY =  max(pop4)-0.000001*(levelfour-1);
minY =  min(pop4)+0.000001*(levelfour-1);
axis([minX maxX minY maxY]);

subplot(3,3,5),plot(Δptmp,pop5);
title('pop5');
maxX =  max(Δptmp);
minX = -maxX;
maxY =  max(pop5)-0.000001*(levelfive-1);
minY =  min(pop5)+0.000001*(levelfive-1);
axis([minX maxX minY maxY]);

subplot(3,3,6),plot(Δptmp,ReXi);
title('ReXi');
maxX =  max(Δptmp);
minX = -maxX;
maxY =  max(ReXi);%+0.000001;
minY =  min(ReXi);%-0.000001;
axis([minX maxX minY maxY]);

subplot(3,3,7),
plot(Δptmp,ImXi);
title('ImXi ');
maxX =  max(Δptmp);
minX = -maxX;
maxY =  max(ImXi);
minY =  min(ImXi);
axis([minX maxX minY maxY]);

subplot(3,3,8),
plot(Δptmp,Transmission+supplot);
title('Transmission');
maxX =  max(Δptmp);
minX = -maxX;
maxY =  max(Transmission);%+0.000001;
minY =  min(Transmission);%-0.000001;
axis([minX maxX minY maxY]);

subplot(3,3,9),
plot(Δptmp,Polarization);
title('Polarization (fraction down)');
maxX =  max(Δptmp);
minX = -maxX;
maxY =  max(Polarization);%+0.000001;
minY =  min(Polarization);%-0.000001;
axis([minX maxX minY maxY]);
```

Appendix E

Mathematica code for the field dependent energy diagrams

```
Clear["Global`*"]
(*Red text inside the program, are parameters that can be changed*)

Ni = 1; (*Number of nuclei*)
Ii = 3 / 2; (*Nuclear spin of each nuclei. Consider all nuclear spins equal*)
L = 0; (*Orbital angular momentum*)
S = 1 / 2; (*total electron spin*)
J = L + S; (*Orbit angular momentum of the electron*)

If [Mod[Ni, 2] == 0 , Itotal = Table[i, {i, 0, Ni * Ii, 1}],
 Itotal = Table[i, {i, Ii, Ni * Ii, 1}]];
(*even number of nuclei Itotal runs from 0 to Ni*Ii in
 steps of 1. Odd runs from Ii to Ni*Ii in steps of 1*)

(*The eigenfunctions has to be
 calculated in each subspace with equal Itotal*)
eigenvalues = ConstantArray[0, Length[Itotal]];
storeF = ConstantArray[0, Length[Itotal]];
(*eigenvectors=ConstantArray[0,Length[Itotal]];*)
(*eigensystem=ConstantArray[0,Length[Itotal]];*)
plot = ConstantArray[0, Length[Itotal]];
(*START OVERALL FORLOOP*)
For[solnr = 1, solnr < Length[Itotal] + 1, solnr++,

 Isubtot = {Itotal[[solnr]]};
 mI = ConstantArray[0, Length[Isubtot]];
 For[x = 1, x < Length[Isubtot] + 1, x++,
   mI[[x]] = Table[i, {i, -Isubtot[[x]], +Isubtot[[x]], 1}]]
  For[x = 1, x < J + 1, x++, mJ = Table[i, {i, -J, +J, 1}
     ];
  ];

 JmJImI = ConstantArray[0, Length[Flatten[mI]] * Length[mJ]];
 q = 1;
 For[x = 1, x < Length[mJ] + 1, x++,
  For[y = 1, y < Length[mI] + 1, y++,
    For[z = 1, z < Length[mI[[y]]] + 1, z++,
     JmJImI[[q]] = {{J, mJ[[x]]}, {Isubtot[[y]], mI[[y, z]]}}; q++]
   ];
 ];

 (*For every Isubtot we need F to run from |Isubtot-J| to Isubtot+J*)
 Ftemp = ConstantArray[0, Length[Isubtot]];
 For[x = 1, x < Length[Isubtot] + 1, x++,
  Ftemp[[x]] = Table[i, {i, Abs[Isubtot[[x]] - J], Isubtot[[x]] + J, 1}];
 ];
```

```
F = Flatten[Ftemp]; (*Flatten is used to rearrange all
 elements from the vector F in one array. NOT USE UNiON HERE!!!*)
storeF[[solnr]] = F;
(*Now create a matrix with all corresponding FmF values*)
mF = ConstantArray[0, Length[F]];
(*the projection of F: mF runs from -F to +F*)
For[x = 1, x < Length[F] + 1, x++, mF[[x]] = Table[i, {i, -F[[x]], +F[[x]], 1}];
];
FmFtemp = ConstantArray[0, Length[F]];
For[x = 1, x < Length[F] + 1, x++,
 FmFtemp[[x]] = Table[{F[[x]], mF[[x, i]]}, {i, Length[mF[[x]]]}];
];

(*Construct the brackets in FmFtemp in a different
 way for ease acces for use with the ClebschGordan solver*)
FmF = ConstantArray[0, Length[Flatten[FmFtemp]] / 2];
(*construct an empty array*)
q = 1;
For[x = 1, x < Length[F] + 1, x++,
 (*For each value of F, collect the corresponding mF values*)
 For[y = 1, y < Length[mF[[x]]] + 1, y++, (*MF values for the corresponding F*)
   FmF[[q]] = {F[[x]], mF[[x, y]]}; q++(*write them in the FmF vector*)
  ];
];

(*Defining Hyperfine energie Hf here*)
Hftemp = ConstantArray[0, Length[Flatten[Ftemp]]];
q = 1;
For[ x = 1, x < Length[Isubtot] + 1, x++,
 For[y = 1, y < Length[Ftemp[[x]]] + 1, y++,
   Hftemp[[q]] = hbar^2 * Ahf / 2 * (Ftemp[[x, y]] * (Ftemp[[x, y]] + 1) -
       Isubtot[[x]] * (Isubtot[[x]] + 1) - J * (J + 1)); q++
  ];
];

(*For each FmF state define theire corresponding hyperfine energy*)
Hf = ConstantArray[0, Length[FmF]];
q = 1;
For[x = 1, x < Length[F] + 1, x++,
 For[y = 1, y < Length[FmFtemp[[x]]] + 1, y++,
   Hf[[q]] = Hftemp[[x]]; q++
  ];
];

(*Constructing States |J,mJ,I,mI>*)
mI = ConstantArray[0, Length[Isubtot]];
For[x = 1, x < Length[Isubtot] + 1, x++,
```

```
 mI[[x]] = Table[i, {i, -Isubtot[[x]], +Isubtot[[x]], 1}];
];
For[x = 1, x < J + 1, x++, mJ = Table[i, {i, -J, +J, 1}];
];
JmJImI = ConstantArray[0, Length[Flatten[mI]] * Length[mJ]];
q = 1;
For[x = 1, x < Length[mJ] + 1, x++,
 For[y = 1, y < Length[mI] + 1, y++,
   For[z = 1, z < Length[mI[[y]]] + 1, z++,
     JmJImI[[q]] = {{J, mJ[[x]]}, {Isubtot[[y]], mI[[y, z]]}};
     q++
    ];
  ];
];

(*Calculating the Clebsch Gordan Coefficients*)
j1 = ConstantArray[0, {Length[JmJImI]}];
m1 = ConstantArray[0, {Length[JmJImI]}];
j2 = ConstantArray[0, {Length[JmJImI]}];
m2 = ConstantArray[0, {Length[JmJImI]}];
j3 = ConstantArray[0, {Length[JmJImI]}];
m3 = ConstantArray[0, {Length[JmJImI]}];
Rule1 = ConstantArray[0, {Length[JmJImI], Length[FmF]}];
Rule2 = ConstantArray[0, {Length[JmJImI], Length[FmF]}];
Rule3 = ConstantArray[0, {Length[JmJImI], Length[FmF]}];
Rule4 = ConstantArray[0, {Length[JmJImI], Length[FmF]}];
ClebschGordanMatrix = ConstantArray[0, {Length[JmJImI], Length[FmF]}];
For[y = 1, y < Length[JmJImI] + 1, y++,
 (*extract all mi and ji put them in an array*)
 j1[[y]] = JmJImI[[y, 1, 1]];
 m1[[y]] = JmJImI[[y, 1, 2]];
 j2[[y]] = JmJImI[[y, 2, 1]];
 m2[[y]] = JmJImI[[y, 2, 2]];
];
For[x = 1, x < Length[FmF] + 1, x++,
 j3[[x]] = FmF[[x, 1]];
 (*For each y extract new F mF values and put refresh the j3 and m3 arrays*)
 m3[[x]] = FmF[[x, 2]];
];

For[x = 1, x < Length[FmF] + 1, x++,
 For[y = 1, y < Length[JmJImI] + 1, y++,
   (*rules from: http://mathworld.wolfram.com/WigIer3j-Symbol.html*)
   Rule1[[y, x]] = If[m1[[y]] + m2[[y]] - m3[[x]] == 0, 1, 0];
   (*MINUS SIgI IN FRONT OF m3!!!*)
   Rule2[[y, x]] = If[Abs[m1[[y]]] <= j1[[y]] &&
      Abs[m2[[y]]] <= j2[[y]] && Abs[m3[[x]]] <= j3[[x]], 1, 0];
```

```
    Rule3[[y, x]] = If[m1[[y]] == 0 && m2[[y]] == 0 && m3[[x]] == 0, Mod[j1[[y]] +
        j2[[y]] + j3[[x]], 2], Mod[j1[[y]] + j2[[y]] + j3[[x]], 1]]; (*If m1=
     m2=m3 → j1+j2+j3=even integer. If satisfied a zero is returned!*)
    Rule4[[y, x]] = If[Abs[j1[[y]] - j2[[y]]] ≤ j3[[x]] &&
       j3[[x]] ≤ j1[[y]] + j2[[y]], 1, 0];
    ClebschGordanMatrix[[y, x]] = If[Rule1[[y, x]] == 1 && Rule2[[y, x]] == 1 &&
       Rule3[[y, x]] == 0 && Rule4[[y, x]] == 1, ClebschGordan[
       {j1[[y]], m1[[y]]}, {j2[[y]], m2[[y]]}, {j3[[x]], m3[[x]]}], 0]
  ];
];
(*Clebsch Gordan Constants for the transformation JmJImI->FmF*)
(*Clebsch Gordan Constants for the transformation FmF->JmJImI*)

(*Zeeman Splitting of the Fine levels*)
Jz = ConstantArray[0, {Length[JmJImI]}]; (*Operator Jz*)
For[x = 1, x < Length[JmJImI] + 1, x++,
 Jz[[x]] = JmJImI[[x, 1, 2]];
];

(*Zeeman Splitting of the Hyperfine levels*)
Iz = ConstantArray[0, {Length[JmJImI]}]; (*Operator Jz*)
For[x = 1, x < Length[JmJImI] + 1, x++,
 Iz[[x]] = JmJImI[[x, 2, 2]];
];

(*HamiltoNian including Hhf and the Hz*)
(*inverse=Inverse[ClebschGordanMatrix];*)
(*this way only have to calculate it once*)
(*A=inverse.(Jz*ClebschGordanMatrix);
B=inverse.(Iz*ClebschGordanMatrix);*)
(*MatrixForm[DiagonalMatrix[-hbar*gJ*omega0*Jz-hbar*gI*omegan*Iz]];*)
(*MatrixForm[ClebschGordanMatrix.DiagonalMatrix[Hf].inverse*hbar^2];*)
(*JmJImI Basis*)
(*Matrix=DiagonalMatrix[Hf]*hbar^2-hbar*gJ*omega0*A-hbar*gI*omegan*B;*)
(*FmF Basis*)
(*eigensystem[[solnr]]=Eigensystem[Matrix];*)
(*eigenvalues[[solnr]]=eigensystem[[solnr,1]];*)
(*eigenvectors[[solnr]]=eigensystem[[solnr,2]];*)
eigenvalues[[solnr]] = Eigenvalues[
  (ClebschGordanMatrix.DiagonalMatrix[Hf].Inverse[ClebschGordanMatrix] +
       DiagonalMatrix[-hbar * gJ * omega0 * Jz - hbar * gI * omegan * Iz]) /
     hbar / (2 * Pi) * 10^(-9)];
(*JmJImI Basis*)
If[ solnr == 1,
 StylePrint["RESULTS:", FontFamily → "Helvetica", FontColor → Red] &&
  Print["The outcome for each subspace of Itotal. Returns the corresponding
     total angular momentum F, and theire hyperfine energy splitting
```

```
      energy relative to the orbital angular momentum here taken zero.\n",
    "Isubtot=", Isubtot], Print["Isubtot=", Isubtot]];
 Print["wherefor F=", F, "<Hhf>=", Hftemp];
 (*];*)(*END OVERALL FORLOOP*)
 (*upto here everything is solved analytically*)
 percentage = N[( solnr / Length[Itotal]) * 100, 4];
 StylePrint[ percentage "% of data is generated.",
  FontFamily → "Helvetica", FontColor → Green];

](*END OVERALL LOOP, all data is generated analytically*)

(*Before filling in the constants, analytical information can be extracted*)
Print[eigenvalues * hbar * (2 * Pi) * 10^(9)];

(*CONSTANTS*)
(*Adjustable*)
Mn = 70 * 1.660538921 * 10^(-27); (*Mass Nucleus average Gallium and Arsenic*)
(*Automatically pick the parameters for the electron or the hole*)
If [L == 0, gJ = +0.44, gJ = 0.2]; (*g-factor electron and g-factor hole*)
If [L == 0, Ahf = +90 * 10^(-6) * e / hbar^2 , Ahf = -15 * 10^(-6) * e / hbar^2 ];
(*Hyperfine coupling in
 Joules.(converting to MHz or eV happens in the Hamiltonian)*)
gL = 1 - me / Mn; (*g-factor "1-me/Mn" orbital angular momentum,
usually set to 1*)
gI = +1.3; (*g-factor nucleus, proton:+5.585694713*)
UptoField = 20; (*in Tesla*)

(*Non-Adjustable,taken from http://physics.nist.gov/cuu/Constants/*)
me = 9.10938291 * 10^(-31); (*Mass electron*)
(*Mu=me*Mn/(me+Mn);*)(*reduced mass*)
e = 1.602176565 * 10^(-19);
hbar = 1.054571726 * 10^(-34);
omega0 = -e / (2 * me) * B0; (*B0 in Gauss*)
omegan = e / (2 * Mn) * B0;
(*mu0=1.2566370614*10^(-6);*)
(*e0=8.854187817*10^(-12);*)
(*a0=4*Pi*e0*hbar^2/(Mu*e^2*Z);*)(*4*Pi*e0*hbar^2/(Mu*e^2*Z);*)
(*5.2917721092*10^(-11)*)(*5.2917721092*10^(-11);*)
(*mun=(e*hbar/(2*Mn));*)(*Nuclear magIeton*)
(*mub=e*hbar/(2*me);*)(*Bohr magneton*)
(*Ahf Hyperfine constant for different levels*)
(*Ahf/hbar*10^(-6)/2/Pi;*)(*Return value of Ahf in Mega Hertz*)
(*1420.40575177 MHz for hydrogen ground level*)

(*In Low field we want to know gF to identify
 which line correspond to which projection of mF*)
Print[ "Calculated gF factors \n (using gI=gn*me/Mn):"];
```

```
gF = ConstantArray[0, Length[Itotal]];
For[solnr = 1, solnr < Length[Itotal] + 1, solnr++,
  (*For every subItotal pick the array with possible F values*)
  gF[[solnr]] = ConstantArray[0, Length[storeF[[solnr]]]];
  For[q = 1, q < Length[storeF[[solnr]]] + 1, q++,
   (*pick the different F values from the array and calculate gF*)
   If [storeF[[solnr, q]] == 0 ,
     gF[[solnr, q]] = 0, (*If F=0 also the projections are zero,
     so in low field there is no zeeman term*)
     gF[[solnr, q]] = gJ * (storeF[[solnr, q]] * (storeF[[solnr, q]] + 1) -
             Itotal[[solnr]] * (Itotal[[solnr]] + 1) + J * (J + 1)) /
           (2 * storeF[[solnr, q]] * (storeF[[solnr, q]] + 1)) +
        me / Mn * gI * (storeF[[solnr, q]] * (storeF[[solnr, q]] + 1) +
             Itotal[[solnr]] * (Itotal[[solnr]] + 1) - J * (J + 1)) /
           (2 * storeF[[solnr, q]] * (storeF[[solnr, q]] + 1));
    ];

  ];
  Print["F values for subItotal=", Itotal[[solnr]], "\n", storeF[[solnr]],
   "\nFor each F their corresponding Lande factor gF \n", gF[[solnr]]];
 ];
(*gF Factor per F, because gF is F dependend*)

StylePrint["Data is now generated, Data is beeing processed to be plotted",
  FontFamily → "Helvetica", FontColor → Green];

(*Store plots*)
For[x = 1, x < Length[eigenvalues] + 1, x++,
  plot[[x]] = Plot[eigenvalues[[x]], {B0, 0, UptoField}, PlotStyle → Black];
  Print["Progress: plot ", x,
   " of ", Length[eigenvalues], " plots processed" ];
 ];
(*show all pLots in one frame*)
Show[plot, PlotRangePadding → None, Frame → True,
 Axes → True, GridLines → Automatic, PlotRange → Automatic,
 FrameLabel → {"B0 (Tesla)", "Energy (GHz)"}]
```

RESULTS:

The outcome for each subspace of Itotal. Returns the corresponding
total angular momentum F, and theire hyperfine energy splitting
energy relative to the orbital angular momentum here taken zero.

Isubtot=

$$\left\{\frac{3}{2}\right\}$$

wherefor F={1, 2}<Hhf>=$$\left\{-\frac{5\ \text{Ahf}\ \text{hbar}^2}{4},\ \frac{3\ \text{Ahf}\ \text{hbar}^2}{4}\right\}$$

100.0 % of data is generated.

$$\left\{\left\{\frac{3\ \text{Ahf}\ \text{hbar}^2}{4}-\frac{\text{gJ}\ \text{hbar}\ \text{omega0}}{2}-\frac{3\ \text{gI}\ \text{hbar}\ \text{omegan}}{2},\right.\right.$$
$$\frac{3\ \text{Ahf}\ \text{hbar}^2}{4}+\frac{\text{gJ}\ \text{hbar}\ \text{omega0}}{2}+\frac{3\ \text{gI}\ \text{hbar}\ \text{omegan}}{2},$$
$$\frac{1}{4}\ \text{hbar}\left(-\text{Ahf}\ \text{hbar}-2\sqrt{4\ \text{Ahf}^2\ \text{hbar}^2+\text{gJ}^2\ \text{omega0}^2-2\ \text{gI}\ \text{gJ}\ \text{omega0}\ \text{omegan}+\text{gI}^2\ \text{omegan}^2}\right),$$
$$\frac{1}{4}\ \text{hbar}\left(-\text{Ahf}\ \text{hbar}+2\sqrt{4\ \text{Ahf}^2\ \text{hbar}^2+\text{gJ}^2\ \text{omega0}^2-2\ \text{gI}\ \text{gJ}\ \text{omega0}\ \text{omegan}+\text{gI}^2\ \text{omegan}^2}\right),$$
$$\frac{1}{4}\ \text{hbar}\left(-\text{Ahf}\ \text{hbar}+4\ \text{gI}\ \text{omegan}-2\sqrt{\left(4\ \text{Ahf}^2\ \text{hbar}^2+2\ \text{Ahf}\ \text{gJ}\ \text{hbar}\ \text{omega0}+\right.\right.\right.$$
$$\left.\left.\left.\text{gJ}^2\ \text{omega0}^2-2\ \text{Ahf}\ \text{gI}\ \text{hbar}\ \text{omegan}-2\ \text{gI}\ \text{gJ}\ \text{omega0}\ \text{omegan}+\text{gI}^2\ \text{omegan}^2\right)}\right),$$
$$\frac{1}{4}\ \text{hbar}\left(-\text{Ahf}\ \text{hbar}+4\ \text{gI}\ \text{omegan}+2\sqrt{\left(4\ \text{Ahf}^2\ \text{hbar}^2+2\ \text{Ahf}\ \text{gJ}\ \text{hbar}\ \text{omega0}+\right.\right.\right.$$
$$\left.\left.\left.\text{gJ}^2\ \text{omega0}^2-2\ \text{Ahf}\ \text{gI}\ \text{hbar}\ \text{omegan}-2\ \text{gI}\ \text{gJ}\ \text{omega0}\ \text{omegan}+\text{gI}^2\ \text{omegan}^2\right)}\right),$$
$$\frac{1}{4}\ \text{hbar}\left(-\text{Ahf}\ \text{hbar}-4\ \text{gI}\ \text{omegan}-2\sqrt{\left(4\ \text{Ahf}^2\ \text{hbar}^2-2\ \text{Ahf}\ \text{gJ}\ \text{hbar}\ \text{omega0}+\right.\right.\right.$$
$$\left.\left.\left.\text{gJ}^2\ \text{omega0}^2+2\ \text{Ahf}\ \text{gI}\ \text{hbar}\ \text{omegan}-2\ \text{gI}\ \text{gJ}\ \text{omega0}\ \text{omegan}+\text{gI}^2\ \text{omegan}^2\right)}\right),$$
$$\left.\left.\frac{1}{4}\ \text{hbar}\left(-\text{Ahf}\ \text{hbar}-4\ \text{gI}\ \text{omegan}+2\sqrt{\left(4\ \text{Ahf}^2\ \text{hbar}^2-2\ \text{Ahf}\ \text{gJ}\ \text{hbar}\ \text{omega0}+\right.\right.\right.\right\}\right\}$$
$$\left.\left.\left.\text{gJ}^2\ \text{omega0}^2+2\ \text{Ahf}\ \text{gI}\ \text{hbar}\ \text{omegan}-2\ \text{gI}\ \text{gJ}\ \text{omega0}\ \text{omegan}+\text{gI}^2\ \text{omegan}^2\right)}\right)$$

Calculated gF factors
(using gI=gn*me/Mn):

F values for subItotal=$\frac{3}{2}$

{1, 2}

For each F their corresponding Lande factor gF

{-0.109987, 0.110008}

Data is now generated, Data is beeing processed to be plotted

Progress: plot 1 of 1 plots processed

Appendix F

Mathematica code for calculating the dipole transition strengths

In[182]:=

```
Clear["Global`*"]

(*LOW FIELD*)
(*{F,mF,J,L,S,I}*)
FmFJLSI1 =
  {(*Lower S1/2 bundle*){1, -1, 1 / 2, 0, 1 / 2, 3 / 2}, {1, 0, 1 / 2, 0, 1 / 2, 3 / 2},
   {1, +1, 1 / 2, 0, 1 / 2, 3 / 2}, {2, +2, 1 / 2, 0, 1 / 2, 3 / 2}(*Upper S1/2 bundle*),
   {2, -2, 1 / 2, 0, 1 / 2, 3 / 2}, {2, -1, 1 / 2, 0, 1 / 2, 3 / 2},
   {2, 0, 1 / 2, 0, 1 / 2, 3 / 2}, {2, +1, 1 / 2, 0, 1 / 2, 3 / 2}};
FmFJLSI2 = (*Lower P3/2 bundle:*){{3, 0, 3 / 2, 1, 1 / 2, 3 / 2},
   {3, +1, 3 / 2, 1, 1 / 2, 3 / 2}, {3, +2, 3 / 2, 1, 1 / 2, 3 / 2},
   {3, +3, 3 / 2, 1, 1 / 2, 3 / 2}(*Second P3/2 bundle:*),
   {3, -1, 3 / 2, 1, 1 / 2, 3 / 2}, {2, 0, 3 / 2, 1, 1 / 2, 3 / 2},
   {2, +1, 3 / 2, 1, 1 / 2, 3 / 2}, {2, +2, 3 / 2, 1, 1 / 2, 3 / 2}(*Third bundle:*),
   {3, -2, 3 / 2, 1, 1 / 2, 3 / 2}, {3, -1, 3 / 2, 1, 1 / 2, 3 / 2},
   {1, 0, 3 / 2, 1, 1 / 2, 3 / 2}, {1, +1, 3 / 2, 1, 1 / 2, 3 / 2}(*Fourth bundle:*),
   {3, -3, 3 / 2, 1, 1 / 2, 3 / 2}, {2, -2, 3 / 2, 1, 1 / 2, 3 / 2},
   {1, -1, 3 / 2, 1, 1 / 2, 3 / 2}, {0, 0, 3 / 2, 1, 1 / 2, 3 / 2}};

(*HIGH FIELD*)
(*{J,mJ,I,mI,L}*)
JmJImILS1 = {(*Lower S1/2 bundle*){1 / 2, +1 / 2, 3 / 2, -3 / 2, 0, 1 / 2},
   {1 / 2, +1 / 2, 3 / 2, -1 / 2, 0, 1 / 2}, {1 / 2, +1 / 2, 3 / 2, +1 / 2, 0, 1 / 2},
   {1 / 2, +1 / 2, 3 / 2, +3 / 2, 0, 1 / 2}(*Upper S1/2 bundle*),
   {1 / 2, -1 / 2, 3 / 2, +3 / 2, 0, 1 / 2}, {1 / 2, -1 / 2, 3 / 2, +1 / 2, 0, 1 / 2},
   {1 / 2, -1 / 2, 3 / 2, -1 / 2, 0, 1 / 2}, {1 / 2, -1 / 2, 3 / 2, -3 / 2, 0, 1 / 2}};
JmJImILS2 = (*Lower P3/2 bundle*){{3 / 2, +3 / 2, 3 / 2, -3 / 2, 1, 1 / 2},
   {3 / 2, +3 / 2, 3 / 2, -1 / 2, 1, 1 / 2}, {3 / 2, +3 / 2, 3 / 2, +1 / 2, 1, 1 / 2},
   {3 / 2, +3 / 2, 3 / 2, +3 / 2, 1, 1 / 2}, (*Second bundle*)
   {3 / 2, +1 / 2, 3 / 2, -3 / 2, 1, 1 / 2}, {3 / 2, +1 / 2, 3 / 2, -1 / 2, 1, 1 / 2},
   {3 / 2, +1 / 2, 3 / 2, +1 / 2, 1, 1 / 2}, {3 / 2, +1 / 2, 3 / 2, +3 / 2, 1, 1 / 2},
   (*Third bundle*){3 / 2, -1 / 2, 3 / 2, -3 / 2, 1, 1 / 2},
   {3 / 2, -1 / 2, 3 / 2, -1 / 2, 1, 1 / 2}, {3 / 2, -1 / 2, 3 / 2, +1 / 2, 1, 1 / 2},
   {3 / 2, -1 / 2, 3 / 2, +3 / 2, 1, 1 / 2}, (*Fourth bundle*)
   {3 / 2, -3 / 2, 3 / 2, -3 / 2, 1, 1 / 2}, {3 / 2, -3 / 2, 3 / 2, -1 / 2, 1, 1 / 2},
   {3 / 2, -3 / 2, 3 / 2, +1 / 2, 1, 1 / 2}, {3 / 2, -3 / 2, 3 / 2, +3 / 2, 1, 1 / 2}};

(*The detail level of the output: 0 only transition strengths,
1 also the outcome of the wigner matrices,
2 also the outcome of all rules of the wigner matrices*)
Detailed = 0;

(*Calculation transition strengths: *)

(*-------------------LOW FIELD---------------------------------*)
```

```
(*Dipole transition strength for FmFJLSI1->FmFJLSI2*)
StylePrint["RESULTS (FmFJLSI1->FmFJLSI2):",
 FontFamily → "Helvetica", FontColor → Red]
StylePrint["LOW FIELD:", FontFamily → "Helvetica", FontColor → Red]
For[q = -1, q < 2, q++, (*-1,0,+1 polarization*)
 Print["--------------------POALARIZATION q= ", q, "----------------------"];
 (*----------------------Factor*WIGNER 3J----------------------*)
 (*Factor=Sqrt[(2J+1)(2J'+1)(2F+1)(2F'+1)]*)
 j1 = ConstantArray[0, {Length[FmFJLSI1]}];
 m1 = ConstantArray[0, {Length[FmFJLSI1]}];
 j2 = ConstantArray[0, {Length[FmFJLSI1]}];
 m2 = ConstantArray[0, {Length[FmFJLSI1]}];
 j3 = ConstantArray[0, {Length[FmFJLSI2]}];
 m3 = ConstantArray[0, {Length[FmFJLSI2]}];
 Rule1 = ConstantArray[0, {Length[FmFJLSI2], Length[FmFJLSI1]}];
 Rule2 = ConstantArray[0, {Length[FmFJLSI2], Length[FmFJLSI1]}];
 Rule3 = ConstantArray[0, {Length[FmFJLSI2], Length[FmFJLSI1]}];
 Rule4 = ConstantArray[0, {Length[FmFJLSI2], Length[FmFJLSI1]}];
 FactorWigner3jMatrix =
  ConstantArray[0, {Length[FmFJLSI2], Length[FmFJLSI1]}];

 For[x = 1, x < Length[FmFJLSI1] + 1, x++,
  j1[[x]] = FmFJLSI1[[x, 1]];
  m1[[x]] = FmFJLSI1[[x, 2]];
  j2[[x]] = 1;
  m2[[x]] = q;
 ];

 For[y = 1, y < Length[FmFJLSI2] + 1, y++,
  j3[[y]] = FmFJLSI2[[y, 1]];
  m3[[y]] = FmFJLSI2[[y, 2]];
 ];

 For[y = 1, y < Length[FmFJLSI2] + 1, y++,
  For[x = 1, x < Length[FmFJLSI1] + 1, x++,
    (*rules from: http://mathworld.wolfram.com/WigIer3j-Symbol.html*)
    Rule1[[y, x]] = If[m1[[x]] + m2[[x]] - m3[[y]] == 0, 1, 0];
    (*MINUS SIgI IN FRONT OF m3!!!*)
    Rule2[[y, x]] = If[Abs[m1[[x]]] <= j1[[x]] &&
       Abs[m2[[x]]] <= j2[[x]] && Abs[m3[[y]]] <= j3[[y]], 1, 0];
    Rule3[[y, x]] = If[m1[[x]] == 0 && m2[[x]] == 0 && m3[[y]] == 0, Mod[j1[[x]] +
        j2[[x]] + j3[[y]], 2], Mod[j1[[x]] + j2[[x]] + j3[[y]], 1]]; (*If m1=
     m2=m3 → j1+j2+j3=even integer. If satisfied a zero is returned!*)
    Rule4[[y, x]] = If[Abs[j1[[x]] - j2[[x]]] ≤ j3[[y]] &&
       j3[[y]] ≤ j1[[x]] + j2[[x]], 1, 0];

    FactorWigner3jMatrix[[y, x]] =
```

```
    If[Rule1[[y, x]] == 1 && Rule2[[y, x]] == 1 && Rule3[[y, x]] == 0 &&
      Rule4[[y, x]] == 1, Sqrt[(2 * FmFJLSI1[[x, 3]] + 1) * (2 * FmFJLSI2[[y, 3]] + 1) *
        (2 * FmFJLSI1[[x, 1]] + 1) * (2 * FmFJLSI2[[y, 1]] + 1)] * ThreeJSymbol[
       {j1[[x]], m1[[x]]}, {j2[[x]], m2[[x]]}, {j3[[y]], -m3[[y]]}], 0];
  ];
];
If[Detailed > 0,
 Print["Factor*Wigner3J = " MatrixForm[FactorWigner3jMatrix]], Null];
If[Detailed == 2,
 Print["Rule1:", Rule1] &&
  Print["Rule2:", Rule2] &&
  Print["Rule3:", Rule3] &&
  Print["Rule4:", Rule4], Null];
(*----------------------Factor*WIGNER 3J----------------------*)

(*----------------------Second WIGNER 6J----------------------*)
(*Wigner6j{j1,j2,j3},{m1,m2,m3}*)

j1 = ConstantArray[0, {Length[FmFJLSI2]}];
m1 = ConstantArray[0, {Length[FmFJLSI1]}];
j2 = ConstantArray[0, {Length[FmFJLSI2]}];
m2 = ConstantArray[0, {Length[FmFJLSI1]}];
j3 = ConstantArray[0, {Length[FmFJLSI1]}];
m3 = ConstantArray[0, {Length[FmFJLSI2]}];
Rule1 = ConstantArray[3, {Length[FmFJLSI2], Length[FmFJLSI1]}];
Rule2 = ConstantArray[0, {Length[FmFJLSI2], Length[FmFJLSI1]}];
Rule3 = ConstantArray[0, {Length[FmFJLSI2], Length[FmFJLSI1]}];
Rule4 = ConstantArray[0, {Length[FmFJLSI2], Length[FmFJLSI1]}];
Rule5 = ConstantArray[0, {Length[FmFJLSI2], Length[FmFJLSI1]}];
SecondWigner6jMatrix =
 ConstantArray[0, {Length[FmFJLSI2], Length[FmFJLSI1]}];

For[x = 1, x < Length[FmFJLSI1] + 1, x++,
 m1[[x]] = FmFJLSI1[[x, 1]];
 j3[[x]] = FmFJLSI1[[x, 6]];
 m2[[x]] = FmFJLSI1[[x, 3]];
];

For[y = 1, y < Length[FmFJLSI2] + 1, y++,
 j1[[y]] = FmFJLSI2[[y, 3]];
 m3[[y]] = 1;
 j2[[y]] = FmFJLSI2[[y, 1]];
];

For[y = 1, y < Length[FmFJLSI2] + 1, y++,
 For[x = 1, x < Length[FmFJLSI1] + 1, x++,
   (*rules from: http://mathworld.wolfram.com/WigIer3j-Symbol.html*)
```

```
    (*Each triad satisfies the triangular inequalities*)
    Rule1[[y, x]] =
     If[Abs[j1[[y]] - j2[[y]]] <= j3[[x]] && j3[[x]] <= j1[[y]] + j2[[y]], 1, 0];
    Rule2[[y, x]] = If[Abs[j1[[y]] - m2[[x]]] <= m3[[y]] &&
       m3[[y]] <= j1[[y]] + m2[[x]], 1, 0];
    Rule3[[y, x]] = If[Abs[m1[[x]] - j2[[y]]] <= m3[[y]] &&
       m3[[y]] <= m1[[x]] + j2[[y]], 1, 0];
    Rule4[[y, x]] = If[Abs[m1[[x]] - m2[[x]]] <= j3[[x]] &&
       j3[[x]] <= m1[[x]] + m2[[x]], 1, 0];
    (*The sum of the elements of each triad is an integer*)
    Rule5[[y, x]] = If[Mod[j1[[y]] + j2[[y]] + j3[[x]], 1] == 0
      (*&&Mod[j1[[y]]+m2[[x]]+m3[[y]],1]==0&&Mod[m1[[x]]+j2[[y]]+m3[[y]],1]==
        0&&Mod[m1[[x]]+m2[[x]]+j3[[x]],1]==0*), 1, 0]; (*If m1=
     m2=m3 → j1+j2+j3=even integer. If satisfied a zero is returned!*)
    SecondWigner6jMatrix[[y, x]] = If[Rule1[[y, x]] == 1 && Rule2[[y, x]] == 1 &&
       Rule3[[y, x]] == 1 && Rule4[[y, x]] == 1 && Rule5[[y, x]] == 1,
      SixJSymbol[{j1[[y]], j2[[y]], j3[[x]]}, {m1[[x]], m2[[x]], m3[[y]]}], 0];
  ];
];
If[Detailed > 0,
 Print["Second Wigner 6j = " MatrixForm[SecondWigner6jMatrix]], Null];
If[Detailed == 2,
 Print["Rule1:", MatrixForm[Rule1]] &&
  Print["Rule2:", MatrixForm[Rule2]] &&
  Print["Rule3:", MatrixForm[Rule3]] &&
  Print["Rule4:", MatrixForm[Rule4]] &&
  Print["Rule5:", MatrixForm[Rule5]] &&
  Print["Rule4*Rule5:", MatrixForm[Rule4 * Rule5]], Null];
(*-----------------------Second WIGNER 6J----------------------*)

(*-----------------------First WIGNER 6J-----------------------*)
(*Wigner6j{j1,j2,j3},{m1,m2,m3}*)

j1 = ConstantArray[0, {Length[FmFJLSI2]}];
m1 = ConstantArray[0, {Length[FmFJLSI1]}];
j2 = ConstantArray[0, {Length[FmFJLSI2]}];
m2 = ConstantArray[0, {Length[FmFJLSI1]}];
j3 = ConstantArray[0, {Length[FmFJLSI1]}];
m3 = ConstantArray[0, {Length[FmFJLSI2]}];
Rule1 = ConstantArray[0, {Length[FmFJLSI2], Length[FmFJLSI1]}];
Rule2 = ConstantArray[0, {Length[FmFJLSI2], Length[FmFJLSI1]}];
Rule3 = ConstantArray[0, {Length[FmFJLSI2], Length[FmFJLSI1]}];
Rule4 = ConstantArray[0, {Length[FmFJLSI2], Length[FmFJLSI1]}];
Rule5 = ConstantArray[0, {Length[FmFJLSI2], Length[FmFJLSI1]}];
FirstWigner6jMatrix = ConstantArray[0, {Length[FmFJLSI2], Length[FmFJLSI1]}];

For[x = 1, x < Length[FmFJLSI1] + 1, x++,
```

```
 m1[[x]] = FmFJLSI1[[x, 3]];
 j3[[x]] = FmFJLSI1[[x, 5]];
 m2[[x]] = FmFJLSI1[[x, 4]];
];

For[y = 1, y < Length[FmFJLSI2] + 1, y++,
 j1[[y]] = FmFJLSI2[[y, 4]];
 m3[[y]] = 1;
 j2[[y]] = FmFJLSI2[[y, 3]];
];

For[y = 1, y < Length[FmFJLSI2] + 1, y++,
 For[x = 1, x < Length[FmFJLSI1] + 1, x++,
   (*rules from: http://mathworld.wolfram.com/WigIer3j-Symbol.html*)
   (*Each triad satisfies the triangular inequalities*)
   Rule1[[y, x]] =
    If[Abs[j1[[y]] - j2[[y]]] <= j3[[x]] && j3[[x]] <= j1[[y]] + j2[[y]], 1, 0];
   Rule2[[y, x]] = If[Abs[j1[[y]] - m2[[x]]] <= m3[[y]] &&
      m3[[y]] <= j1[[y]] + m2[[x]], 1, 0];
   Rule3[[y, x]] = If[Abs[m1[[x]] - j2[[y]]] <= m3[[y]] &&
      m3[[y]] <= m1[[x]] + j2[[y]], 1, 0];
   Rule4[[y, x]] = If[Abs[m1[[x]] - m2[[x]]] <= j3[[x]] &&
      j3[[x]] <= m1[[x]] + m2[[x]], 1, 0];
   (*The sum of the elements of each triad is an integer*)
   Rule5[[y, x]] = If[Mod[j1[[y]] + j2[[y]] + j3[[x]], 1] == 0 &&
      Mod[j1[[y]] + m2[[x]] + m3[[y]], 1] == 0 && Mod[m1[[x]] + j2[[y]] + m3[[y]],
        1] == 0 && Mod[m1[[x]] + m2[[x]] + j3[[x]], 1] == 0, 1, 0]; (*If m1=
    m2=m3 → j1+j2+j3=even integer. If satisfied a zero is returned!*)

   FirstWigner6jMatrix[[y, x]] = If[Rule1[[y, x]] == 1 && Rule2[[y, x]] == 1 &&
      Rule3[[y, x]] == 1 && Rule4[[y, x]] == 1 && Rule5[[y, x]] == 1,
     SixJSymbol[{j1[[y]], j2[[y]], j3[[x]]}, {m1[[x]], m2[[x]], m3[[y]]}], 0];
  ];
];
If[Detailed > 0,
 Print["First Wigner 6j = " MatrixForm[FirstWigner6jMatrix]], Null];
If[Detailed == 2,
 Print["Rule1:", Rule1] &&
  Print["Rule2:", Rule2] &&
  Print["Rule3:", Rule3] &&
  Print["Rule4:", Rule4] &&
  Print["Rule5:", Rule5], Null];
(*----------------------First WIGNER 6J----------------------*)

(*-------------------DIPOLE TRANSITION STRENGTH---------------*)
If[Detailed > 0,
 Print[
```

```
    "(FactorWigner3jMatrix*FirstWigner6jMatrix*SecondWigner6jMatrix)^2 = ",
    MatrixForm[
     (FactorWigner3jMatrix * FirstWigner6jMatrix * SecondWigner6jMatrix)^2]],
   Print["Transition strengths:", MatrixForm[
     (FactorWigner3jMatrix * FirstWigner6jMatrix * SecondWigner6jMatrix)^2]]];
  (*-------------DIPOLE TRANSITION STRENGTH----------------------*)
];Print["horizontal order of states (FmFJLSI) is:", FmFJLSI1,
 "\n vertical order of states (FmFJLSI) is:\n", FmFJLSI2];

(*-------------------------HIGH FIELD--------------------------*)

(*Dipole transition strength for JmJImILS1->JmJImILS2*)
StylePrint["HIGH FIELD (JmJImILS1->JmJImILS2):",
 FontFamily → "Helvetica", FontColor → Red]
For[q = -1, q < 2, q++, (*-1,0,+1 polarization*)
 Print["----------------POALARIZATION q= ", q, "----------------------"];
 (*-----------------------Factor*WIGNER 3J----------------------*)
 (*Factor=Sqrt[(2J+1)(2J'+1)(2F+1)(2F'+1)]*)
 j1 = ConstantArray[0, {Length[JmJImILS1]}];
 m1 = ConstantArray[0, {Length[JmJImILS1]}];
 j2 = ConstantArray[0, {Length[JmJImILS1]}];
 m2 = ConstantArray[0, {Length[JmJImILS1]}];
 j3 = ConstantArray[0, {Length[JmJImILS2]}];
 m3 = ConstantArray[0, {Length[JmJImILS2]}];
 Rule1 = ConstantArray[0, {Length[JmJImILS2], Length[JmJImILS1]}];
 Rule2 = ConstantArray[0, {Length[JmJImILS2], Length[JmJImILS1]}];
 Rule3 = ConstantArray[0, {Length[JmJImILS2], Length[JmJImILS1]}];
 Rule4 = ConstantArray[0, {Length[JmJImILS2], Length[JmJImILS1]}];
 FactorWigner3jMatrix =
  ConstantArray[0, {Length[JmJImILS2], Length[JmJImILS1]}];

 For[x = 1, x < Length[JmJImILS1] + 1, x++,
  j1[[x]] = JmJImILS1[[x, 1]];
  m1[[x]] = JmJImILS1[[x, 2]];
  j2[[x]] = 1;
  m2[[x]] = q;
 ];

 For[y = 1, y < Length[JmJImILS2] + 1, y++,
  j3[[y]] = JmJImILS2[[y, 1]];
  m3[[y]] = JmJImILS2[[y, 2]];
 ];

 For[y = 1, y < Length[JmJImILS2] + 1, y++,
  For[x = 1, x < Length[JmJImILS1] + 1, x++,
    (*rules from: http://mathworld.wolfram.com/WigIer3j-Symbol.html*)
    Rule1[[y, x]] = If[m1[[x]] + m2[[x]] - m3[[y]] == 0, 1, 0];
```

```
    (*MINUS SIGN IN FRONT OF m3!!!*)
    Rule2[[y, x]] = If[Abs[m1[[x]]] <= j1[[x]] &&
       Abs[m2[[x]]] <= j2[[x]] && Abs[m3[[y]]] <= j3[[y]], 1, 0];
    Rule3[[y, x]] = If[m1[[x]] == 0 && m2[[x]] == 0 && m3[[y]] == 0, Mod[j1[[x]] +
        j2[[x]] + j3[[y]], 2], Mod[j1[[x]] + j2[[x]] + j3[[y]], 1]]; (*If m1=
     m2=m3 → j1+j2+j3=even integer. If satisfied a zero is returned!*)
    Rule4[[y, x]] = If[Abs[j1[[x]] - j2[[x]]] ≤ j3[[y]] &&
       j3[[y]] ≤ j1[[x]] + j2[[x]], 1, 0];

    FactorWigner3jMatrix[[y, x]] = If[Rule1[[y, x]] == 1 &&
       Rule2[[y, x]] == 1 && Rule3[[y, x]] == 0 && Rule4[[y, x]] == 1,
      Sqrt[(2 * JmJImILS1[[x, 3]] + 1) * (2 * JmJImILS2[[y, 3]] + 1)] *
       ThreeJSymbol[{j1[[x]], m1[[x]]}, {j2[[x]], m2[[x]]},
        {j3[[y]], -m3[[y]]}], 0];(*MINUS SIGN IN FRONT OF m3!!!*)
  ];
];
If[Detailed > 0,
 Print["Factor*Wigner3J = " MatrixForm[FactorWigner3jMatrix]], Null];
If[Detailed == 2,
 Print["Rule1:", Rule1] &&
  Print["Rule2:", Rule2] &&
  Print["Rule3:", Rule3] &&
  Print["Rule4:", Rule4], Null];
(*-----------------------Factor*WIGNER 3J----------------------*)

(*---------------------------WIGNER 6J-------------------------*)
(*Wigner6j{j1,j2,j3},{m1,m2,m3}*)

j1 = ConstantArray[0, {Length[JmJImILS2]}];
m1 = ConstantArray[0, {Length[JmJImILS1]}];
j2 = ConstantArray[0, {Length[JmJImILS2]}];
m2 = ConstantArray[0, {Length[JmJImILS1]}];
j3 = ConstantArray[0, {Length[JmJImILS1]}];
m3 = ConstantArray[0, {Length[JmJImILS2]}];
Rule1 = ConstantArray[0, {Length[JmJImILS2], Length[JmJImILS1]}];
Rule2 = ConstantArray[0, {Length[JmJImILS2], Length[JmJImILS1]}];
Rule3 = ConstantArray[0, {Length[JmJImILS2], Length[JmJImILS1]}];
Rule4 = ConstantArray[0, {Length[JmJImILS2], Length[JmJImILS1]}];
Rule5 = ConstantArray[0, {Length[JmJImILS2], Length[JmJImILS1]}];
Rule6 = ConstantArray[0, {Length[JmJImILS2], Length[JmJImILS1]}];
Wigner6jMatrix = ConstantArray[0, {Length[JmJImILS2], Length[JmJImILS1]}];

For[x = 1, x < Length[JmJImILS1] + 1, x++,
 m1[[x]] = JmJImILS1[[x, 1]];
 j3[[x]] = JmJImILS1[[x, 6]];
 m2[[x]] = JmJImILS1[[x, 5]];
];
```

```
For[y = 1, y < Length[JmJImILS2] + 1, y++,
 j1[[y]] = JmJImILS2[[y, 5]];
 m3[[y]] = 1;
 j2[[y]] = JmJImILS2[[y, 1]];
];

For[y = 1, y < Length[JmJImILS2] + 1, y++,
 For[x = 1, x < Length[JmJImILS1] + 1, x++,
   (*rules from: http://mathworld.wolfram.com/WigIer3j-Symbol.html*)
   (*Each triad satisfies the triangular inequalities*)
   Rule1[[y, x]] =
    If[Abs[j1[[y]] - j2[[y]]] <= j3[[x]] && j3[[x]] <= j1[[y]] + j2[[y]], 1, 0];
   Rule2[[y, x]] = If[Abs[j1[[y]] - m2[[x]]] <= m3[[y]] &&
      m3[[y]] <= j1[[y]] + m2[[x]], 1, 0];
   Rule3[[y, x]] = If[Abs[m1[[x]] - j2[[y]]] <= m3[[y]] &&
      m3[[y]] <= m1[[x]] + j2[[y]], 1, 0];
   Rule4[[y, x]] = If[Abs[m1[[x]] - m2[[x]]] <= j3[[x]] &&
      j3[[x]] <= m1[[x]] + m2[[x]], 1, 0];
   (*The sum of the elements of each triad is an integer*)
   Rule5[[y, x]] = If[Mod[j1[[y]] + j2[[y]] + j3[[x]], 1] == 0 &&
      Mod[j1[[y]] + m2[[x]] + m3[[y]], 1] == 0 && Mod[m1[[x]] + j2[[y]] + m3[[y]],
        1] == 0 && Mod[m1[[x]] + m2[[x]] + j3[[x]], 1] == 0, 1, 0]; (*If m1=
    m2=m3 → j1+j2+j3=even integer. If satisfied a zero is returned!*)
   Rule6[[y, x]] = If[Abs[JmJImILS1[[x, 3]] - JmJImILS2[[y, 3]]] == 0 &&
      Abs[JmJImILS1[[x, 4]] - JmJImILS2[[y, 4]]] == 0, 1, 0];
   (*extra restriction, no nuclear flip may occur*)
   Wigner6jMatrix[[y, x]] = If[Rule1[[y, x]] == 1 && Rule2[[y, x]] == 1 && Rule3[[y,
        x]] == 1 && Rule4[[y, x]] == 1 && Rule5[[y, x]] == 1 && Rule6[[y, x]] == 1,
     SixJSymbol[{j1[[y]], j2[[y]], j3[[x]]}, {m1[[x]], m2[[x]], m3[[y]]}], 0];
  ];
];

If[Detailed > 0,
 Print["Wigner6j" MatrixForm[Wigner6jMatrix]], Null];
If[Detailed == 2,
 Print["Rule1:", Rule1] &&
  Print["Rule2:", Rule2] &&
  Print["Rule3:", Rule3] &&
  Print["Rule4:", Rule4] &&
  Print["Rule5:", Rule5] &&
  Print["Rule6:", Rule6], Null];

(*--------------DIPOLE TRANSITION STRENGTH------------------*)
If[Detailed > 0,
 Print["(FactorWigner3jMatrix*Wigner6jMatrix)^2 = "
   MatrixForm[(FactorWigner3jMatrix * Wigner6jMatrix)^2]],
```

```
    Print["Transition strengths:" MatrixForm[
       (FactorWigner3jMatrix * Wigner6jMatrix)^2]]];
   (*------------DIPOLE TRANSITION STRENGTH--------------------*)

  ]; Print["horizontal order of states (JmJImILS) is:", JmJImILS1,
   "\n vertical order of states (JmJImILS) is:\n", JmJImILS2];
```

RESULTS (FmFJLSI1->FmFJLSI2):

LOW FIELD:

----------POALARIZATION q= -1----------

Transition strengths:

$$\begin{pmatrix}
0 & 0 & 0 & 0 & 0 & 0 & 0 & \frac{1}{15} \\
0 & 0 & 0 & \frac{1}{45} & 0 & 0 & 0 & 0 \\
0 & 0 & 0 & 0 & 0 & 0 & 0 & 0 \\
0 & 0 & 0 & 0 & 0 & 0 & 0 & 0 \\
0 & 0 & 0 & 0 & 0 & 0 & \frac{2}{15} & 0 \\
0 & 0 & \frac{1}{36} & 0 & 0 & 0 & 0 & \frac{1}{12} \\
0 & 0 & 0 & \frac{1}{18} & 0 & 0 & 0 & 0 \\
0 & 0 & 0 & 0 & 0 & 0 & 0 & 0 \\
0 & 0 & 0 & 0 & 0 & \frac{2}{9} & 0 & 0 \\
0 & 0 & 0 & 0 & 0 & 0 & \frac{2}{15} & 0 \\
0 & 0 & \frac{5}{36} & 0 & 0 & 0 & 0 & \frac{1}{60} \\
0 & 0 & 0 & \frac{1}{30} & 0 & 0 & 0 & 0 \\
0 & 0 & 0 & 0 & \frac{1}{3} & 0 & 0 & 0 \\
\frac{1}{6} & 0 & 0 & 0 & 0 & \frac{1}{18} & 0 & 0 \\
0 & \frac{5}{36} & 0 & 0 & 0 & 0 & \frac{1}{180} & 0 \\
0 & 0 & \frac{1}{9} & 0 & 0 & 0 & 0 & 0
\end{pmatrix}$$

----------POALARIZATION q= 0----------

Transition strengths:

$$\begin{pmatrix} 0 & 0 & 0 & 0 & 0 & 0 & \frac{1}{5} & 0 \\ 0 & 0 & 0 & 0 & 0 & 0 & 0 & \frac{8}{45} \\ 0 & 0 & 0 & \frac{1}{9} & 0 & 0 & 0 & 0 \\ 0 & 0 & 0 & 0 & 0 & 0 & 0 & 0 \\ 0 & 0 & 0 & 0 & 0 & \frac{8}{45} & 0 & 0 \\ 0 & \frac{1}{9} & 0 & 0 & 0 & 0 & 0 & 0 \\ 0 & 0 & \frac{1}{12} & 0 & 0 & 0 & 0 & \frac{1}{36} \\ 0 & 0 & 0 & \frac{1}{9} & 0 & 0 & 0 & 0 \\ 0 & 0 & 0 & 0 & \frac{1}{9} & 0 & 0 & 0 \\ 0 & 0 & 0 & 0 & 0 & \frac{8}{45} & 0 & 0 \\ 0 & 0 & 0 & 0 & 0 & 0 & \frac{1}{45} & 0 \\ 0 & 0 & \frac{5}{36} & 0 & 0 & 0 & 0 & \frac{1}{60} \\ 0 & 0 & 0 & 0 & 0 & 0 & 0 & 0 \\ 0 & 0 & 0 & 0 & \frac{1}{9} & 0 & 0 & 0 \\ \frac{5}{36} & 0 & 0 & 0 & 0 & \frac{1}{60} & 0 & 0 \\ 0 & \frac{1}{9} & 0 & 0 & 0 & 0 & 0 & 0 \end{pmatrix}$$

----------POALARIZATION q= 1----------

Transition strengths:

$$\begin{pmatrix} 0 & 0 & 0 & 0 & 0 & \frac{1}{15} & 0 & 0 \\ 0 & 0 & 0 & 0 & 0 & 0 & \frac{2}{15} & 0 \\ 0 & 0 & 0 & 0 & 0 & 0 & 0 & \frac{2}{9} \\ 0 & 0 & 0 & \frac{1}{3} & 0 & 0 & 0 & 0 \\ 0 & 0 & 0 & 0 & \frac{1}{45} & 0 & 0 & 0 \\ \frac{1}{36} & 0 & 0 & 0 & 0 & \frac{1}{12} & 0 & 0 \\ 0 & \frac{1}{12} & 0 & 0 & 0 & 0 & \frac{1}{12} & 0 \\ 0 & 0 & \frac{1}{6} & 0 & 0 & 0 & 0 & \frac{1}{18} \\ 0 & 0 & 0 & 0 & 0 & 0 & 0 & 0 \\ 0 & 0 & 0 & 0 & \frac{1}{45} & 0 & 0 & 0 \\ \frac{5}{36} & 0 & 0 & 0 & 0 & \frac{1}{60} & 0 & 0 \\ 0 & \frac{5}{36} & 0 & 0 & 0 & 0 & \frac{1}{180} & 0 \\ 0 & 0 & 0 & 0 & 0 & 0 & 0 & 0 \\ 0 & 0 & 0 & 0 & 0 & 0 & 0 & 0 \\ 0 & 0 & 0 & 0 & \frac{1}{30} & 0 & 0 & 0 \\ \frac{1}{9} & 0 & 0 & 0 & 0 & 0 & 0 & 0 \end{pmatrix}$$

horizontal order of states (FmFJLSI) is:

$$\left\{\left\{1,-1,\frac{1}{2},0,\frac{1}{2},\frac{3}{2}\right\},\left\{1,0,\frac{1}{2},0,\frac{1}{2},\frac{3}{2}\right\},\left\{1,1,\frac{1}{2},0,\frac{1}{2},\frac{3}{2}\right\},\left\{2,2,\frac{1}{2},0,\frac{1}{2},\frac{3}{2}\right\},\right.$$
$$\left.\left\{2,-2,\frac{1}{2},0,\frac{1}{2},\frac{3}{2}\right\},\left\{2,-1,\frac{1}{2},0,\frac{1}{2},\frac{3}{2}\right\},\left\{2,0,\frac{1}{2},0,\frac{1}{2},\frac{3}{2}\right\},\left\{2,1,\frac{1}{2},0,\frac{1}{2},\frac{3}{2}\right\}\right\}$$

vertical order of states (FmFJLSI) is:

$$\left\{\left\{3,0,\frac{3}{2},1,\frac{1}{2},\frac{3}{2}\right\},\left\{3,1,\frac{3}{2},1,\frac{1}{2},\frac{3}{2}\right\},\left\{3,2,\frac{3}{2},1,\frac{1}{2},\frac{3}{2}\right\},\left\{3,3,\frac{3}{2},1,\frac{1}{2},\frac{3}{2}\right\},\right.$$
$$\left\{3,-1,\frac{3}{2},1,\frac{1}{2},\frac{3}{2}\right\},\left\{2,0,\frac{3}{2},1,\frac{1}{2},\frac{3}{2}\right\},\left\{2,1,\frac{3}{2},1,\frac{1}{2},\frac{3}{2}\right\},\left\{2,2,\frac{3}{2},1,\frac{1}{2},\frac{3}{2}\right\},$$
$$\left\{3,-2,\frac{3}{2},1,\frac{1}{2},\frac{3}{2}\right\},\left\{3,-1,\frac{3}{2},1,\frac{1}{2},\frac{3}{2}\right\},\left\{1,0,\frac{3}{2},1,\frac{1}{2},\frac{3}{2}\right\},\left\{1,1,\frac{3}{2},1,\frac{1}{2},\frac{3}{2}\right\},$$
$$\left.\left\{3,-3,\frac{3}{2},1,\frac{1}{2},\frac{3}{2}\right\},\left\{2,-2,\frac{3}{2},1,\frac{1}{2},\frac{3}{2}\right\},\left\{1,-1,\frac{3}{2},1,\frac{1}{2},\frac{3}{2}\right\},\left\{0,0,\frac{3}{2},1,\frac{1}{2},\frac{3}{2}\right\}\right\}$$

HIGH FIELD (JmJImILS1->JmJImILS2):

----------POALARIZATION q= -1----------

Transition strengths:

$$\begin{pmatrix}
0 & 0 & 0 & 0 & 0 & 0 & 0 & 0 \\
0 & 0 & 0 & 0 & 0 & 0 & 0 & 0 \\
0 & 0 & 0 & 0 & 0 & 0 & 0 & 0 \\
0 & 0 & 0 & 0 & 0 & 0 & 0 & 0 \\
0 & 0 & 0 & 0 & 0 & 0 & 0 & 0 \\
0 & 0 & 0 & 0 & 0 & 0 & 0 & 0 \\
0 & 0 & 0 & 0 & 0 & 0 & 0 & 0 \\
0 & 0 & 0 & 0 & 0 & 0 & 0 & 0 \\
\frac{2}{9} & 0 & 0 & 0 & 0 & 0 & 0 & 0 \\
0 & \frac{2}{9} & 0 & 0 & 0 & 0 & 0 & 0 \\
0 & 0 & \frac{2}{9} & 0 & 0 & 0 & 0 & 0 \\
0 & 0 & 0 & \frac{2}{9} & 0 & 0 & 0 & 0 \\
0 & 0 & 0 & 0 & 0 & 0 & 0 & \frac{2}{3} \\
0 & 0 & 0 & 0 & 0 & 0 & \frac{2}{3} & 0 \\
0 & 0 & 0 & 0 & 0 & \frac{2}{3} & 0 & 0 \\
0 & 0 & 0 & 0 & \frac{2}{3} & 0 & 0 & 0
\end{pmatrix}$$

----------POALARIZATION q= 0----------

Transition strengths:

$$\begin{pmatrix} 0 & 0 & 0 & 0 & 0 & 0 & 0 & 0 \\ 0 & 0 & 0 & 0 & 0 & 0 & 0 & 0 \\ 0 & 0 & 0 & 0 & 0 & 0 & 0 & 0 \\ 0 & 0 & 0 & 0 & 0 & 0 & 0 & 0 \\ \frac{4}{9} & 0 & 0 & 0 & 0 & 0 & 0 & 0 \\ 0 & \frac{4}{9} & 0 & 0 & 0 & 0 & 0 & 0 \\ 0 & 0 & \frac{4}{9} & 0 & 0 & 0 & 0 & 0 \\ 0 & 0 & 0 & \frac{4}{9} & 0 & 0 & 0 & 0 \\ 0 & 0 & 0 & 0 & 0 & 0 & 0 & \frac{4}{9} \\ 0 & 0 & 0 & 0 & 0 & 0 & \frac{4}{9} & 0 \\ 0 & 0 & 0 & 0 & 0 & \frac{4}{9} & 0 & 0 \\ 0 & 0 & 0 & 0 & \frac{4}{9} & 0 & 0 & 0 \\ 0 & 0 & 0 & 0 & 0 & 0 & 0 & 0 \\ 0 & 0 & 0 & 0 & 0 & 0 & 0 & 0 \\ 0 & 0 & 0 & 0 & 0 & 0 & 0 & 0 \\ 0 & 0 & 0 & 0 & 0 & 0 & 0 & 0 \end{pmatrix}$$

----------POALARIZATION q= 1----------

Transition strengths:

$$\begin{pmatrix} \frac{2}{3} & 0 & 0 & 0 & 0 & 0 & 0 & 0 \\ 0 & \frac{2}{3} & 0 & 0 & 0 & 0 & 0 & 0 \\ 0 & 0 & \frac{2}{3} & 0 & 0 & 0 & 0 & 0 \\ 0 & 0 & 0 & \frac{2}{3} & 0 & 0 & 0 & 0 \\ 0 & 0 & 0 & 0 & 0 & 0 & 0 & \frac{2}{9} \\ 0 & 0 & 0 & 0 & 0 & 0 & \frac{2}{9} & 0 \\ 0 & 0 & 0 & 0 & 0 & \frac{2}{9} & 0 & 0 \\ 0 & 0 & 0 & 0 & \frac{2}{9} & 0 & 0 & 0 \\ 0 & 0 & 0 & 0 & 0 & 0 & 0 & 0 \\ 0 & 0 & 0 & 0 & 0 & 0 & 0 & 0 \\ 0 & 0 & 0 & 0 & 0 & 0 & 0 & 0 \\ 0 & 0 & 0 & 0 & 0 & 0 & 0 & 0 \\ 0 & 0 & 0 & 0 & 0 & 0 & 0 & 0 \\ 0 & 0 & 0 & 0 & 0 & 0 & 0 & 0 \\ 0 & 0 & 0 & 0 & 0 & 0 & 0 & 0 \\ 0 & 0 & 0 & 0 & 0 & 0 & 0 & 0 \end{pmatrix}$$

horizontal order of states (JmJImILS) is:

$$\left\{\left\{\frac{1}{2}, \frac{1}{2}, \frac{3}{2}, -\frac{3}{2}, 0, \frac{1}{2}\right\}, \left\{\frac{1}{2}, \frac{1}{2}, \frac{3}{2}, -\frac{1}{2}, 0, \frac{1}{2}\right\},\right.$$
$$\left\{\frac{1}{2}, \frac{1}{2}, \frac{3}{2}, \frac{1}{2}, 0, \frac{1}{2}\right\}, \left\{\frac{1}{2}, \frac{1}{2}, \frac{3}{2}, \frac{3}{2}, 0, \frac{1}{2}\right\}, \left\{\frac{1}{2}, -\frac{1}{2}, \frac{3}{2}, \frac{3}{2}, 0, \frac{1}{2}\right\},$$
$$\left.\left\{\frac{1}{2}, -\frac{1}{2}, \frac{3}{2}, \frac{1}{2}, 0, \frac{1}{2}\right\}, \left\{\frac{1}{2}, -\frac{1}{2}, \frac{3}{2}, -\frac{1}{2}, 0, \frac{1}{2}\right\}, \left\{\frac{1}{2}, -\frac{1}{2}, \frac{3}{2}, -\frac{3}{2}, 0, \frac{1}{2}\right\}\right\}$$

vertical order of states (JmJImILS) is:

$$\left\{\left\{\frac{3}{2}, \frac{3}{2}, \frac{3}{2}, -\frac{3}{2}, 1, \frac{1}{2}\right\}, \left\{\frac{3}{2}, \frac{3}{2}, \frac{3}{2}, -\frac{1}{2}, 1, \frac{1}{2}\right\},\right.$$
$$\left\{\frac{3}{2}, \frac{3}{2}, \frac{3}{2}, \frac{1}{2}, 1, \frac{1}{2}\right\}, \left\{\frac{3}{2}, \frac{3}{2}, \frac{3}{2}, \frac{3}{2}, 1, \frac{1}{2}\right\}, \left\{\frac{3}{2}, \frac{1}{2}, \frac{3}{2}, -\frac{3}{2}, 1, \frac{1}{2}\right\},$$
$$\left\{\frac{3}{2}, \frac{1}{2}, \frac{3}{2}, -\frac{1}{2}, 1, \frac{1}{2}\right\}, \left\{\frac{3}{2}, \frac{1}{2}, \frac{3}{2}, \frac{1}{2}, 1, \frac{1}{2}\right\}, \left\{\frac{3}{2}, \frac{1}{2}, \frac{3}{2}, \frac{3}{2}, 1, \frac{1}{2}\right\},$$
$$\left\{\frac{3}{2}, -\frac{1}{2}, \frac{3}{2}, -\frac{3}{2}, 1, \frac{1}{2}\right\}, \left\{\frac{3}{2}, -\frac{1}{2}, \frac{3}{2}, -\frac{1}{2}, 1, \frac{1}{2}\right\},$$
$$\left\{\frac{3}{2}, -\frac{1}{2}, \frac{3}{2}, \frac{1}{2}, 1, \frac{1}{2}\right\}, \left\{\frac{3}{2}, -\frac{1}{2}, \frac{3}{2}, \frac{3}{2}, 1, \frac{1}{2}\right\}, \left\{\frac{3}{2}, -\frac{3}{2}, \frac{3}{2}, -\frac{3}{2}, 1, \frac{1}{2}\right\},$$
$$\left\{\frac{3}{2}, -\frac{3}{2}, \frac{3}{2}, -\frac{1}{2}, 1, \frac{1}{2}\right\}, \left\{\frac{3}{2}, -\frac{3}{2}, \frac{3}{2}, \frac{1}{2}, 1, \frac{1}{2}\right\}, \left\{\frac{3}{2}, -\frac{3}{2}, \frac{3}{2}, \frac{3}{2}, 1, \frac{1}{2}\right\}\right\}$$